Faculty of Electrical Technology and Engineering

DEVELOPMENT OF A FISH TANK WASTE CLEANER USING SOLAR POWER CHARGING SYSTEM WITH IOT CONTROLLING

MOHAMAD LOKMAN HAKIM BIN MOHAMED NOOR

Bachelor of Electrical Engineering Technology with Honours

2024

DEVELOPMENT OF A FISH TANK WASTE CLEANER USING SOLAR POWER CHARGING SYSTEM WITH IOT CONTROLLING

MOHAMAD LOKMAN HAKIM BIN MOHAMED NOOR

A project report submitted
in partial fulfillment of the requirements for the degree of
Bachelor of Electrical Engineering Technology with Honours

Faculty of Electrical Technology and Engineering

UNIVERSITI TEKNIKAL MALAYSIA MELAKA

2024

DECLARATION

I declare that this project report entitled "Development of a fish tank waste cleaner using solar power charging system with IoT controlling" is the result of my own research except as cited in the references. The project report has not been accepted for any degree and is not concurrently submitted in candidature of any other degree.

Signature	:	
Student Name	:	MOHAMAD LOKMAN HAKIM BIN MOHAMED NOOR
Date	:	3/1/2025

APPROVAL

I approve that this Bachelor Degree Project 2 (PSM2) report entitled “Development of a fish tank waste cleaner using solar power charging system with IoT controlling” is sufficient for submission.

Signature	:	
Supervisor Name	:	TS. DR. SUZIANA BINTI AHMAD
Date	:	3/1/2025

APPROVAL

I hereby declare that I have checked this project report and in my opinion, this project report is adequate in terms of scope and quality for the award of the degree of Bachelor of Electrical Engineering Technology with Honours.

Signature :

Supervisor Name : TS. DR. SUZIANA BINTI AHMAD

Date : 3/1/2025

Signature :

Co-Supervisor Name (if any) :

Date :

DEDICATION

This research paper is dedicated to my beloved parents, whose unwavering love, support, and sacrifices have laid the foundation for my education and aspirations. Their constant encouragement and inspiration have motivated me to stay determined and resilient in the face of every challenge, enabling me to strive for excellence.

I extend my heartfelt gratitude to my family for their unconditional support, understanding, and patience throughout this journey. Their unwavering belief in my abilities has been a driving force behind my success.

To my friends, thank you for your support during difficult times, your advice, and your motivation, which have made this journey both meaningful and fulfilling.

My deepest appreciation goes to my supervisor, whose expertise, guidance, and invaluable insights have been instrumental in shaping and completing this project. Their unwavering support and constructive feedback have been a guiding light throughout my academic journey.

Above all, I am profoundly grateful to ALLAH SWT for blessing me with the strength, good health, and perseverance to overcome challenges and successfully complete this project. It is through His guidance and mercy that I have achieved this milestone.

Lastly, I thank myself for the hard work, dedication, and commitment I have shown in bringing this research to fruition.

ABSTRACT

In the current era of globalization, technology is a one of the best initiatives for improving the quality of aquatic environments. Developing a fish tank waste cleaner powered by solar energy represents an innovative approach to meeting the demand for eco-friendly and efficient cleaning solutions in aquatic settings. By utilizing solar energy to operate the waste cleaner, this project aims to contribute to environmental conservation and enhance energy efficiency in maintaining fish tanks. Traditional methods of fish tank cleaning often rely on manual labour or non-renewable energy sources, which can harm the environment and are not very efficient. The primary objective of this project is to use solar power to create an underwater cleaner for fish tanks. The goal is to improve cleaning efficiency and utilize energy more effectively. The aim is to demonstrate that this project can effectively clean fish tanks using sustainable methods that benefit the environment and save energy. To achieve this, This project is combining solar panels, microcontrollers such as ESP8266, and various electronic components such as IR sensors, motor drivers, DC motors, relay modules, DC water pumps, and rechargeable batteries to create a solar-powered fish tank cleaner. Additionally, This project integrating an IoT system to enable real-time controlling by users. This project is continuously testing and refining the cleaner in real-world scenarios, optimizing its functionality and software to ensure it performs well and conserves energy. The solar power system consistently generates and stores energy, effectively powering the fish tank waste cleaner. Real-world testing has demonstrated its effectiveness underwater, showing that it is possible to manage fish tank waste sustainably and efficiently. The result shows the proposed project able to clean the fish tank with the provided power supply.

ABSTRAK

Dalam era globalisasi sekarang, teknologi merupakan salah satu inisiatif terbaik untuk meningkatkan kualiti persekitaran akuatik. Membangunkan pembersih sisa tangki ikan yang dikuasakan oleh tenaga suria mewakili pendekatan inovatif untuk memenuhi permintaan untuk penyelesaian pembersihan yang mesra alam dan cekap dalam tetapan akuatik. Dengan menggunakan tenaga suria untuk mengendalikan pembersih sisa, projek ini bertujuan untuk menyumbang kepada pemuliharaan alam sekitar dan meningkatkan kecekapan tenaga dalam menyelenggara tangki ikan. Kaedah tradisional pembersihan tangki ikan sering bergantung kepada tenaga kerja manual atau sumber tenaga tidak boleh diperbaharui, yang boleh membahayakan alam sekitar dan tidak begitu cekap. Objektif utama projek ini adalah untuk menggunakan tenaga solar untuk mencipta pembersih bawah air untuk tangki ikan. Matlamatnya adalah untuk meningkatkan kecekapan pembersihan dan menggunakan tenaga dengan lebih berkesan. Matlamatnya adalah untuk menunjukkan bahawa projek ini boleh membersihkan tangki ikan dengan berkesan menggunakan kaedah mampan yang memberi manfaat kepada alam sekitar dan menjimatkan tenaga. Untuk mencapai matlamat ini, Projek ini menggabungkan panel solar, mikropengawal seperti ESP8266, dan pelbagai komponen elektronik seperti penderia IR, pemacu motor, motor DC, modul geganti, pam air DC, dan bateri boleh dicas semula untuk mencipta pembersih tangki ikan berkuasa solar. . Selain itu, Projek ini menyepadukan sistem IoT untuk membolehkan kawalan masa nyata oleh pengguna. Projek ini secara berterusan menguji dan memperhalusi pembersih dalam senario dunia sebenar, mengoptimumkan fungsi dan perisiannya untuk memastikan ia berfungsi dengan baik dan menjimatkan tenaga. Sistem tenaga suria secara konsisten menjana dan menyimpan tenaga, menjana tenaga pembersih sisa tangki ikan dengan berkesan. Ujian dunia sebenar telah menunjukkan keberkesanannya di bawah air, menunjukkan bahawa adalah mungkin untuk menguruskan sisa tangki ikan secara mampan dan cekap. Hasilnya menunjukkan projek yang dicadangkan mampu membersihkan tangki ikan dengan bekalan kuasa yang disediakan.

ACKNOWLEDGEMENTS

First and foremost, I would like to extend my deepest gratitude to my supervisor, TS. DR. SUZIANA BINTI AHMAD, for her invaluable guidance, insightful advice, and unwavering patience throughout the course of this project. Her expertise and support have been instrumental in helping me navigate challenges and achieve my goals.

I would also like to express my heartfelt appreciation to my parents and family members for their unconditional love, constant prayers, and encouragement during my studies. Their unwavering support has been my greatest source of strength and motivation throughout this journey.

Lastly, my sincere thanks go to the dedicated staff at UTEM, my fellow colleagues and classmates, and the esteemed faculty members for their cooperation, assistance, and kindness. I am also grateful to all other individuals, whether mentioned here or not, who have offered their support and contributions to the success of this project.

TABLE OF CONTENTS

LIST OF TABLES

LIST OF FIGURES

LIST OF SYMBOLS

LIST OF ABBREVIATIONS

V	-	Voltage
A	-	Ampere
W	-	Watts
Volts	-	Voltages
Amps	-	Amperes
PV	-	Photovoltaics
Isc	-	Short circuit current
Voc	-	Open circuit voltage

LIST OF APPENDICES

CHAPTER 1

INTRODUCTION

1.1 Background

Maintaining a healthy aquatic environment in fish tanks and aquariums is essential for the well-being of the aquatic inhabitant’s ecosystem. However, one of the primary challenges in aquarium maintenance is managing the accumulation of waste, which can degrade water quality and endanger the health of fish, plants, and other aquatic organisms. Traditional waste management methods often involve manual cleaning or reliance on mechanical filtration systems, which can be time-consuming, labor-intensive, and prone to inefficiencies.

In response to these challenges, there has been a growing interest in developing innovative solutions for automated waste management in fish tanks and aquariums. Fish tank waste cleaners, also known as aquarium vacuum cleaners, have emerged as a promising technology to address this need. These devices utilize various mechanisms, such as suction or filtration, to remove debris, uneaten food, and accumulated waste from the substrate and water column of the aquarium.

The development of fish tank waste cleaners represents a convergence of advancements in aquaculture technology, automation, and engineering. These devices are designed to streamline the maintenance process, making it more efficient, convenient, and environmentally friendly. By automating waste removal tasks, fish tank waste cleaners help to maintain optimal water quality, reduce the risk of disease outbreaks, and promote the overall health and vitality of the aquarium ecosystem.

Moreover, integrating solar charging systems into fish tank waste cleaners further enhances their sustainability and autonomy. By harnessing solar energy to power these devices, they become independent of grid electricity, reducing their environmental footprint and operating costs. Solar-powered charging systems provide continuous energy to the devices, ensuring uninterrupted waste management and contributing to the sustainability of aquarium ecosystems. This project provides an overview of the background, design principles, and applications of fish tank waste cleaners, with a focus on the integration of solar charging systems to promote sustainable aquaculture practices.

This project builds upon this existing research by proposing a microcontroller for fish tank waste cleaner. Using microcontroller technology, the system can automate the cleaning process based on sensor data, offering a cost-effective and efficient solution compared to traditional methods. The project aims to contribute to the development of practical's that can improve the overall performance and maintenance efficiency of fish tank waste cleaner.

1.2 Problem Statement

Traditional electricity sources such as coal mining and burning for electrical generation can lead to air pollution. Solar energy is a renewable source of power that doesn't harm the environment. Therefore, solar is one of the renewables in that can overcome air pollution. This situation aligns with sustainable development goals SDG 7, which aims to provide affordable, reliable, sustainable, and modern energy for all. SDG 7 focuses on increasing the proportion of renewable energy in the global energy mix, improving energy efficiency, and expanding infrastructure and technology to deliver clean energy, particularly in developing countries. The development of a fish tank waste cleaner using solar power charging system with IoT monitoring contributes to this goal by utilizing renewable energy sources, thus decreasing dependence on fossil fuels, and promoting environmental sustainability. Solar energy use aids the transition to cleaner energy and represents innovative solutions that are both cost-effective and accessible, aligning with SDG 7's broader objective of making sustainable energy available to everyone. Furthermore, compared to Arduino Uno, Arduino Uno lacks built-in connectivity options like Wi-Fi or Bluetooth, which means Arduino Uno needs to use additional modules or shields to connect to the internet or other devices. While ESP8266 is a versatile microcontroller that can handle tasks such as data processing, communication, and sensor integration. It also offers Wi-Fi connectivity, which can be useful for remote monitoring and control of the waste cleaner. This situation aligns with sustainable development goals SDG 9, which aims to build resilient infrastructure, promote inclusive and sustainable industrialization, and foster innovation. SDG 9 highlights the necessity for quality infrastructure to support economic growth and human well-being, the importance of innovation and technological advancement, and the encouragement of sustainable industrial development. The creation of a solar-powered fish tank waste cleaner contributes to the goal of fostering innovation and advancing sustainable technologies. The use of solar energy in this innovative solution represents the development of resilient and eco-friendly infrastructure that can be broadly adopted. This supports SDG 9's broader goals of enhancing industrial capabilities, promoting technological progress, and ensuring that infrastructure development is sustainable and inclusive, benefiting both communities and the environment. Floating cleaners are designed to only clean on the surface of the water, they can be effective in removing the surface of floating waste. However, for deeper cleaning and reaching areas at the bottom of the tank, an underwater cleaner may be more suitable. It can target and remove waste that has settled at the bottom, ensuring a thorough cleaning of the entire tank.

1.3 Project Objective

a) To design a solar power charging system using solar panels, a charge controller, and a battery.
b) To design a fish tank waste cleaner using an ESP8266, motor driver, and DC motor.
c) To analyse the performance of a solar-powered waste cleaner using real-time experiments.

1.4 Scope of Project

The scope of this project are as follows:

a) Design and building a fish tank waste cleaner using suction method capable of removing uneaten food, small waste particles, controlled by microcontroller (ESP 8266).
b) Focus on implementation of a solar power charging system using on a single panel or a small number of the panels for initial development and testing to provide sustainable and renewable energy for powering the waste cleaner.
c) Design and fabrication of the waste cleaner to ensure durability, efficiency, and compatibility with aquarium environments.
d) Testing and validation of the waste cleaner's performance and efficiency through real-time experiments conducted in various aquarium settings.

e) Evaluation of the waste cleaner's effectiveness in removing debris and maintaining water quality, considering factors such as cleaning capacity, energy consumption, and operational reliability.

CHAPTER 2

LITERATURE REVIEW

2.1 Introduction

The increasing demand for energy is a major challenge we face today. It's crucial for us to shift towards renewable energy sources due to the limited availability of fossil fuels. Renewable energies, like solar power, offer a sustainable and environmentally friendly alternative. The sun, being the largest energy source, provides us with an abundance of energy. In fact, just one hour of solar energy absorbed by the Earth can meet the world's annual energy needs[1].The literature review section provides an overview of existing research and knowledge related to the project. It helps establish the current understanding of underwater waste cleaning technologies, solar power charging systems, and their applications in fish tank maintenance.

By reviewing relevant studies, articles, and publications certainly can identify gaps in the existing knowledge and build upon previous work to contribute to the field. The literature review will serve as a foundation of the project, allowing to explore the latest advancements, best practices, and potential challenges in developing a solar-powered underwater fish tank waste cleaner.

2.2 Renewable energy

Renewable energy sources are becoming increasingly crucial in meeting the world's future energy requirements. They are gradually replacing conventional energy sources, there by mitigating the risks associated with the widespread use of traditional energy sources[2]. Renewable energy comes from natural sources that are constantly replenished. Here are the main types of renewable energy such as Solar Energy[3], [4], [5], Wind Energy[2], [6], [7], Hydropower energy [8] and thermal energy[9], [10], [11].

Additionally, it's important to note that fossil fuels have limited availability and cannot serve as a long-term energy solution. As a result, renewable energy sources offer a viable alternative to these traditional resources, renewable energy aligns with the sustainable objectives set by the United Nations for 2030, as many member countries aim to achieve affordable and clean energy. Goal seven of this agenda specifically emphasizes the importance of renewables and innovative approaches to their implementation[10].

However, renewable energy sources possess a distinctive characteristic that they are often unpredictable and intermittent. This unpredictability can lead to significant challenges concerning the stability of electricity grids[2].

2.2.1 Wind energy

Wind energy is a type of renewable energy that harnesses the power of the wind to generate electricity. It works by using wind turbines, which have large blades that spin when the wind blows. As the blades rotate, it turns a generator that produces electricity. Figure 2.1 shows the operational concept of the wind energy system.

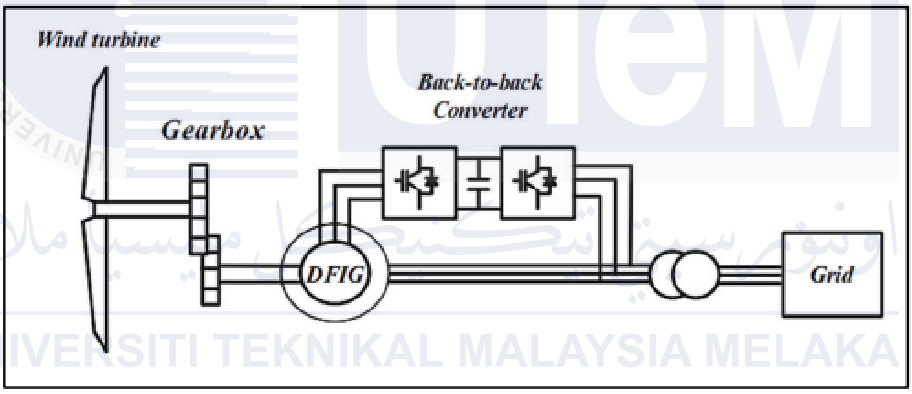

Figure 2.1 Operational concept of the wind energy system[2].

A wind energy system captures the wind's power to make electricity. It has a tall tower with big blades that look like propellers, called turbines. When the wind blows, it spins these turbines, which are connected to a generator[2].

Main advantages on the wind energy are flexible operation and control, the cost reduction of wind energy in the last decades happened together with a significant increase in turbine size. Wind energy is clean, abundant, and doesn't produce greenhouse gas emissions like fossil fuels do[2]. The amount of power produced by a turbine is influenced by the speed of the wind at the specific location where it's installed. The stronger the wind, the more power the turbine can generate.

Although wind energy conversion systems offer many environmental benefits, large additions of wind energy conversion can pose a threat to system reliability. Thus, the proper selection of wind turbines (WTs) and their installation is considered a major challenge. Unlike fossil fuels, which are finite and contribute to pollution, wind energy relies on the natural movement of air, which is constantly replenished. One drawback of wind energy is its unpredictable and intermittent nature[12]. This can pose challenges in maintaining a stable electricity grid. Thus, the fluctuating availability of wind can make it difficult to ensure a consistent and reliable power supply. However, due to rising fuel prices, it is predicted that in the near future, the cost of power produced by wind energy-based systems would decrease even more while the cost of electricity generated from traditional energy sources will rise in other developing nations.

2.2.2 Hydropower energy

Hydropower energy is a form of renewable energy that harnesses the power of flowing or falling water to generate electricity. It is often generated by building dams on rivers or utilizing the natural flow of water in rivers and streams. The force of the moving water turns turbines, which then spin generators to produce electricity. The typical block diagram as Figure 2.2.

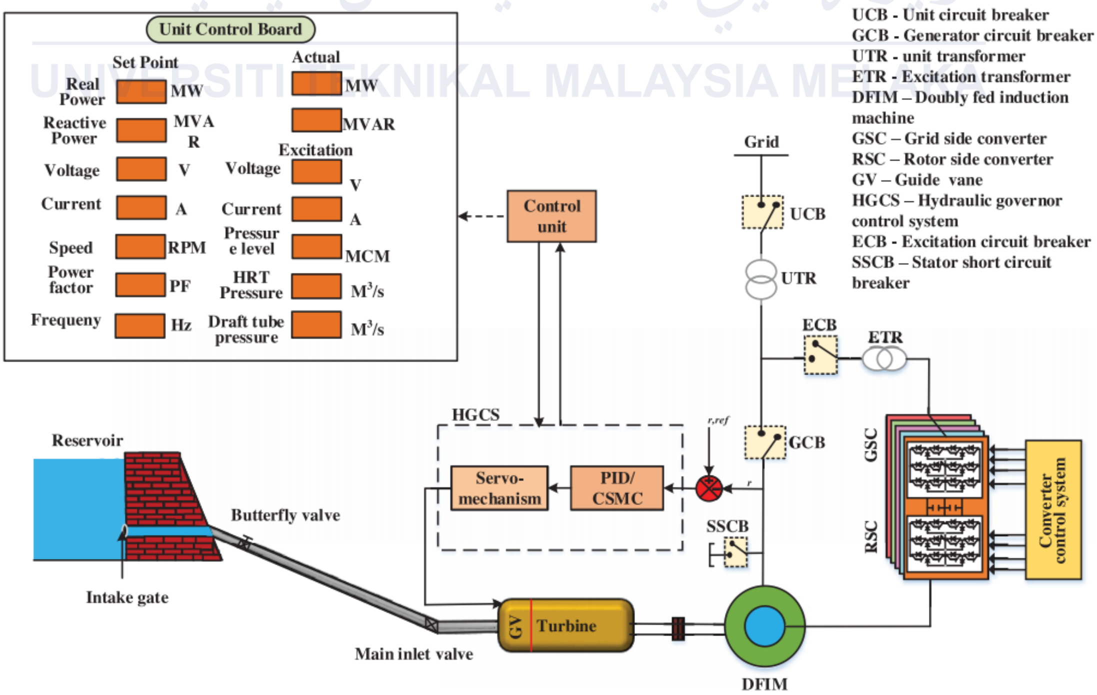

Figure 2.2 Block diagram of a typical hydroplant control system [8].

A typical hydroplant control system uses sensors to monitor water flow, turbine speed, and power output. This data feeds into a central control system, which adjusts guide vanes in the turbine to regulate water flow and maintain consistent power generation while also incorporating safety features and communicating with the power grid to meet fluctuating electricity demands.

Hydropower generation is an environmentally friendly, sustainable form of energy that offers numerous social and economic advantages also it is a clean and renewable energy source with no pollution. The Chinese government has made the decision to offer incentives and subsidies for exporting hydropower, these benefits are included in the price of green electricity. Due to China's economic growth and the desire to enhance people's quality of life, there has been a significant increase in the construction of hydropoaar stations in the country, this expansion is driven by the aim to meet the rising energy demands and provide clean and renewable electricity to support economic development while improving the well-being of the population. Hydropower companies will not only prioritize the energy advantages but also consider the positive impacts of their automatic generation control (AGC) in response to the area control error (ACE) signal[8]. The review highlights that Ultra-low head hydropower has the potential to tackle environmental issues, hydropower has been utilized for centuries as a renewable energy source, powering mills and machinery, in the 19th century, it became a significant electricity source for industrialized societies. One big benefit of using pump mode in hydropower is the ability to control and adjust the flow of active power, which helps maintain a balanced energy distribution on the grid.

However, hydropower energy can be the potential environmental impact caused by the construction of dams and reservoirs, also these projects can lead to the displacement of communities, loss of wildlife habitats, and alteration of natural river ecosystems, the creation of dams can disrupt the natural flow of rivers, affecting downstream ecosystems and potentially causing water scarcity in certain areas. A hydropower unit is a complex mechanical system with various devices working together in a confined space, using numerous permanent magnets in this system can make processing, transportation, installation, and maintenance challenging, it can also pose safety risks due to the potential for magnets falling off under the strong centrifugal force.

2.2.3 Thermal energy

Thermal energy is the energy that is generated from the heat of an object or a system. It is a form of kinetic energy that arises from the movement of particles within a substance. The temperature of an object or system is directly related to its thermal energy. Thermal energy can be easily converted into other forms of energy, such as electricity or mechanical power. Thermal energy can be stored for later use, providing flexibility in energy supply. This type of energy can be harnessed and utilized for various purposes, such as heating buildings, generating electricity in thermal power plants, or even cooking food. Figure 2.3 shows energy flow diagram of retrofitted thermal plants with TES.

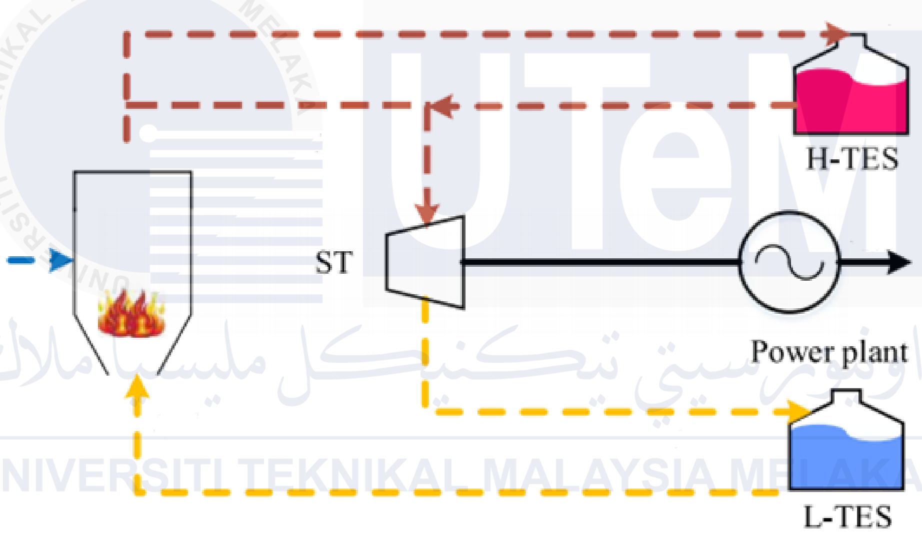

Figure 2.3 Energy flow diagram of retrofitted thermal plants with TES[28].

Upgraded power plants with thermal batteries (TES) work by adding a heat storage loop. Excess heat from the plant (like from a boiler) gets pumped into the TES unit, which can be molten rock, salt, or sand. This stored heat can then be used later to make steam and run the turbines to generate electricity during high-demand periods, without needing the original fuel source[28].

According to the data by 2060 in China, wind power and solar power generation together make up more than 60% of the total electricity generation, reaching around 11.0 trillion kWh, thermal power generation accounts for less than 20% with approximately 2.5 trillion kWh, this indicates a significant shift towards renewable energy sources in the future[9]. Thermal energy storage is an affordable and adaptable solution that improves the integration of intermittent solar power, it offers short-term storage for peak-shifting and addressing short-term fluctuations caused by renewable energy sources, in medium-term and long-term thermal energy storage can provide flexibility for weekly and seasonal energy needs. The series resistance cable serves as a thermal energy source and is composed of a high resistivity material, this material offers the benefits of cost-effectiveness and a long lifespan[13].

However, to properly install and repair electrical heat tracing systems, it is necessary to closely attach the heating cables to heated objects and surround them with thermal insulation materials, this process often involves removing the thermal insulation layer and replacing all of the heating cables[13]. Another requirement for installing thermal power plants is the availability of ample open spaces, these large free spaces are necessary to accommodate the infrastructure and equipment needed for the plants, by having access to sufficient land is indeed a crucial factor to consider when planning and setting up thermal energy facilities. We must explore and invest in renewable energy sources that have a smaller environmental footprint and can provide sustainable energy in the long run.

2.2.4 Solar energy

Solar energy works by harnessing the power of sunlight and converting it into usable energy. This process is done through the use of solar panels, which are made up of photovoltaic (PV) cells. These cells are made of semiconductor materials that generate an electric current when exposed to sunlight. When sunlight hits the solar panels, the PV cells absorb the photons and create an electric field. This electric field then allows the flow of electrons, generating direct current (DC) electricity. The DC electricity is then converted into alternating current (AC) electricity through an inverter, making it compatible with the electrical grid or for direct use in homes or businesses. Figure 2.4 shows example design machine using photovoltaic (PV) technologies[14].

Figure 2.4 Example design machine using photovoltaic (PV) technologies [14]

The prototype design includes different components like Arduino UNO, a solar panel, a DC motor, a motor driver, rechargeable batteries, and some other electronic parts. To control and communicate with the prescribed network, the Arduino UNO was programmed using Arduino IDE software. The remote control of the Grasscutter was achieved through the Blynk app on an Android mobile device. The movement of the Grasscutter's wheels is controlled by the DC motor, which receives specific commands from the processor[14].

Solar PV systems are widely recognized as a renewable energy source due to their cost-effectiveness, low maintenance requirements, high efficiency, and reliable performance. These systems offer a sustainable and environmentally friendly solution for generating electricity, making them a popular choice in the renewable energy sector, it plays a vital role in promoting sustainable and clean energy practices, contributing to a greener future. By utilizing solar panels, we can tap into this abundant source of energy and reduce our reliance on fossil fuels, and it aligns with the Sustainable Development Goal 7: Affordable and Clean Energy, as it helps to reduce air pollution and combat climate change. The process of converting sunlight into electricity through photovoltaics doesn't rely on any fuel and doesn't have any ongoing costs. It's a clean and sustainable way to generate power. In fact, the installation of solar panels is projected to contribute to about a quarter of the world's electricity needs. This widespread adoption of solar energy is a great example of its growing popularity and effectiveness[1].

Solar energy has numerous advantages, but it also has a few disadvantages to consider. One of the major drawbacks of solar energy is the initial cost of installing solar panels can be quite high, although it is important to note that the long-term savings on energy bills can offset this investment[1]. When it comes to constructing a solar power plant, it is necessary to allocate a substantial land area to ensure that all panels receive optimal sunlight and radiation. Additionally, the climate conditions play a pivotal role in determining the energy output from solar cells, overcast and foggy weather conditions lead to reduced sunlight, resulting in decreased energy production from photovoltaic (PV) modules[1].Another challenge is the need for sufficient space to accommodate the solar panels, especially for large-scale installations. As technology continues to advance and costs decrease, solar energy is becoming an increasingly attractive choice for a greener and more sustainable environment.

Photovoltaic modules are well-established, commercially accepted systems that have been generating electricity since 1995. The efficiency of solar energy produced by photovoltaic modules can be affected by two main factors, environmental which is such as humidity, wind speed, precipitation, and temperature, another main factor is non-environmental, which takes into account factors such as atmospheric pollution, dust accumulation, and bird droppings[15]. Dust accumulation, dirt, and bird dropping are some leading causes that lead to the poor functionality of solar panels. Figure 2.5 shows distribution of dust intensity around the world[15].

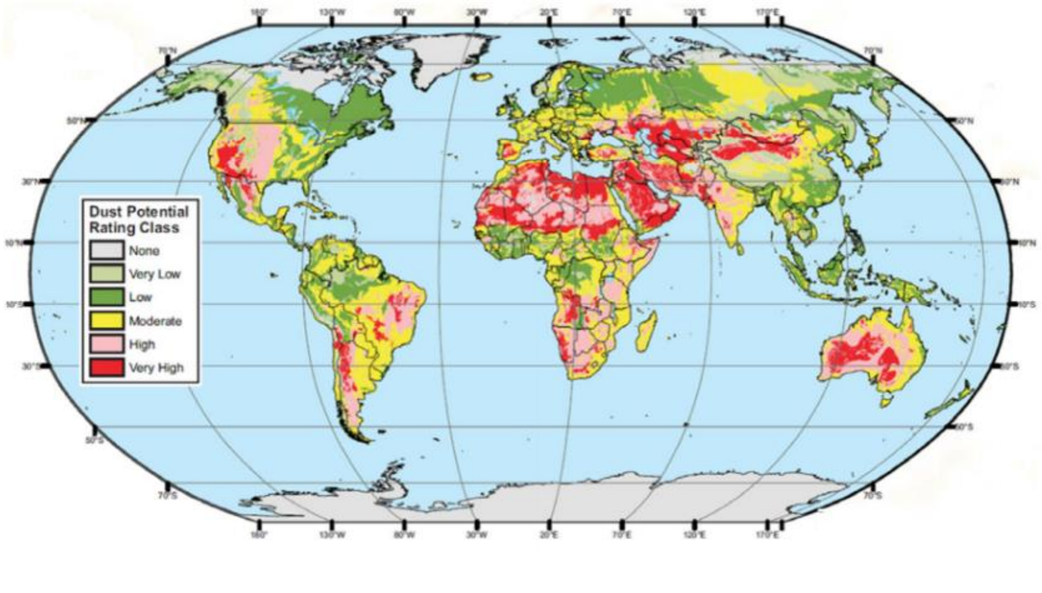

Figure 2.5 Distribution of dust intensity around the world [15].

This research is focusing a comprehensive review of automatic cleaning systems of solar panels from a College of Engineering and Technology, American University of the Middle East, Kuwait[15]. The method of this project is using the electrostatic cleaning system, which is recommended for regions with scarce water resources. Moreover, their objective of this project is reviewing the different automatic cleaning systems designed to remove dust and improve the functionality of photovoltaic modules at solar panels. Figures 2.6, and 2.7 show the effect of dust accumulation density, and comparison of indicators and features of five cleaning.

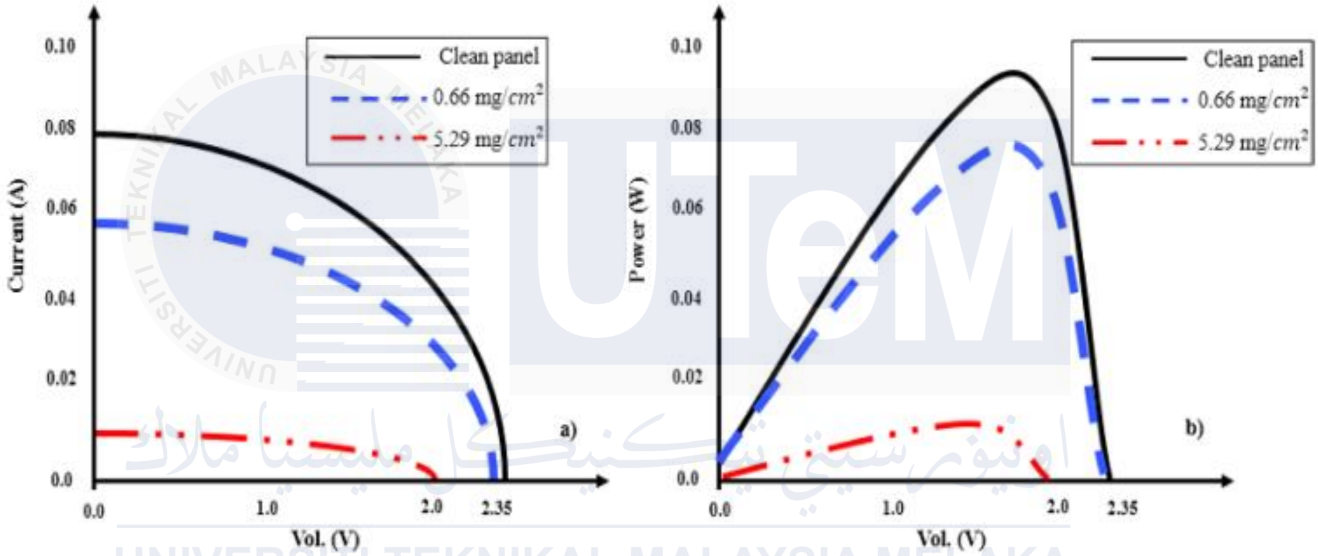

Figure 2.6 Effect of dust accumulation density on current, power, and voltage[7].

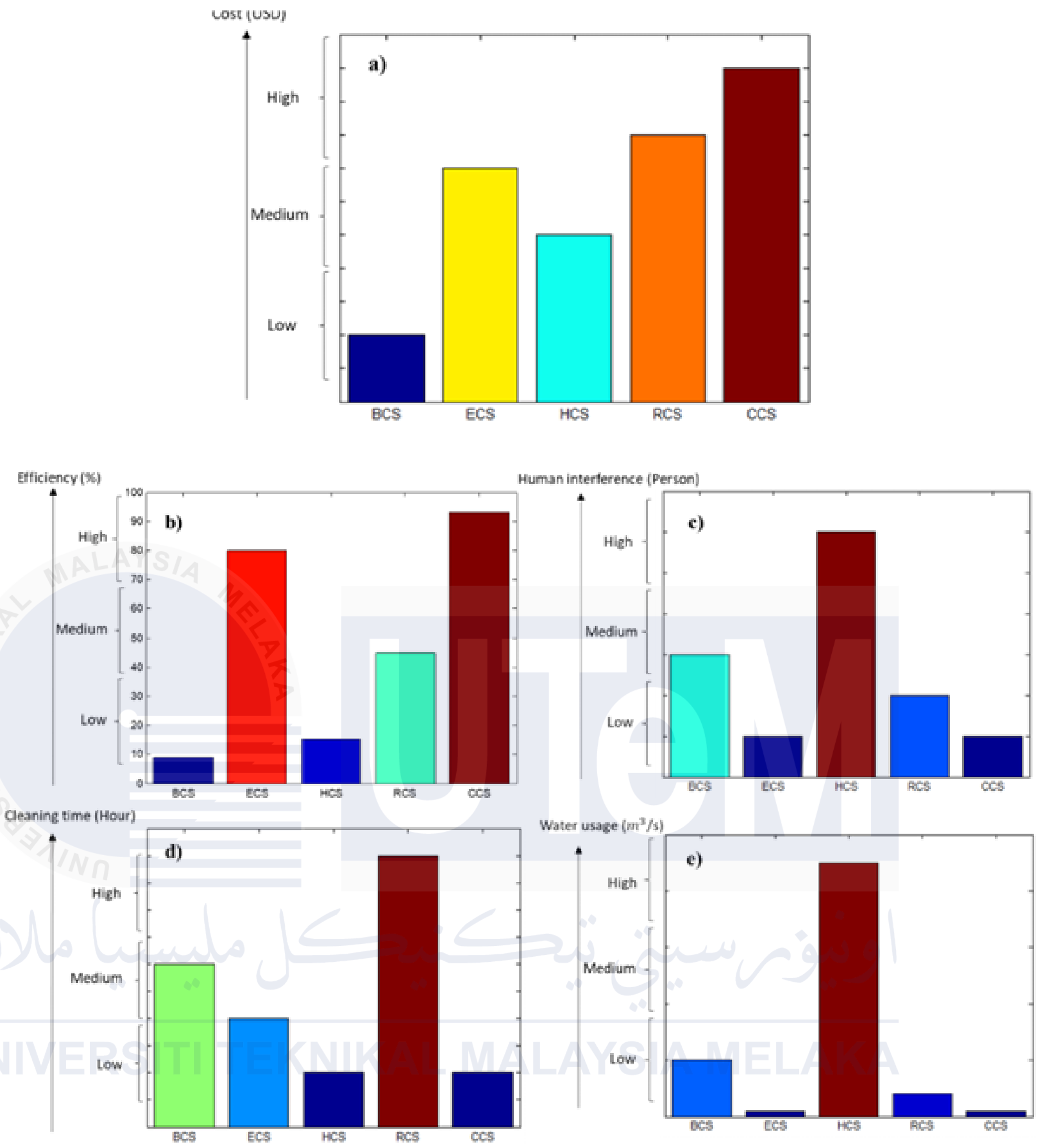

Figure 2.7 Comparison of indicators and features of five cleaning systems on comparison of labor work, water usage, efficiency, and required cleaning time[7].

2.3 Waste cleaner device

A garbage waste cleaner is a device or system designed to collect and dispose of garbage and waste. It can refer to various methods, such as manual waste collection by sanitation workers or automated systems like garbage trucks equipped with mechanical arms to pick up and empty trash bins. There are also specialized machines and robots that can clean up waste in specific environments. These robots are equipped with sensors, cameras, or mechanical parts that help them move around and collect trash in different environments[16]. This project can be programmed with different methods, like using suction to collect waste or identifying and picking up various types of small waste and debris. Waste cleaner device can be classified into three major field such as ground[16], [17], water surface[1], [4],and underwater[18], [19], [20].

2.3.1 Ground

A waste cleaner device is a specialized robot designed to navigate and clean up waste in various environments, both outdoors and indoors. These robots are specifically built to operate on the ground, allowing them to efficiently move around and collect waste in different areas. They are equipped with sensors and advanced navigation systems to detect and avoid obstacles, ensuring effective waste management. Figure 2.5 shows the actual model of a street sweeping machine.

Figure 2.8 Actual model of street sweeping machine[33].

This developed a solar operated street sweeping machine that can be used for cleaning small streets. The machine consists of a solar panel mounted on its top and a battery unit which can be used to power the entire machine. The electricity generated using the solar panel is stored in the battery which can be used to provide energy to operate the motor. The method of this project is generating electricity that powers the sweeping mechanism controlled by Arduino uno and the aim of this project is to propose a solution for the limitations of manual street sweeping by developing a solar powered street sweeping machine. Moreover, these robots can be programmed to utilize environmentally friendly cleaning solutions and run on renewable energy sources such as solar power, this not only helps to reduce the carbon footprint of cleaning operations but also promotes a more sustainable approach to keeping our surroundings clean.

Ground-based waste cleaner robots offer several advantages in terms of efficiency, environmental impact, and operational costs. One of the main advantages of ground-based waste cleaner robots is their operational efficiency, these robots can function continuously without the need for human intervention, ensuring that large areas stay consistently clean. Cost-effectiveness is indeed a crucial advantage of robotic waste cleaners, while the initial investment in these robots may be substantial, the long-term savings are quite significant. Over time, the efficiency and continuous operation of these robots can lead to reduced labor costs and increased productivity, making them a financially viable solution[21].

Ground-based waste cleaner robots do have some notable disadvantages that need to be taken into consideration. High initial costs and technical limitations can be a barrier for some organizations or communities looking to implement these robots. One major drawback is the substantial upfront expenses associated with acquiring and installing robotic waste cleaners, these costs can pose a challenge, particularly for small businesses with limited financial resources[22].Technical limitations also present a challenge. Ground-based robots may struggle with complex or cluttered environments, which can impede their effectiveness. Ground-based waste cleaner robots is their complexity in planning and the limitation of not supporting wet cleaning, it can be inconvenient for users as they have to reset the location each time the robot is used in a new area and these factors can make the operation of the robot more challenging and less efficient[17].

2.3.2 Water surface

A waste cleaner device on surface water is a specialized robot designed to clean up waste and debris floating on bodies of water such as rivers, lakes, or oceans. These robots are equipped with sensors, cameras, and collection systems to detect and collect various types of waste, including plastic, debris, and other pollutants. This are typically autonomous or remotely operated, allowing them to navigate and clean large areas of water effectively.

The water surface device or called cleaning robot are widely used to collect garbage as seen in Figure 2.9 and Figure 2.10.

Figure 2.9 Prototype of the miniature water surface garbage cleaning robot[41].

Figure 2.9 demonstrates a garbage cleaning method using a suction system, where the robot moves along the water's surface to collect floating debris through suction. This technique is especially effective for capturing small, lightweight particles, helping to keep the water free from litter[23].

Figure 2.10 Wireless water surface cleaning robot using conveyor belt[42].

Figure 2.10 shows a robot fitted with a conveyor belt system, also operating on the water's surface. This robot utilizes the conveyor belt to gather and transfer larger pieces of trash onto the robot, where they are stored until they can be disposed of[24].

Waste cleaner robots used on surface water offer several advantages in terms of environmental impact, operational efficiency, and cost-effectiveness. One of the primary advantages is the significant positive environmental impact. These robots help reduce pollution in bodies of water by effectively collecting and removing floating debris, plastics, and other pollutants, the suggested approach for cleaning lake water not only helps to maintain the natural beauty of the lakes but also successfully retrieves 95% of the waste that is floating on the surface. Surface water cleaning robots can operate continuously and autonomously, covering large areas without the need for constant human supervision. This project developed a versatile unmanned surface vehicle that serves multiple purposes, including obstacle avoidance, water quality detection, and surface cleaning, this vehicle utilizes sensor fusion technology to combine different sensors for enhanced performance and the robot is capable of autonomously detecting obstacles, navigating, and detecting and cleaning the water surface[4]. Cost-effectiveness is also a notable advantage, while the initial investment for these robots can be high and the long-term savings are substantial, automated systems reduce the need for manual labor and associated costs, such as wages and safety equipment.

While waste cleaner robots used on surface water offer several advantages, they also come with notable disadvantages. A drawback is the considerable upfront expense associated with procuring and deploying robotic systems. The initial cost can be a barrier for many organizations, encompassing not only the purchase of the robots themselves but also the installation of essential infrastructure and the training of personnel[25]. Certain drawbacks that limit its effectiveness in small water bodies, these limitations include its large size, displacement, noise, and the need for manual operation of the hull, which can be costly. Consequently, large-scale integrated clean ships are not suitable for cleaning garbage in small waters[26].

2.3.3 Underwater

An underwater waste cleaner robot is a specialized robot designed to clean up waste and debris from underwater such as rivers, lakes, or fish tank. These robots are equipped with sensors, cameras, and collection systems to detect and collect various types of waste, including waste, debris, and other pollutants. This project are typically autonomous or remotely operated, allowing them to navigate and clean large areas of water effectively. Figure 2.11 shows the prototype 3D design of underwater robot.

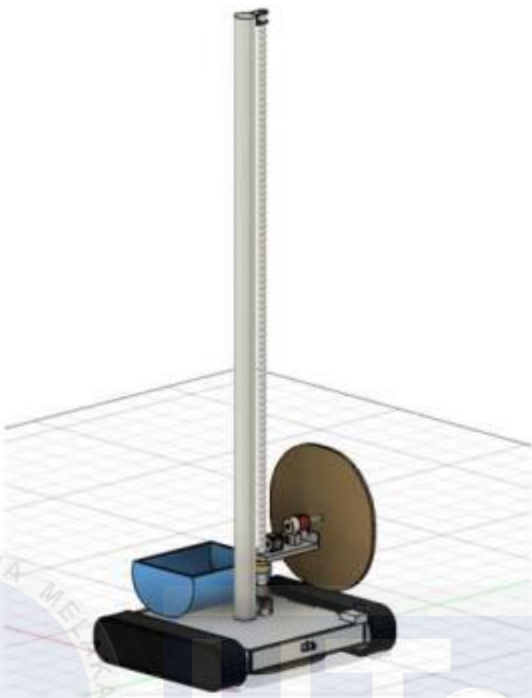

Figure 2.11 Prototype 3D design of underwater robot[44].

The robot's lightweight design allows for easy to move in different water environments, while its speed ensures quick and efficient cleaning operations, with safety features in place, the robot minimizes the risk of harm to itself and marine life, its effectiveness in detecting and collecting waste helps maintain the cleanliness and health of underwater ecosystems[27].

Underwater waste cleaner robots offer several advantages. Underwater wireless optical communication (UWOC) has emerged as a promising option with several notable benefits, these advantages include fast data transmission, minimal delay, compact size, and low cost[28]. Underwater robots can operate continuously and autonomously, covering large areas without the need for constant human supervision, equipped with advanced navigation systems and sensors, these robots can efficiently locate and collect underwater waste.

Underwater waste cleaner robots do have some notable disadvantages that need to be taken into consideration. Underwater robots are complex machines, and their development and operation can be expensive. The cost of building and maintaining these robots, along with the human support they require, can be a significant barrier to small organization[27]. Underwater environments can be quite complex with obstacles, these factors can challenge a robot's ability to navigate effectively and efficiently, fragile ecosystems and marine life must be avoided during cleaning operations. One challenge with underwater waste cleaner robots is the need to empty their collected waste before they can continue their operation, this can pose a logistical hurdle, particularly in deep waters or large areas[27].

2.4 Microcontroller for waste cleaner robot

A microcontroller is a small chip that is designed to control specific operations in embedded systems. It consists of a processor, memory, and input/output peripherals, all integrated into a single circuit. Microcontrollers are commonly used in devices like appliances, cars, and medical instruments. Unlike general-purpose computers, microcontrollers are optimized for specific tasks, making them efficient and reliable for real-time applications. They are widely used in automated systems, providing cost-effective and energy-efficient solutions for controlling various electronic devices and machinery.

A microcontroller operates by following a set of instructions stored in its memory. These instructions, typically written in languages like C or assembly, guide the microcontroller in controlling the inputs and outputs of electronic devices. When powered on, the microcontroller runs its programmed code, which includes tasks such as reading sensor data, processing information, and controlling actuators. It continuously loops through these instructions, monitoring inputs from peripherals and adjusting outputs accordingly. The integrated architecture of a microcontroller allows for precise timing and efficient handling of real-time operations, making it well-suited for embedded systems with specific tasks. Microcontroller can be classified into four major field such as Arduino Uno[29], [30], Raspberry Pi[31], [32],ESP32[33], and ESP8266[34], [35], [36], [37].

2.4.1 Arduino uno

The Arduino Uno is a popular open-source microcontroller board that is based on the ATmega328P microcontroller. It offers digital and analog input/output pins, a USB connection for programming and power, and a user-friendly interface. This makes it a great choice for beginners and hobbyists in electronics. To operate the board, users can write code in a simplified version of C/C++ using the Arduino Integrated Development Environment (IDE). Once the code is uploaded to the board, the microcontroller executes the instructions, allowing it to interact with various components such as sensors, LEDs, motors, and more.

Its versatility and ease of use make it ideal for creating a wide range of interactive projects and prototypes. Figure 2.12 shows Arduino UNO R3 and Atmega328P pin out.

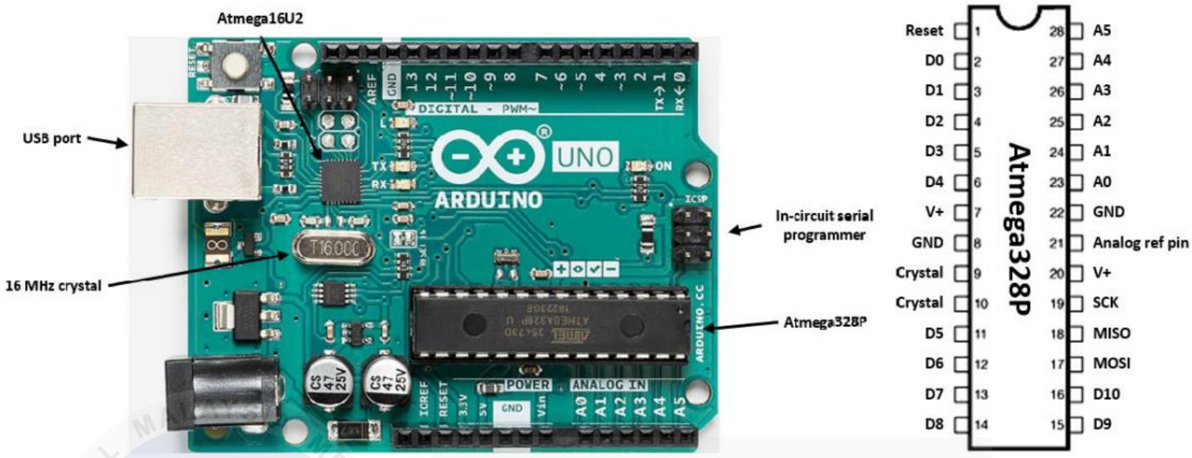

Figure 2.12 Arduino UNO R3 and Atmega328P pin out[60].

One of the primary advantages of the Arduino Uno is its ease of use, the board is designed to be accessible for beginners, with a straightforward setup process and a user-friendly programming environment. Recently, with the rise of Arduino devices, the Atmega328P microcontroller is gaining popularity for its user-friendly design and versatility. This small chip is now a common choice for research projects, both personal and industrial.

The strong community support surrounding the Arduino Uno is another key advantage. A large and active community of users and developers continuously shares resources, tutorials, and libraries, which significantly enhances the learning curve and project development process. Another advantage of the Arduino Uno is its cost-effectiveness. It is a relatively affordable option compared to other microcontroller platforms, making it accessible to students and small-scale developers, this affordability factor contributes to its popularity and widespread usage in various projects and applications[30].

Despite its many advantages, the Arduino Uno do have some notable disadvantages that need to be taken into consideration. One of the primary disadvantages of the Arduino Uno is its limited processing power, the ATmega328P microcontroller on the Arduino Uno operates at a frequency of 16 MHz and this speed is suitable for simple tasks, it may not be sufficient for more demanding applications that require higher processing capabilities. Power inefficiency is indeed a concern with the Arduino Uno. It is not specifically designed for low-power consumption, which can be a drawback for applications or projects that rely on battery power or require energy efficiency, this limitation should be taken into consideration when choosing the appropriate microcontroller for such scenarios. Another disadvantage is the lack of advanced features. It does not support functionalities like multi-threading, high-resolution analog-to-digital conversion, or high-speed communication protocols, which are available in more advanced microcontroller platforms, this limitation should be considered when working on projects that require these advanced capabilities[38].

2.4.2 Raspberry pi

The Raspberry Pi is a compact and cost-effective single-board computer specifically designed to promote computer science education and facilitate hobbyist projects. It features a processor, memory, and various input/output options, including USB ports, HDMI, and GPIO pins. These capabilities allow for seamless integration with a wide range of peripherals and accessories. Operating on a Linux-based operating system, typically Raspberry Pi OS, it supports multiple programming languages like Python and C++. This enables users to engage in tasks such as web browsing, programming, multimedia playback, and even electronic project development. Figure 2.13 shows the ports that the Raspberry Pi offers[32].

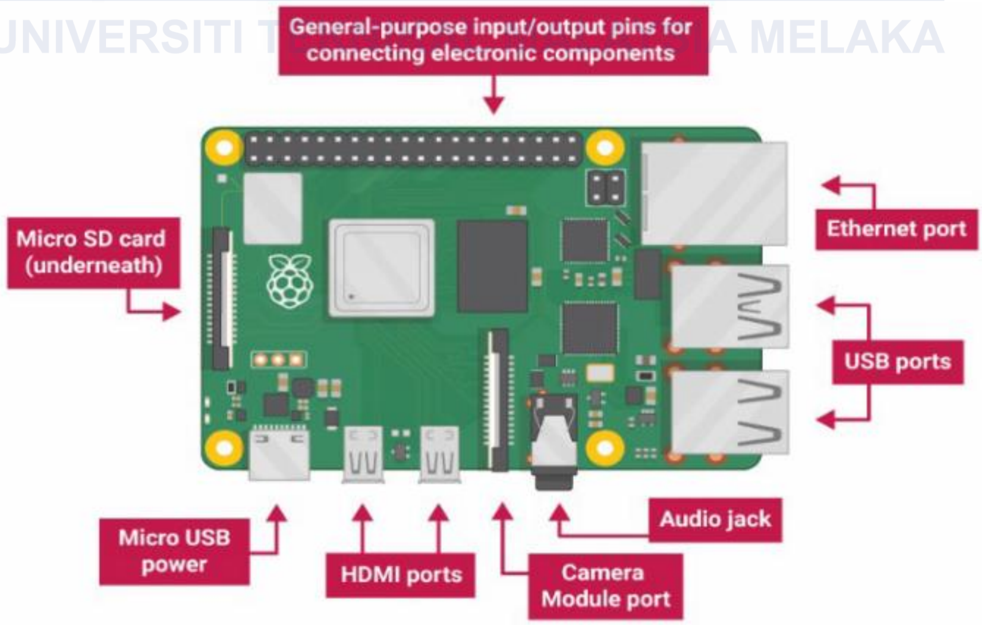

Figure 2.13 Ports that the Raspberry Pi offers[32].

One of the main benefits of the Raspberry Pi is its impressive processing power. With its multi-core ARM processor, the Raspberry Pi is capable of handling complex computations and multitasking, surpassing the capabilities of simpler microcontroller boards, this enhanced processing capability opens up a world of possibilities for users, allowing them to tackle more demanding projects and applications that require robust computational power[32].

One of the primary advantages of the Raspberry Pi is versatility, it supports a wide range of operating systems, including various Linux distributions, making it highly adaptable for diverse projects like home automation, web servers, and media centers, this flexibility allows users to tailor the Raspberry Pi to their specific needs and utilize it for a multitude of professional applications. Another significant advantage of the Raspberry Pi is its affordability, despite its impressive features and capabilities, the Raspberry Pi remains relatively inexpensive, this makes it accessible to a wide range of individuals, including students, hobbyists, and professionals[31]. The Raspberry Pi benefits greatly from its extensive community support, which is a major advantage, there is a large and active global community that constantly shares valuable resources, tutorials, and libraries. This collaborative environment significantly enhances the learning curve and project development process for users[31].

While The Raspberry Pi offers several advantages, the Raspberry Pi do have some notable disadvantages that need to be taken into consideration. One of the challenges faced by the Raspberry Pi is limited RAM capacity, even the latest models of the Raspberry Pi offer a maximum of 8GB of RAM, which can be limiting for memory-intensive tasks, this restriction can pose challenges when dealing with applications or projects that require a significant amount of memory to operate efficiently[32]. Storage limitations are also a concern. The Raspberry Pi typically uses microSD cards for storage, which can be slower and less reliable compared to solid-state drives (SSDs) or hard disk drives (HDDs), this can impact the performance of applications that require fast read/write speeds or substantial storage capacity. While the Raspberry Pi is impressive in terms of its size and cost, it does have a drawback when it comes to processing power compared to full-fledged desktop computers. Although the Raspberry Pi is quite powerful for its size, it may struggle with high-end applications like complex simulations, video editing, and heavy multitasking, these resource-intensive tasks often require the capabilities of more powerful desktop computers to handle them efficiently[32].

2.4.3 ESP 32

The ESP32 is a powerful, low-cost microcontroller with integrated Wi-Fi and Bluetooth capabilities, developed by Espressif Systems. It features a dual-core processor, various input/output pins, and a wide range of peripherals, making it ideal for IoT applications. The ESP32 operates by running code written in languages such as C or Python, typically uploaded via the Arduino IDE or Espressif's own development tools. Once programmed, it can connect to Wi-Fi networks, interact with sensors, and control devices, enabling users to create smart, connected projects such as home automation systems, wearable technology, and wireless sensors. Its combination of connectivity and processing power makes it a versatile and popular choice for developers. Figure 2.14 shows the port that the ESP32 offers.

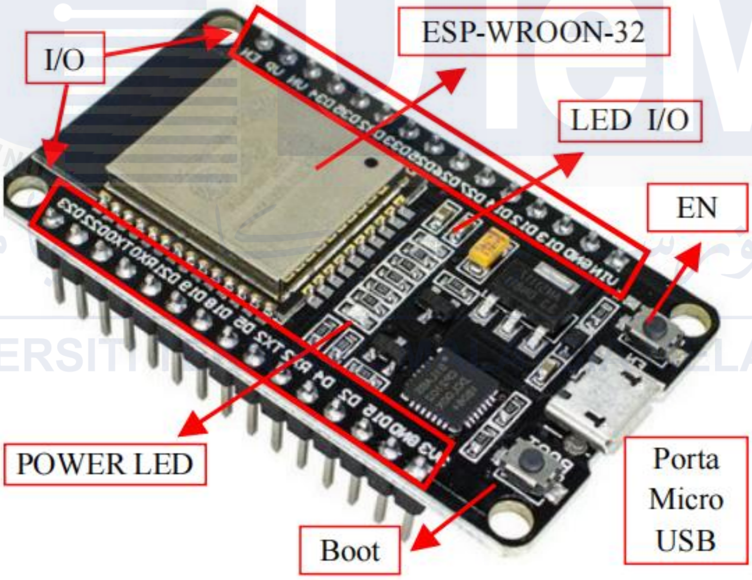

Figure 2.14 Port that the ESP32 offer[64].

The ports on the ESP32 as doorways that let it talk to other devices. One type of port is called GPIO, which can connect buttons, sensors, or other electronic stuff. Then there are UART ports, which are like doors for talking to devices using serial communication, like GPS or Bluetooth modules. The ESP32 also has I2C and SPI ports, which are like doors for connecting to displays or sensors[64].

One of the significant advantages of the ESP32 is its dual-core processor. Unlike many other microcontrollers, the ESP32 is equipped with two CPU cores, allowing it to effectively handle multiple tasks concurrently, this dual-core architecture greatly enhances multitasking capabilities and overall performance, making it well-suited for applications that demand real-time responsiveness, with the ESP32, users can efficiently manage and execute multiple tasks simultaneously, resulting in improved efficiency and performance in their projects. Another major advantage of the ESP32 is its low power consumption, despite its impressive capabilities, the ESP32 is designed to operate efficiently in low-power modes, making it a great choice for applications that are battery-powered or require energy efficiency. The ESP32 provides a wide range of peripheral interfaces, such as ADCs, DACs, GPIOs, and PWM channels. These interfaces offer developers extensive hardware capabilities to connect and interact with external components. This allows for the implementation of intricate control systems, audio processing, and analog sensing applications. The ESP32 is well-suited for IoT applications, which is a significant advantage, with its built-in Wi-Fi and Bluetooth capabilities, along with its low power consumption and extensive connectivity options, the ESP32 is an excellent platform for developing IoT devices and systems, its integrated features make it convenient for connecting and communicating with other devices, enabling seamless integration into IoT networks[39].

While the ESP32 microcontroller offers numerous advantages, it also comes with certain disadvantages. Some users may find complex programming environments to be a drawback, although the ESP32 supports multiple programming languages and development frameworks, setting up the development environment and configuring the toolchain can be challenging, especially for beginners. One notable drawback is the relatively limited availability of development tools and resources compared to more established microcontroller platforms. While the ESP32 has gained popularity in recent years, it may not have the same extensive support and documentation as other platforms like Arduino, this can make it slightly more challenging to find specific resources or troubleshooting guidance for ESP32-based projects[33].

2.4.4 Esp 8266

The ESP8266 is a highly integrated Wi-Fi microcontroller system on small chip developed by Espressif Systems. It is widely used for IoT applications due to its low cost, low power consumption, and built-in Wi-Fi connectivity. The ESP8266 features a single-core processor, on-board memory, and various input/output pins, allowing it to interface with sensors, actuators, and other electronic components. It operates by executing code written in languages like C or Lua, typically uploaded using the Arduino IDE or Espressif's own development tools. Once programmed, it can connect to Wi-Fi networks, send, and receive data over the internet, and interact with other devices, the ESP8266 can enabling a wide range of IoT projects such as home automation, smart devices, and remote monitoring systems. Figure 2.15 shows the port that the ESP8266 offer.

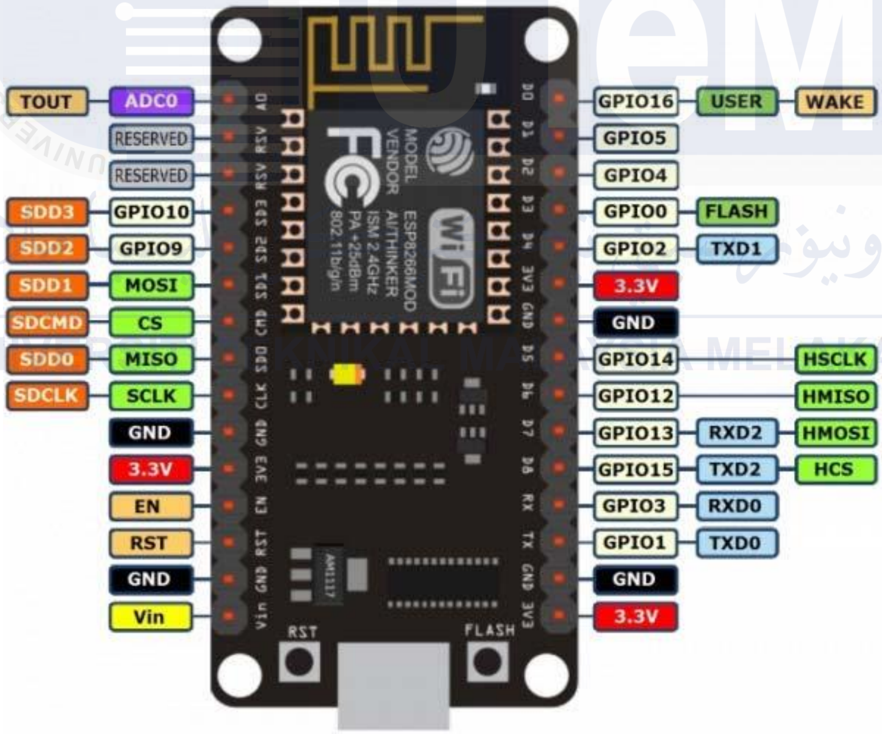

Figure 2.15 Port that the ESP8266 offer[57].

The ESP8266 has different ports that act like gateways for communication with other devices. These ports allow the ESP8266 to connect and interact with different components. One of the common ports is called GPIO, which is like a door that you can use to connect buttons, sensors, or other electronic gadgets. Another port is UART, which is like a door specifically made for serial communication. It helps the ESP8266 connect with devices like GPS modules or Bluetooth modules[35].

The ESP8266 microcontroller, widely used in IoT applications, is known for its built-in Wi-Fi capabilities, cost-effectiveness, and versatility. It can connect to wireless networks without extra modules, function as a standalone device, and be programmed using the Arduino IDE, which supports Windows, macOS, and Linux. The ESP8266 supports multiple architectures (AVR, ARM, Tensilica), offering flexibility for various projects. Its strong community provides resources like tutorials, libraries, and forums. Ideal for IoT projects such as smart home devices, environmental monitoring, and industrial automation, the ESP8266 excels in real-time data collection, processing, and transmission[36].

The ESP8266 microcontroller has notable drawbacks despite its advantages. Its single-core 160 MHz processor limits its suitability for demanding applications, and its limited GPIO pins restrict connectivity with multiple sensors and actuators. The lack of advanced security features, such as hardware encryption and secure boot, poses risks in IoT applications. Additionally, it struggles with complex networking tasks, including handling multiple connections and large data loads, which can lead to performance issues or instability[40].

2.5 Previous researches on waste cleaner using solar power charging system.

Many related research papers have been done in order to complete this project. The first research paper in the list is the projects that are researched and build by Manasa M et al., 2021 presents smart vacuum cleaner [41]. The method in this project is equipping an RC car with an ultrasonic sensor to detect and avoid obstacles while cleaning using Arduino Uno. The objective of this project is to develop an autonomous vacuum cleaner to clean environments with minimal human intervention. The application of this project aims to build a smart vacuum cleaner. Figures 2.16, 2.17, and 2.18 show the RC car, vacuum cleaner, and block diagram.

Figure 2.16 RC car [41].

Figure 2.17 Vacuum cleaner [41].

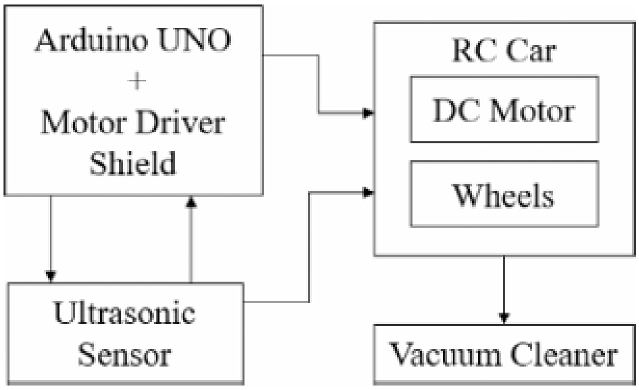

Figure 2.18 Block diagram [41].

The second research in the list is from a Department of Mechanical Engineering, Kongu Engineering College, India by A. Abubakkar et al., 2022 presents design and fabrication of mobile app-controlled floor sweeper[42]. The accumulation of dust and scrap in the floors of workshops and warehouses creates untidiness and many occupational hazards. To have a dust free and safe working environment inside the workshop, it is necessary to sweep and clean them periodically. Mostly the cleaning is done using hand sweepers, ride on sweepers and walk behind type sweepers. The objective of this project is to automate floor cleaning in workshops and warehouses to minimize human effort. This project method is a combination of a cylindrical brush for main cleaning and two side brushes to reach corners and edges using Arduino Mega. Figures 2.19, 2.20, and 2.21 show the 3D model of the floor cleaning machine, block diagram circuit connection, and screenshot of the mobile apps.

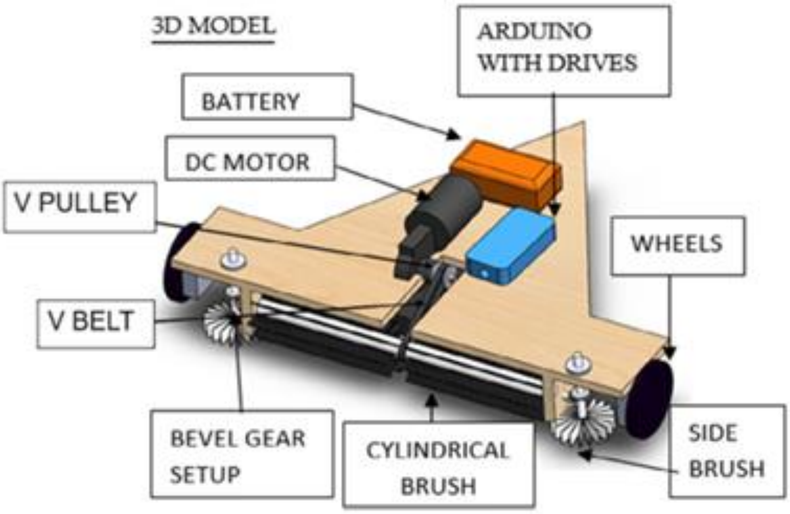

Figure 2.19 3D model of the floor cleaning machine [42].

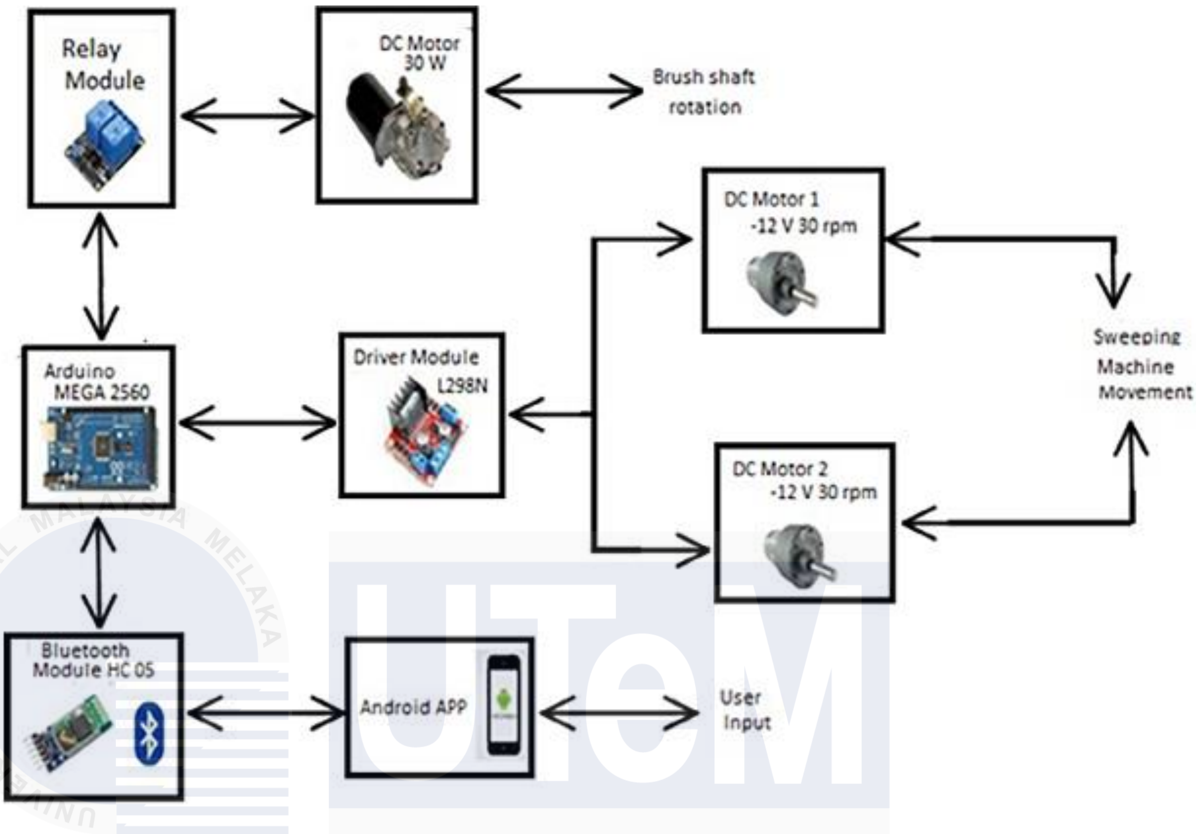

Figure 2.20 Block diagram circuit connection [42].

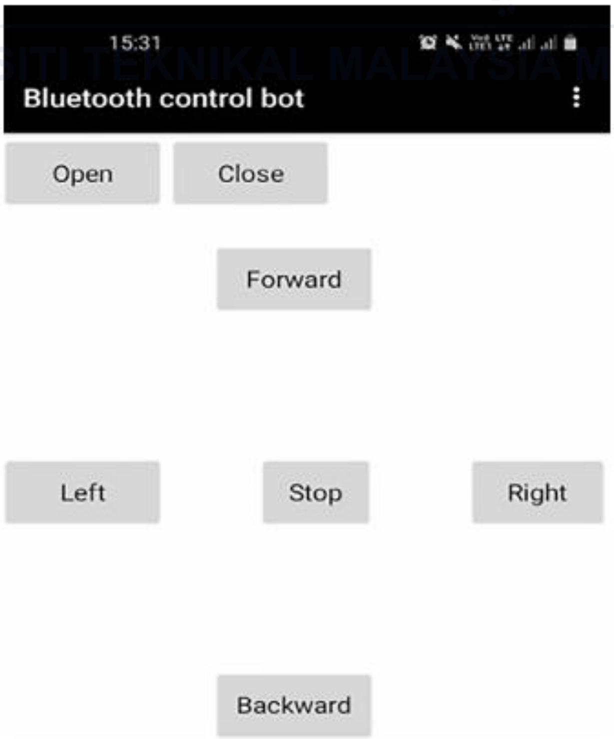

Figure 2.21 Screenshot of the mobile apps [42].

Further in the list is research from Ladoke Akintola University of Technology, Nigeria by T. B. Asafa et al., 2018 presents development of a vacuum cleaner robot[21] and their project is development of a vacuum cleaner robot with a disk-shaped robot with ultrasonic sensors for obstacle detection and navigation using Arduino Uno. The developed robot is disk shaped, equipped with vacuuming and cleaning technology and controlled by Arduino mega microcontroller. It sucks dirt via a retractable dustbin on top of which a cooling fan is mounted, and two sweepers each driven by a 3VDC motor. The robot navigates via two motor shield controlled rear wheels and a front caster wheel which also governs its turning. Four ultrasonic sensors, placed at 90 degrees apart, detect obstacles and subsequently help the robot navigate. The robot is powered by 3 batteries (28.8VDC), rechargeable via an embedded AC-DC adapter. It is 12 cm wide and 9cm tall making it easy for maneuvering its environment.

Because of the lightweight battery, cardboard based dustbin and small blower used, its weight is about 1.5 kg. The total current consumed is 1102mA. When fully charged, a 2200mAh-capacity battery works continuously for two hours and cleans the floor efficiently[21]. The objective is to develop a compact and efficient robot vacuum cleaner for everyday use in homes and offices. Figure 2.22, 2.23 show prototype vacuum cleaner robot and result before and after cleaning process.

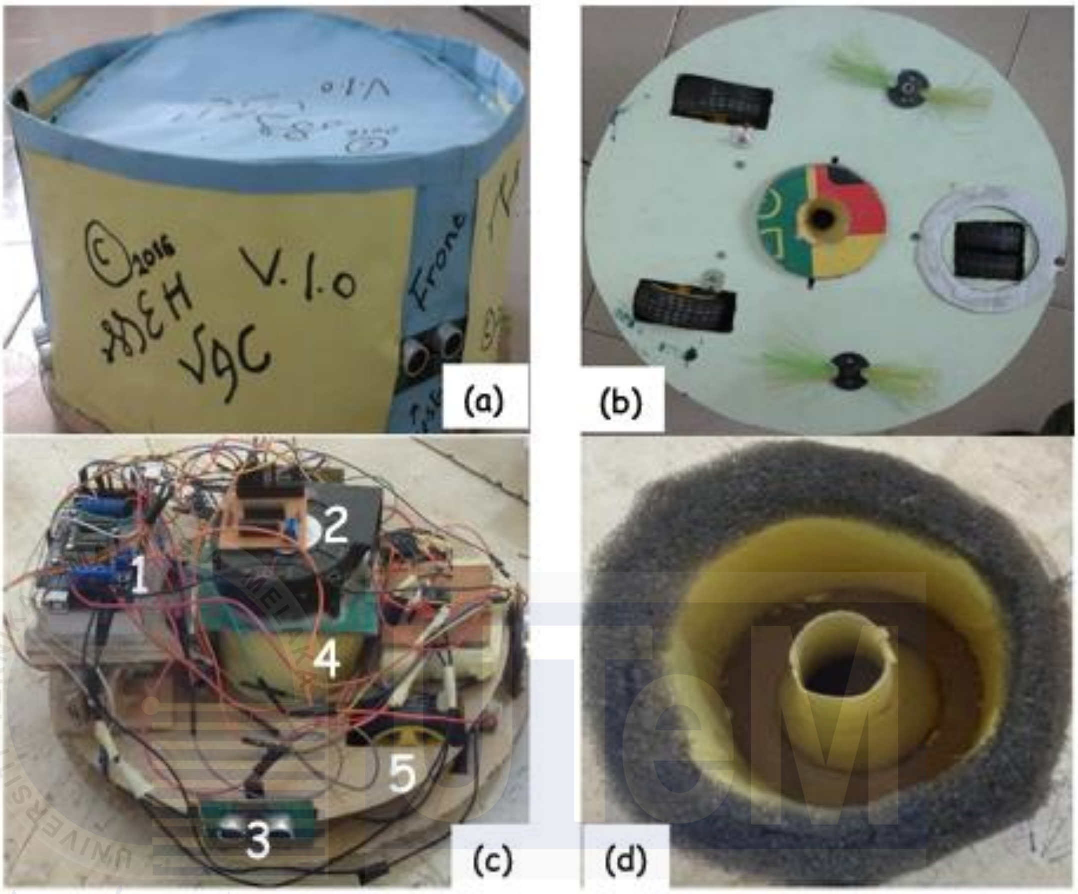

Figure 2.22 Prototype vacuum cleaner robot [21].

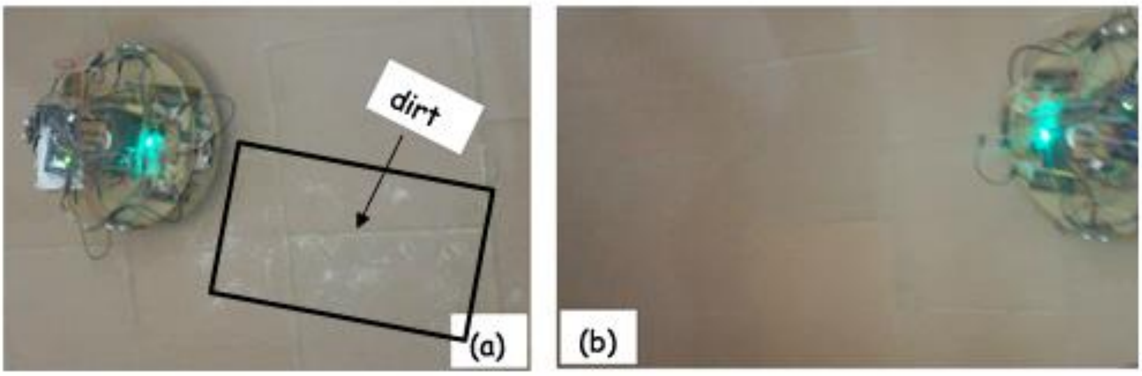

Figure 2.23 Result before and after cleaning [21].

The next research list continues with the research from a Heriot-Watt University, United Kingdom by Nathan Western et al., 2021 presents design a train cleaning robot for the train carriage interior[43]. The analysis informs the development of three robot designs.

These designs are assessed in their appropriateness for development against a baseline design that uses readily available parts. Among the three designs developed, one uses vacuum powered arm similar to the type utilized in manufacturing plants, one is based on the dustpan and brush used in domestic cleaning, and one is based on a conveyor belt. These designs are assigned a percentage suitability for implementation in the automated train carriage cleaning system[43]. The method of this project is a conveyor belt system to collect and remove waste from the train environment and the target application is at a train carriage interior. Figure 2.24, 2.25, 2.26 shows the vacuum manipulator design, the design with the split scoop manipulator, and the conveyor and box design.

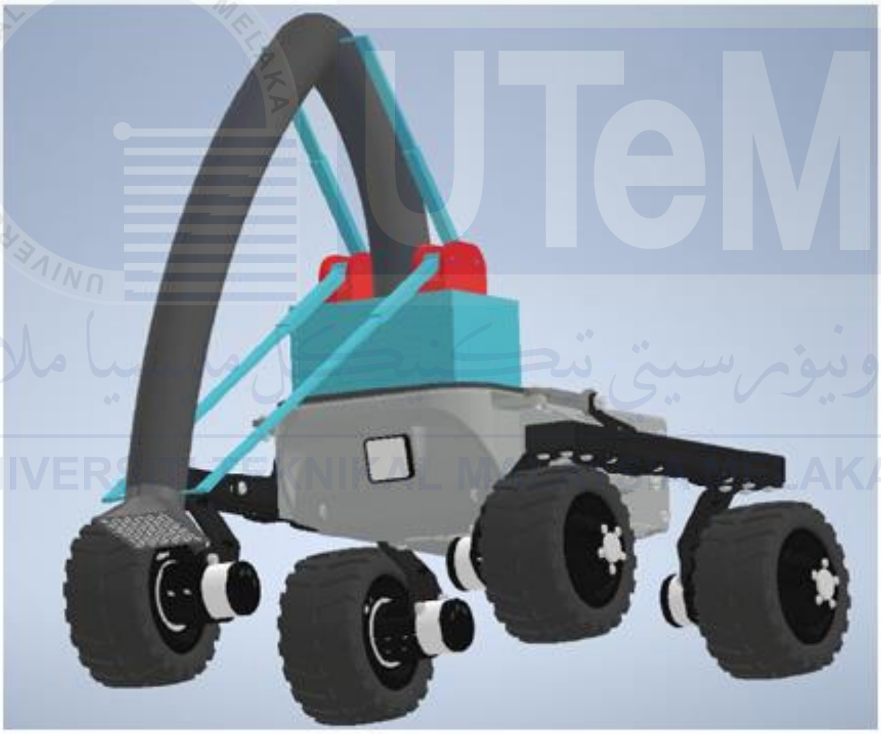

Figure 2.24 The vacuum manipulator design [43].

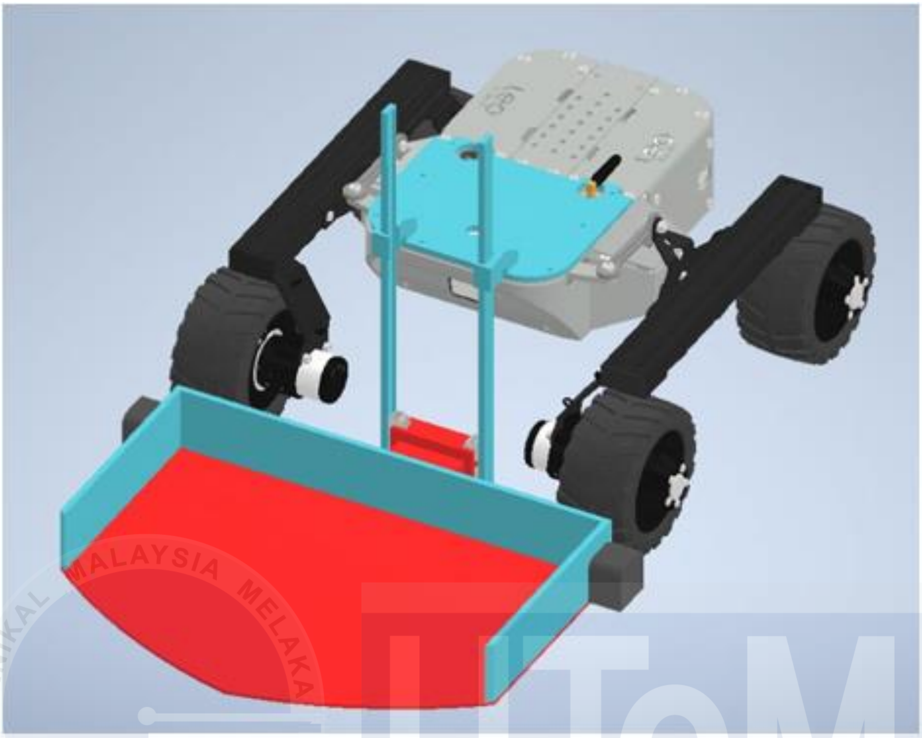

Figure 2.25 The design with the split scoop manipulator [43].

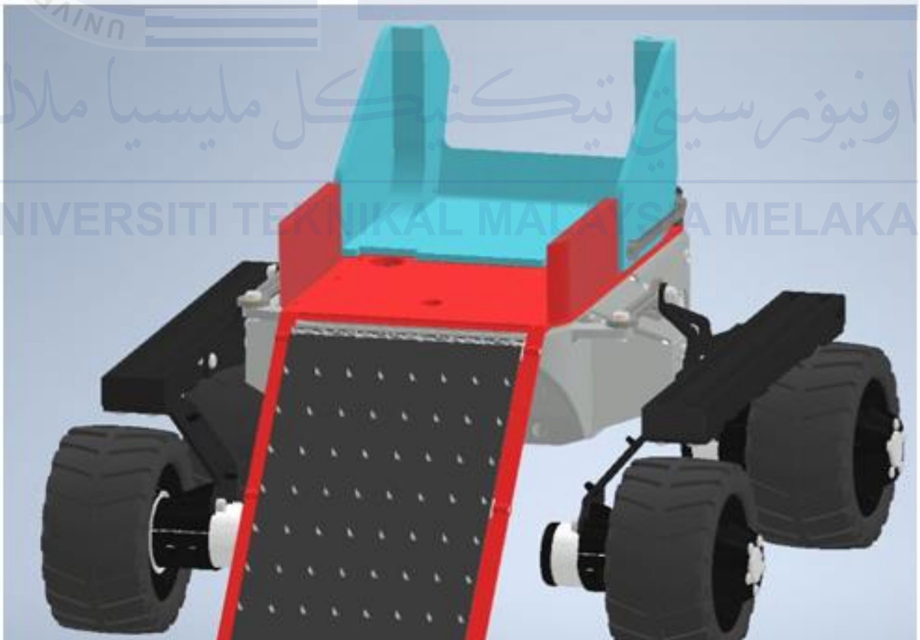

Figure 2.26 The conveyor and box design [43].

The last research paper in the list is from Jawaharlal Nehru Technological University Anantapur, India by K. Kalyani Radha et al., presents fabrication of solar robotic vacuum cleaner[5]. The main objective of this project is to develop a solar-powered vacuum cleaner to reduce reliance on non-renewable energy sources and human labor for floor cleaning. The method of this project is to convert sunlight into electricity that powers the vacuum cleaner using solar panel and the whole project is controlled by Arduino uno. A fabrication of solar robotic vacuum cleaner consists of solar-powered outdoor vacuum cleaner with a dc motor-driven suction pump. A receptacle to contain the litter will be attached to the pump's exit. The battery that is set to supply power to the dc motor will be recharged by the solar panels placed above the apparatus. In challenging circumstances, it is possible to utilize the power to charge battery[5]. Figures 2.27 and 2.28 show the model of solar robotic vacuum cleaner and component of solar robotic vacuum cleaner.

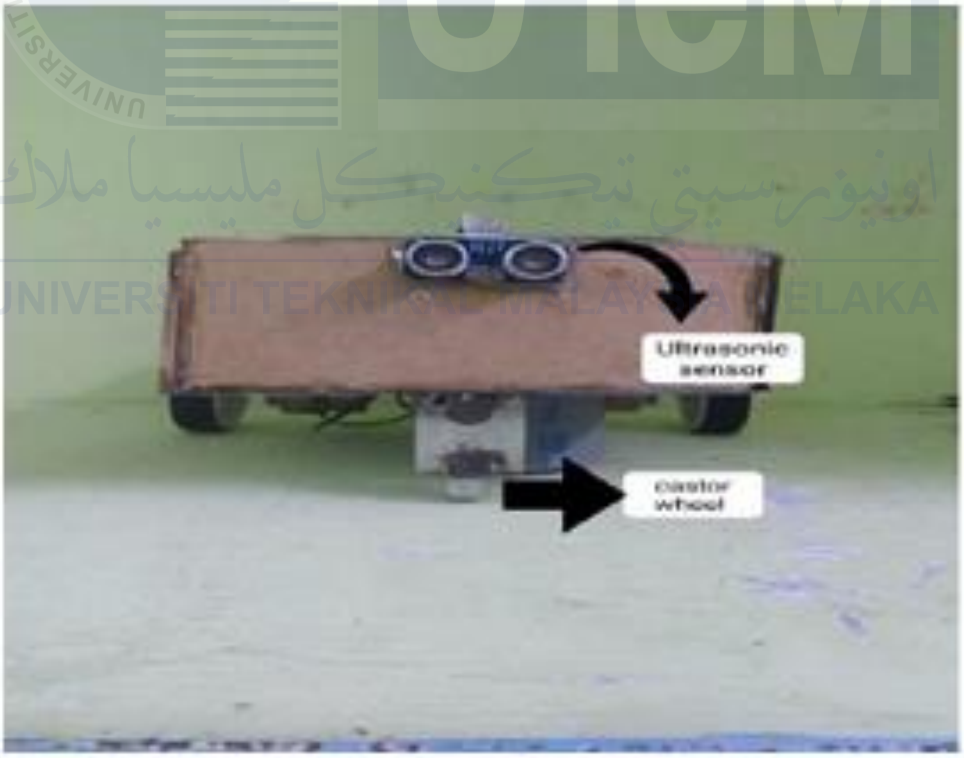

Figure 2.27 Model of solar robotic vacuum cleaner [5].

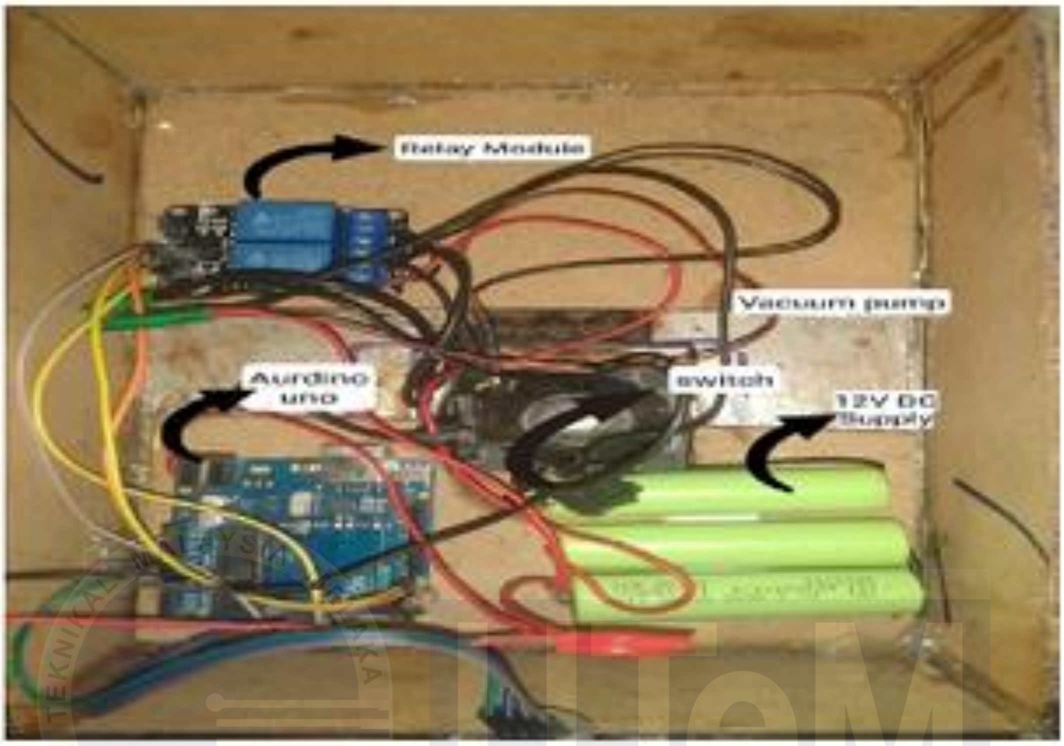

Figure 2.28 Component of solar robotic vacuum cleaner [5].

2.6 Summary of previous researches on underwater waste cleaner for various method applications.

The table shows comparison between previous journals or research paper in terms of method and application. Table 2.1, 2.2, 2.3, 2.4, and 2.5 shows comparison between previous journals.

Table 2.1 Previous research on underwater Robot.

No	Author	Application	Elements	Method
1	[44]	Underwater ship hull	Design and develop a negative-pressure adsorptive underwater climbing robot that can effectively climb and clean vertical ship hulls underwater.	Bernoulli negative-pressure generation mechanism.
2	[45]	Underwater ship hull	Ensure accurate trajectory tracking for the underwater cleaning vehicle, even in the presence of	A model-parameter-free nonsingular fixed-

			system uncertainties, cavitation water, tether force, and other unknown external disturbances.	time sliding mode control.
3	[46]	Underwater ship hull	Develop a flexible wheel-leg composite moving mechanism for ship hull cleaning robots.	Relation equations of flip angle, pitching angle, turning angle, and hull curvature radius.
4	[47]	Underwater ship hull	Develop an algorithm for the rapid and accurate identification of biofouling in underwater images.	Filter-Guided Inverse Dark Channel Inversion Exposure Compensation (FIDCE) algorithm.
5	[20]	Underwater ship hull	Develop a solution for effectively cleaning ship hulls, overcoming the limitations of existing technologies.	Utilization of six thrusters and two crawler belts to drive the robot.
6	[19]	Underwater cleaning robots	Enhance the capabilities of underwater cleaning robots by implementing a deep-learning-based biofouling recognition algorithm and a computer-vision-based boundary tracking method.	Fast-SCNN network model accelerated by TensorRT.
7	[48]	Underwater inspection robot	Detect and assess underwater structures is crucial for maintaining their safety.	Parameters to extract the corresponding adhesion force, torque, and energy efficiency ratio.
8	[18]	Underwater hull	Propose a novel design for an underwater hull cleaning robot that	SolidWorks.

		cleaning robot	can efficiently and non-destructively clean hull surfaces, reducing transportation costs.	
9	[49]	Underwater Robot	Develop an automatic navigation system for underwater piles using a modified ROV.	Prototyped automatic navigation software.

Table 2.2 Previous research on Solar charging system for various application.

No	Author	Application	Elements	Method
1	[50]	Electrical vehicle	Design a solar-powered EV charging station that utilizes a 400V DC bus voltage and is powered by both a PV system and a utility grid.	Implementation of an Energy Management Algorithm (EMA).
2	[51]	EV charging	Investigate the feasibility of solar energy for residential buildings with EV charging in the Vistara Residential Enclave at Madurai.	HOMER software.
3	[52]	Smart EV charging	Assess the optimal urban-scale energy matching potentials in a net-zero energy city powered by wind and solar energy.	Quadratic programming.
4	[1]	Suction robot	Design and test a new solar panel cleaning robot, MFv01.	Development of the MFv01 robot.
5	[53]	Air conditioning	Develop and test a microclimate solar cooling system (SPVTEAC) for localized air conditioning.	Building and testing an SPVTEAC prototype.
6	[54]	Swarm robot	Explore the potential of using swarm robotics inspired by ant or	Literature survey.

			bee colonies for material handling tasks related to solar energy.	
7	[14]	Grasscutter robot	Design a solar-powered, remote-controlled grasscutter for use in public areas like parks and hotels.	Arduino UNO
8	[3]	Mobile Metal Detector Robot	Develop a remotely operated, solar-powered metal detector robot for landmine detection.	Building a robot
9	[55]	Drone	Develop a sustainable solution for integrating UAV (drone) operations in smart cities.	Integrated multi-objective charging infrastructure coverage optimization model.

Table 2.3 Previous research on cleaning robots.

No	Author	Application	Elements	Method
1	[56]	PV panels	Understand the impact of dust accumulation on the performance and efficiency of PV systems, as well as to propose effective cleaning mechanisms to restore their power generation output.	Mathematical models to understand how dust accumulation affects PV panel performance.
2	[41]	Smart vacuum cleaner	Develop an autonomous vacuum cleaner to clean environments with minimal human intervention.	Arduino Uno.
3	[38]	Glass wall	Provide a multi-functional cleaning solution that eliminates the need for human intervention in dangerous tasks.	A combination of an electric ducted fan (EDF) and support ropes.

4	[42]	Floor sweeper	Automate floor cleaning in workshops and warehouses to minimize human effort.	Arduino Mega.
5	[57]	Modular window	Improve the window-cleaning capabilities of robots on building facades.	A modular robot design called Mantis.
6	[21]	Vacuum cleaner robot	Develop a compact and efficient robot vacuum cleaner for everyday use in homes and offices.	Arduino Uno.
7	[43]	Train carriage interior	Design a robot platform for collecting and disposing of waste in passenger trains.	A conveyor belt system.
8	[15]	Solar panels	Review the different automatic cleaning systems designed to remove dust and improve the functionality of photovoltaic modules.	The electrostatic cleaning system.
9	[22]	Street sweeping machine	Propose a solution for the limitations of manual street sweeping by developing a solar-operated street sweeping machine.	Generate electricity that powers the sweeping mechanism.
10	[16]	Trash Sweep Medi-waste separator	Develop a more affordable robotic cleaner specifically designed for cleaning clinics.	A simpler sensor-based obstacle avoidance strategy.
11	[5]	solar robotic vacuum cleaner	Develop a solar-powered vacuum cleaner to reduce reliance on non-renewable energy sources and human labour for floor cleaning.	Arduino Uno.

Table 2.4 Previous research on cleaning robots and IoT systems.

No	Author	Application	Elements	Method
1	[42]	floor sweeper	Automate floor cleaning in workshops and warehouses to minimize human effort.	Arduino Mega.

Table 2.5 Previous research on cleaning robots and solar power.

No	Author	Application	Objective	Method
1	[22]	street sweeping machine	Propose a solution for the limitations of manual street sweeping by developing a solar-operated street sweeping machine.	Generate electricity that powers the sweeping mechanism.
2	[5]	solar robotic vacuum cleaner	Develop a solar-powered vacuum cleaner to reduce reliance on non-renewable energy sources and human labour for floor cleaning.	Arduino Uno.

2.7 Summary

The growing demand for energy and the necessity to transition to renewable sources make solar power an appealing option. Renewable energies, like solar power, provide a sustainable and environmentally friendly alternative to finite fossil fuels, which contribute to pollution. The literature review explores various renewable energy sources, including wind, hydropower, and thermal energy, each with unique advantages and challenges. Wind energy is clean but unpredictable and can destabilize the grid. Hydropower is environmentally friendly but can have significant ecological impacts. Thermal energy offers flexibility but requires large spaces and complex installation. Solar energy, harnessing sunlight through photovoltaic cells, provides a cost-effective, low-maintenance, and reliable electricity source. Despite the initial installation costs and climate dependence, solar energy's long-term benefits and alignment with sustainable development goals make it the preferred choice for developing a fish tank waste cleaner with a solar power charging system.

Waste cleaner devices can be designed for ground, water surface, or underwater operation, each presenting distinct advantages and challenges. Ground-based robots are efficient and cost-effective for cleaning large areas but have high initial costs and technical limitations in complex environments. Water surface robots effectively remove floating debris and improve environmental cleanliness but only function at water surface and less suited for small water bodies. Underwater robots, equipped with advanced sensors and navigation systems, excel in cleaning submerged waste and maintaining underwater ecosystems. Despite their higher complexity and cost, their ability to operate autonomously and efficiently in underwater environments makes them the preferred choice over ground or water surface cleaners for waste management in fish tanks and similar settings.

Microcontrollers are integrated circuits designed for specific tasks in embedded systems. The Arduino Uno is popular for its ease of use and community support but has limited processing power and energy inefficiency. The Raspberry Pi offers strong processing power and versatility but is constrained by RAM and storage. The ESP32, ideal for IoT projects, features low power consumption and a dual-core processor but has a complex programming environment. The ESP8266, with built-in Wi-Fi, affordability, and strong support, is a great choice for IoT despite its single-core processor and limited GPIO pins. For my waste cleaner robot project, I chose the ESP8266 for its cost-effectiveness and versatility.

CHAPTER 3

METHODOLOGY

3.1 Introduction

The methodology section of this study describes the systematic process used to develop and evaluate a solar-powered fish tank waste cleaner. It covers the design and construction phases, including the choice of components like the ESP8266 microcontroller for its connectivity and energy efficiency. The section also discusses the integration of solar panels for sustainable power, sensor implementation for waste detection, and the programming logic for autonomous operation. Furthermore, it outlines the testing procedures to assess the cleaner's performance under various conditions, the data collection methods, and the criteria for evaluating effectiveness and efficiency. This structured approach ensures the development process is reproducible, and the results are reliable and valid.

3.1.1 Methodology

The methodology for this project outlines a systematic approach to developing and evaluating a solar-powered fish tank waste cleaner. The process starts with designing and constructing the solar charging system, which involves selecting and assembling key components such as solar panels, a charge controller, a battery, and a voltage regulator. This system is tested to ensure its ability to reliably convert and store solar energy. After validation, the construction of the fish tank waste cleaner begins, integrating the ESP8266 microcontroller due to its superior connectivity and energy efficiency compared to alternatives like the Arduino Uno. The cleaner is equipped with sensors, including an IR sensor for obstacle detection, and a water pump, all controlled by ESP8266 for autonomous operation. The integration phase also involves installing two DC motors for mobility within the tank, with each component undergoing thorough testing to ensure functionality.

Once both the solar charging system and the waste cleaner are successfully assembled, the IoT system is set up. This involves connecting the waste cleaner to a smartphone application via Wi-Fi for remote monitoring and control, utilizing the ESP8266's built-in connectivity features. Real-time testing is conducted in an actual fish tank to observe the cleaner's performance, particularly its effectiveness in removing waste from various areas within the tank. Data collection methods include analyzing sensor data to verify the system's proper functioning and overall efficiency. This structured approach ensures that each phase of development is reproducible, and the results are reliable and valid, providing a strong foundation for sustainable aquaculture practices.

3.1.2 Flowchart of the fish tank waste cleaner using solar power charging system.

The flowchart explains the development process of a fish tank waste cleaner using a solar power charging system. It begins with the setup of the solar charging system, involving the selection and assembly of the solar panel, battery, solar charge controller, and voltage regulator. Following this, the system shows the test of the system. If the test is successful, the process moves to the assembly of the fish tank waste cleaner, which includes integrating the electronic components and sensors. This phase also includes testing the waste cleaner device to ensure proper functionality.

After both the solar charging system and the fish tank waste cleaner system have successfully passed their respective tests, the Internet of Things (IoT) system is established. This involves connecting the fish tank waste cleaner device to a smartphone application for data monitoring.

The final stage involves real-time testing in the fish tank. This includes operating the system within the fish tank and monitoring its performance, particularly its effectiveness in cleaning the waste from the water. During this stage, data testing is also conducted, which involves analyzing sensor data to verify the system's proper functioning. Figure 3.1 illustrates the overall system development flowchart for the fish tank waste cleaner using a solar power charging system.

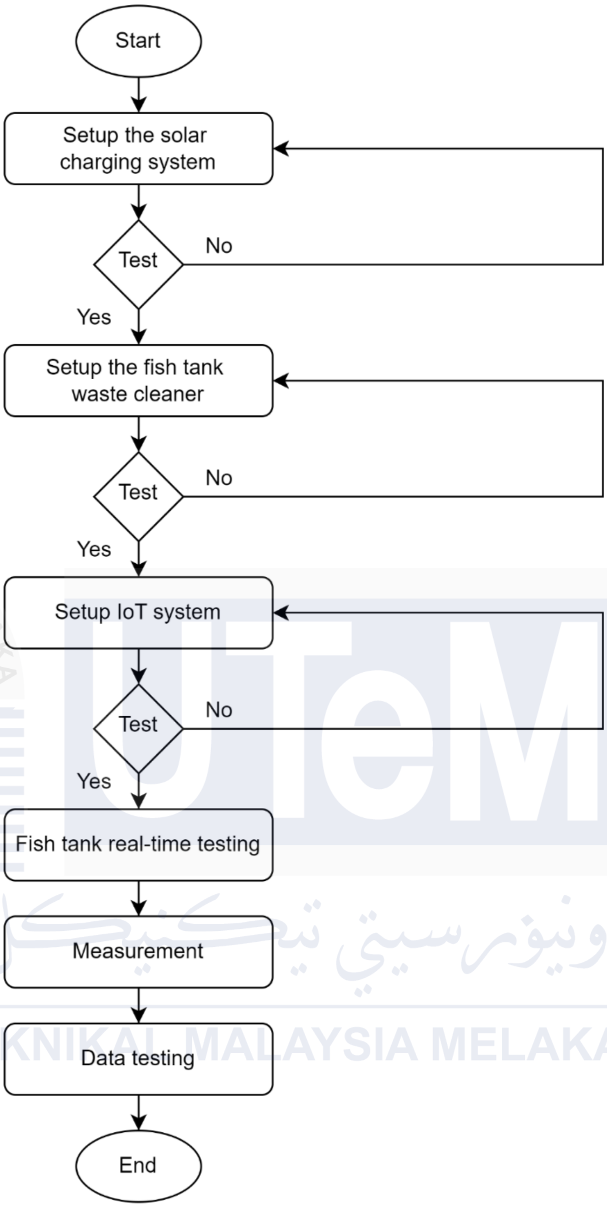

Figure 3.1 Flowchart of the fish tank waste cleaner using solar power charging system.

3.1.3 Flowchart of solar charging system.

The flowchart outlines the setup process for a solar charging system with a data collector. The initial step involves installing the solar panels, depicted as a polycrystalline photovoltaic (PV) module. Next, the solar panels are connected to a battery and a solar charge controller, followed by testing the system. If the test is successful, the process advances to setting up the data collector.

Following this, the installation of a voltage regulator to convert 12VDC to 3.6VDC is depicted. Another test is conducted after this step. If successful, the process proceeds to connect the data collector to the 3.6V battery for measurement. Alternatively, the flowchart shows using a different voltage regulator to convert the 12VDC output to 5VDC for the load at fish tank waste cleaner device. A final test is then conducted, and if successful, the data collector is connected to the 5V battery for measurement. Figure 3.2 illustrates the flowchart of the solar charging system.

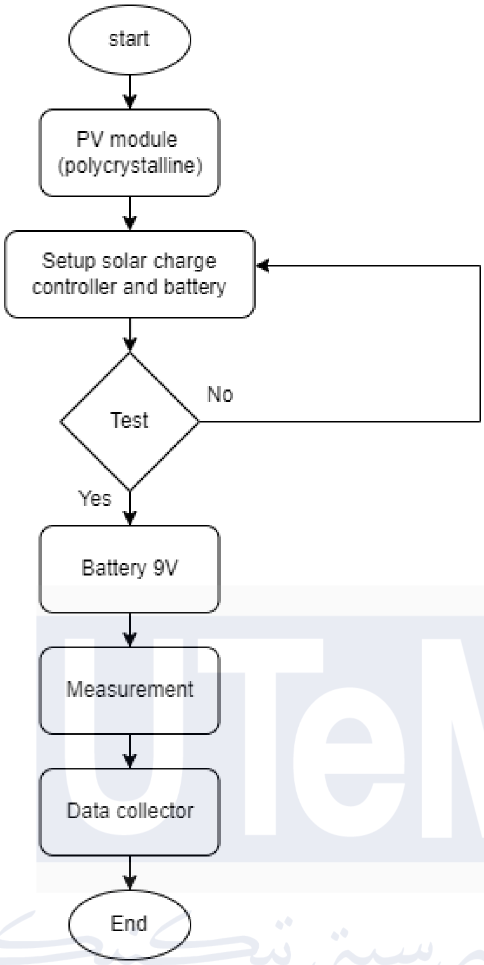

Figure 3.2 Flowchart of solar charging system.

3.1.4 Flowchart of fish tank waste cleaner.

The flowchart outlines the setup process for a fish tank waste cleaner device. The process begins with the installation of the ESP8266 microcontroller board, which will control the device. Next, the flowchart shows the setup of an infrared (IR) sensor used for obstacle detection. After setting up the IR sensor, tests are conducted to ensure both the ESP8266, and the IR sensor are functioning correctly. If either test fails, the flowchart directs you to revisit the setup step for the faulty component.

Once both the ESP8266 and IR sensor pass their tests, the next step is to set up a water pump, followed by a test to confirm its correct operation. The process continues with the setup of two DC motors connected to tires, which will enable the device to move through the tank. Each motor is tested after installation to ensure proper functionality. If all components pass their individual tests, the flowchart concludes that the setup process is complete. Figure 3.3 shows the flowchart of fish tank waste cleaner.

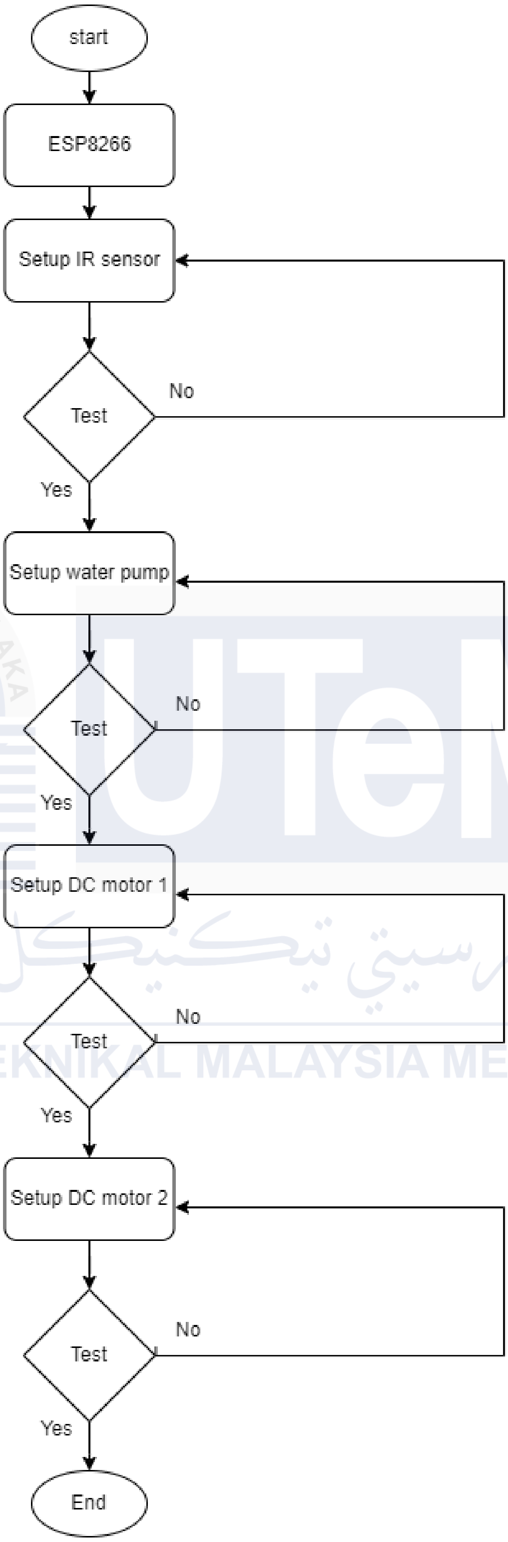

Figure 3.3 Flowchart of fish tank waste cleaner.

3.1.5 Block diagram of a fish tank waste cleaner using solar power charging system.

Figure 3.4 shows the block diagram illustrates the entire system integrated with an IoT monitoring setup. Sunlight is converted into electricity by the solar panel, and a solar charge controller regulates this electricity to safely charge the battery, preventing overcharging. The stored energy in the sealed lead-acid battery can then be used to power various devices. Central to remote management is the ESP8266 microcontroller, which connects to the internet using the Blynk app on your smartphone, allowing real-time monitoring of system performance. The system can also include an optional IR sensor to trigger actions based on obstacle detection. Additionally, a motor driver and relay module enable the control of a water pump. Figure 3.4 shows the block diagram of a fish tank waste cleaner using solar power charging system.

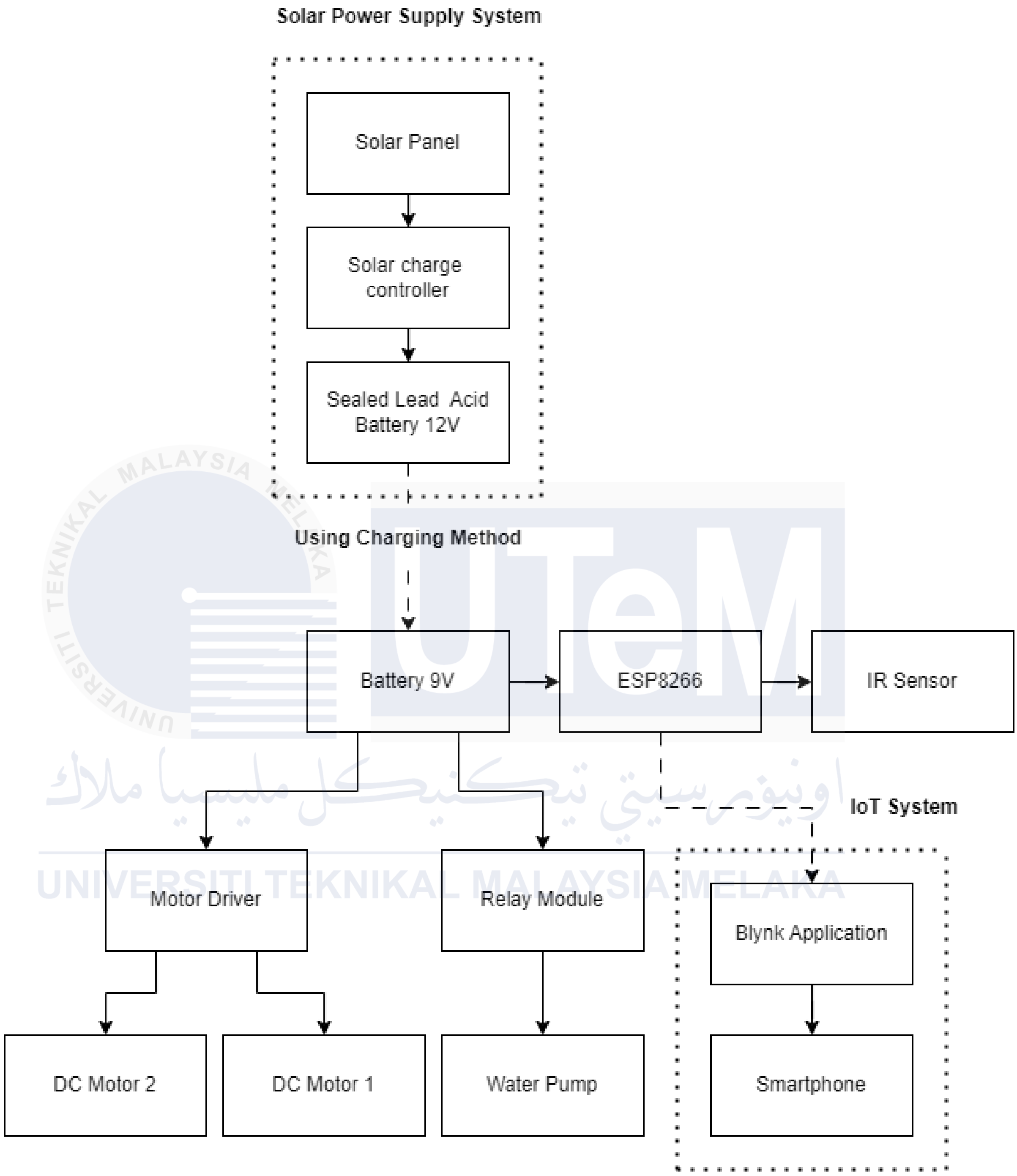

Figure 3.4 Block diagram of a fish tank waste cleaner using solar power charging system.

3.1.6 Development of the project.

The development of the fish tank waste cleaner was carried out in a structured manner, progressing through five key stages as outlined in Table 3.1. The first stage focused on the development of the solar charging system's circuitry, ensuring a sustainable and eco-friendly power source for the device. In the second stage, the fish tank waste cleaner's circuitry was designed and implemented, integrating essential components such as the ESP8266 microcontroller, water pump, motor driver, and sensors to form the core functionality of the system. The third stage involved the physical design of the cleaner, which included prototyping and optimizing the device's structure for buoyancy, mobility, and operational efficiency. In the fourth stage, an IoT system was developed to enable remote monitoring and control, allowing users to interact with the cleaner via a smartphone application. Finally, the fifth stage encompassed a comprehensive performance analysis of the device, assessing its cleaning efficiency and overall functionality under real-world conditions. Table 3.1 shows development of the project.

Table 3.1 Development of the project.

Stage 1	Development of solar charging system's circuitry
Stage 2	Development of fish tank waste cleaner's circuitry
Stage 3	Design of fish tank waste cleaner
Stage 4	Development of IoT system
Stage 5	Performance analysis on fish tank waste cleaner.

3.2 Development of solar charging system

The solar charging system utilize polycrystalline specification of maximum rated power of 10 watts, the output tolerance is 3%, meaning the actual power output can vary up to 3% above or below 10 watts. The maximum power current is 0.58 amps, and the maximum power voltage is 17.5 volts. The short circuit current is 0.63 amps, and the open circuit voltage is 21.24 volts. The above specification is presented as in **APPENDIX B**.

3.2.1 List of Solar charging Components.

The solar charging system consists of several components, each playing a crucial role in the system's operation. The total expenditure for these components is RM140.00, as outlined in the corresponding table 3.2.

Table 3.2 List of Solar charging Components.

No	Component	Quantity	Image	Price (RM)
1.	Polycrystalline Solar PV Panel	1		RM 80.00
2.	Solar charge controller (SCC)	1		RM 20.00

3.	12v Sealed Lead Acid Battery	1		RM40.00

3.2.2 Block diagram of solar power supply system.

This solar power supply system uses solar panels to generate DC electricity. The solar charge controller regulates this electricity to safely charge the battery. The battery stores the DC electricity and supplies power to the 9V battery using charging method. The ESP8266 controls the entire system and can use sensor data, such as from an IR sensor, to detect any obstacle. Figure 3.5 shows the block diagram of the solar power supply system.

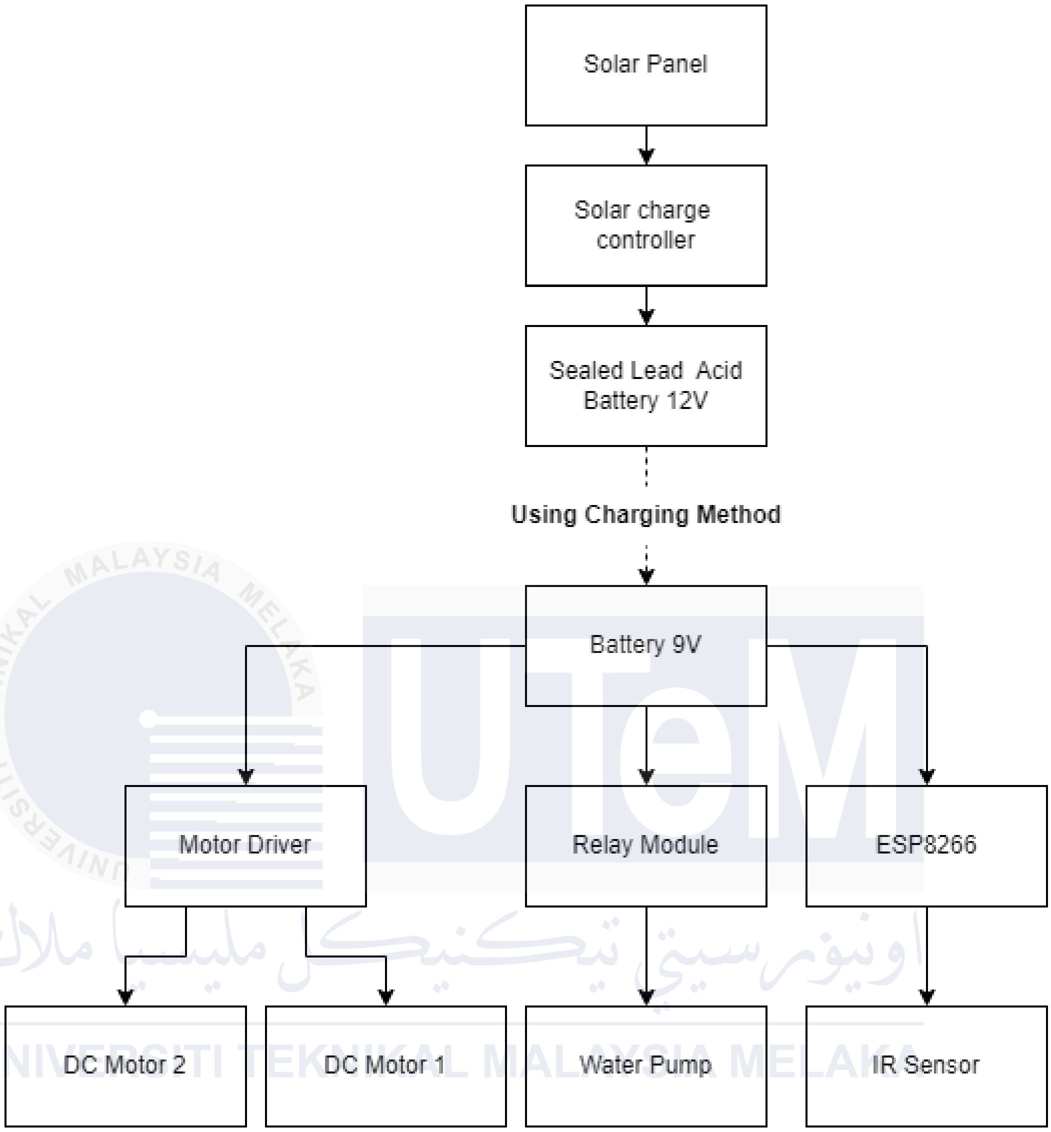

Figure 3.5 Block diagram of solar power supply system.

3.2.3 Hardware setup of solar charging system.

There are several methods to measure a solar charging system. One way is to measure the output voltage and output current of the solar panel is using a multimeter. The solar panel converts sunlight into electricity, which then flows to a solar charge controller as in Figure 3.6. The solar charge controller protects the battery from overcharging and the battery stores the electricity generated by the solar panel. Figure 3.6 shows the wiring connections of solar charging system.

Figure 3.6 Wiring of solar charging system.

The positive and negative terminals of the battery are connected to the solar charge controller. The solar PV panel is connected to the solar charge controller, and the multimeter is connected either in series with the solar PV panel to measure current or in parallel to measure voltage and the load is connected to the solar charge controller.

3.2.4 Design development of solar charging system.

The 3D design of the solar charging system was meticulously created using SolidWorks software, known for its capability to produce highly detailed and accurate 3D models. This design incorporates all essential components, including the solar charging system powered by a 12V battery, a solar PV panel, and a solar charge controller. SolidWorks facilitated precise alignment and fitting of the components, resulting in a compact and efficient design tailored to the actual dimensions of the solar PV panel. Figure 3.7, 3.8, 3.9 shows the design of solar charging system, top view 3D design of solar charging system, and side view 3D design of solar charging system.

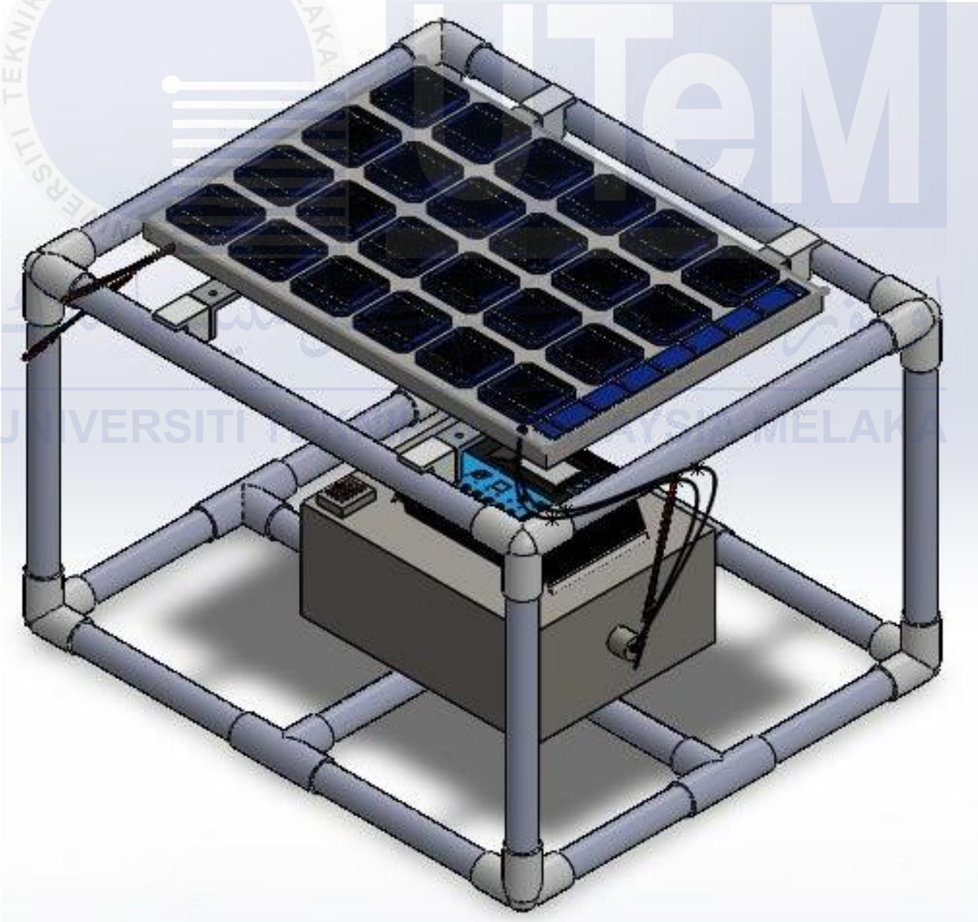

Figure 3.7 3D design of solar charging system.

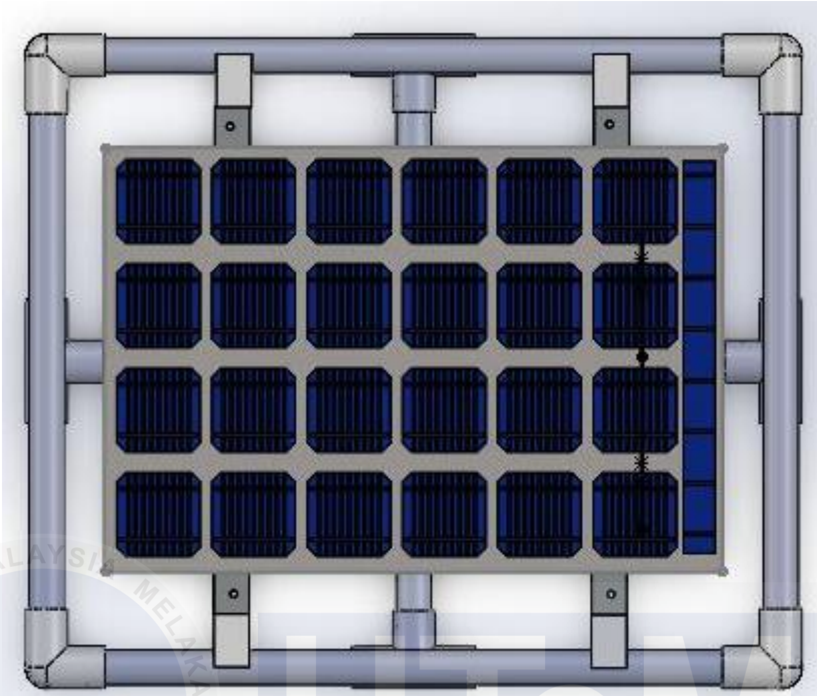

Figure 3.8 Top view 3D design of solar charging system.

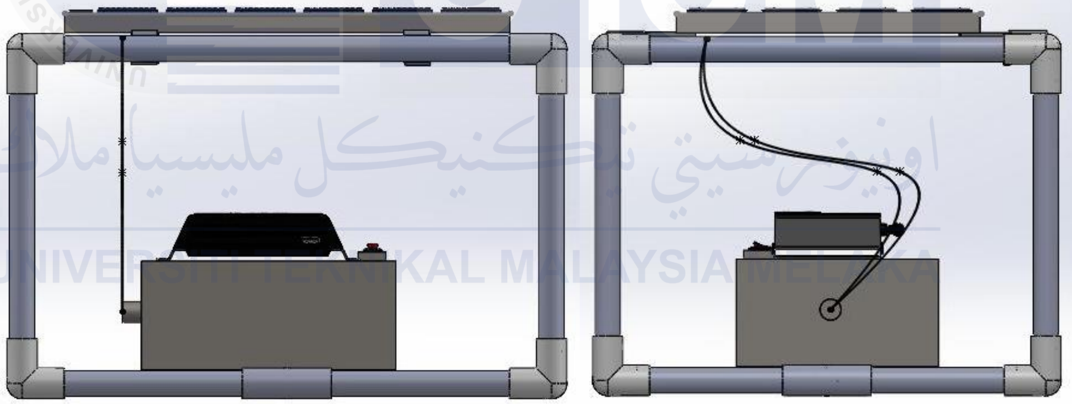

Figure 3.9 Side view 3D design of solar charging system.

3.2.5 Isometric view of solar charging system.

The isometric view of the solar charging system provides a comprehensive three-dimensional representation of the design, showcasing all key components and their spatial arrangement. Created using SolidWorks software, this view highlights the integration of the solar PV panel, 12V rechargeable battery, solar charge controller, and supporting structural elements. The dimensions of the solar PV panel are accurately represented to reflect real-world measurements, ensuring compatibility with standard solar panels. The structural framework is designed to provide stability and protection, with precise dimensions allocated for the secure mounting of the solar charge controller and junction box. Figure 3.10 show isometric view of solar charging system.

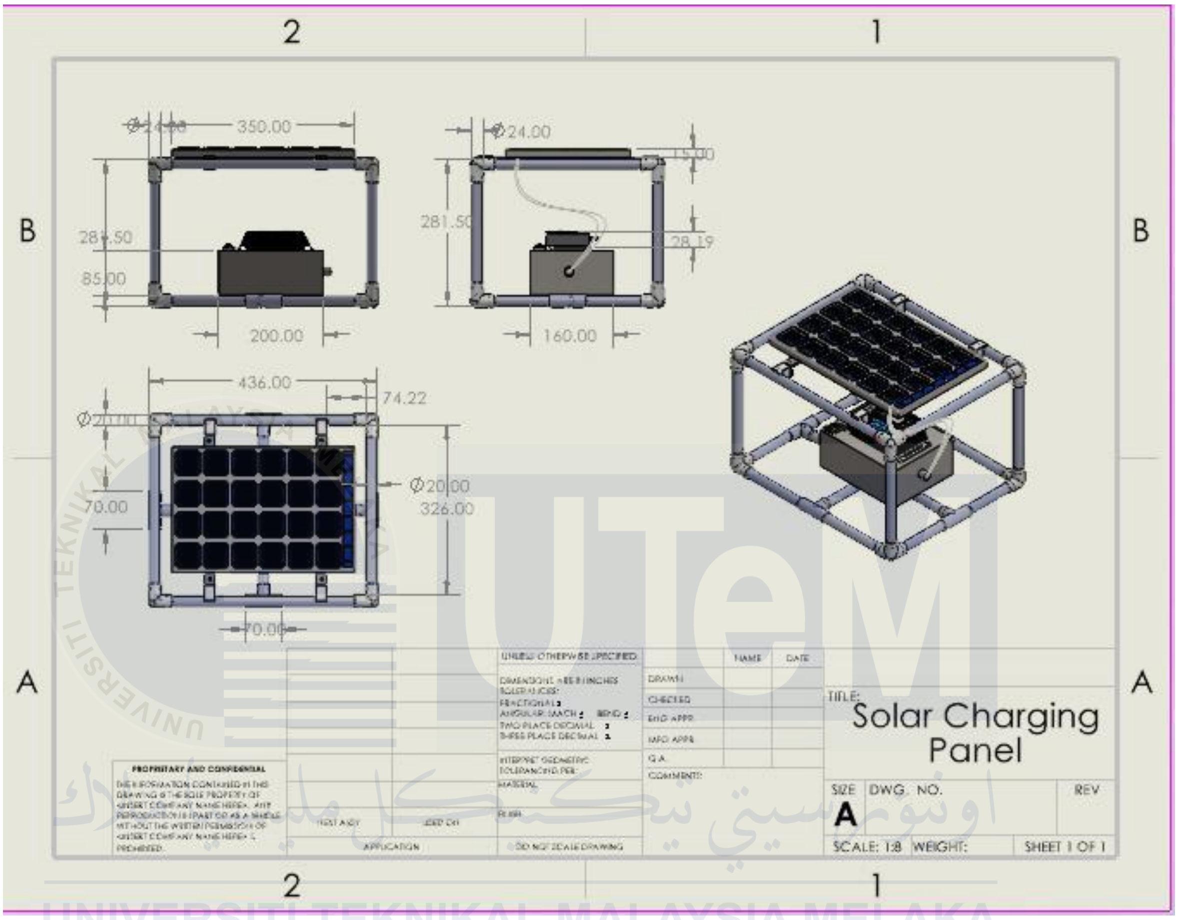

Figure 3.10 Isometric view of solar charging system.

3.2.6 Measurement of solar charging system.

The figures below illustrate the real-time wiring connections. The multimeter is used to measure the voltage and current coming from the solar PV panel. However, the measurement of solar PV panel are using voltage open circuit (Voc) and short circuit current (Isc). The multimeter range is set to 20V for voltage open circuit (Voc) measurements and 10A for short circuit current (Isc) measurements. Set the multimeter to DC voltage mode, connect the red lead to the positive terminal of the solar PV panel and the black lead to the negative terminal of the solar PV panel. Place the solar PV panel in direct sunlight and observe the voltage open circuit (Voc) and short circuit current (Isc) reading on the multimeter. Figures 3.11, 3.12, 3.13, and 3.14 show Real-time wiring connection of measurement solar charging system, the view of solar charging system, placement junction box of solar charging system, arrangement inside junction box of solar charging system.

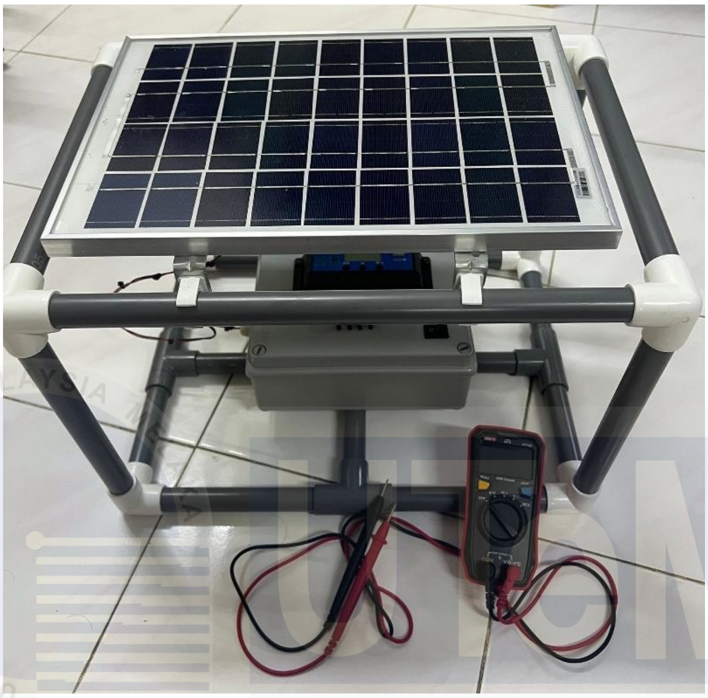

Figure 3.11 Real-time wiring connection of measurement solar charging system.

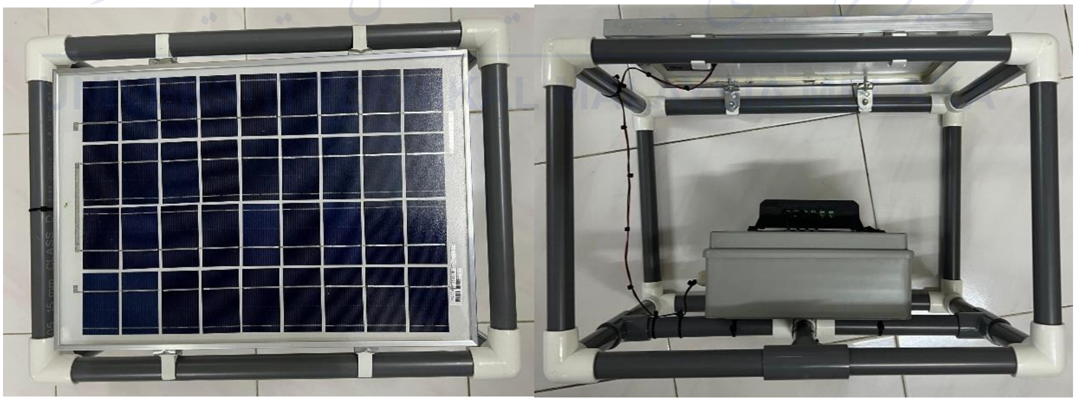

Figure 3.12 The view of solar charging system.

Figure 3.13 Placement junction box of solar charging system.

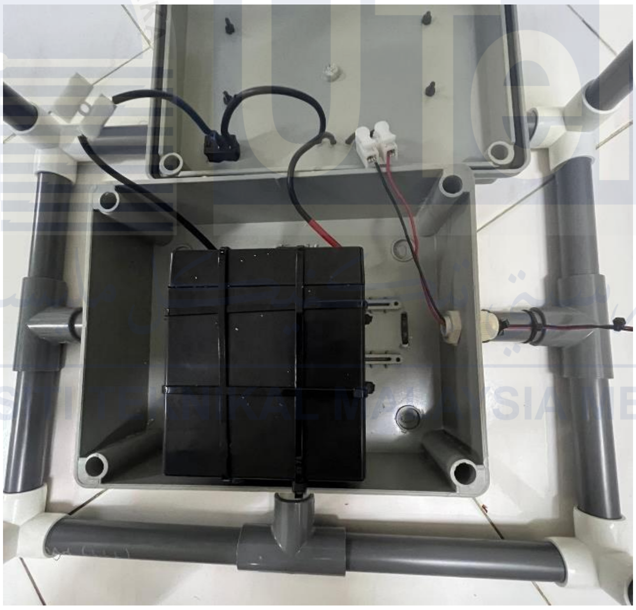

Figure 3.14 Arrangement inside junction box of solar charging system.

3.3 Development of fish tank waste cleaner's circuitry.

The fish tank waste cleaner, developed with a solar power charging system and IoT monitoring, incorporates various components for efficient and automated functionality. The ESP8266 microcontroller serves as the core processor, enabling wireless connectivity. Obstacle detection is facilitated by an IR sensor, while a DC motor, controlled by a motor driver, powers the device's movement within the tank. A DC water pump ensures water circulation and filtration, managed by a 3V relay module for switching. The device is powered by 1000mAh 9V rechargeable batteries, providing sufficient energy for seamless operation.

3.3.1 List of fish tank waste cleaner components.

The fish tank waste cleaner consists of several components, each playing a crucial role in the system's operation. The total expenditure for these components is RM88.50, as outlined in the corresponding table 3.3.

Table 3.3 List of fish tank waste cleaner components.

No	Component	Quantity	Image	Price (RM)
1.	ESP8266	1		RM 15.00

2.	IR Infrared Obstacle Avoidance Sensor	1		RM 3.00
3.	3V - 6V 130 Mini DC Motor	2		RM 3.00
4.	Motor Driver	1	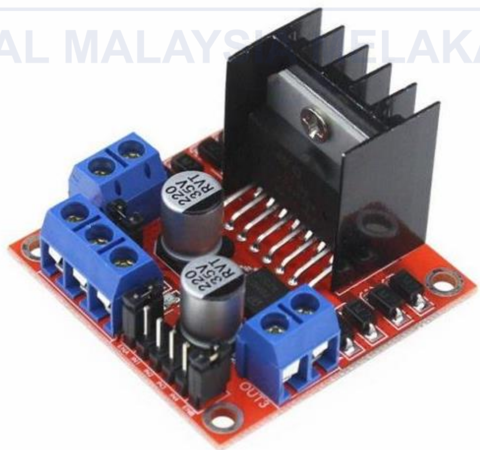	RM 7.00

5.	DC 12V Brushless Water Pump Waterproof	1		RM18.00
6.	Relay module 3V	1	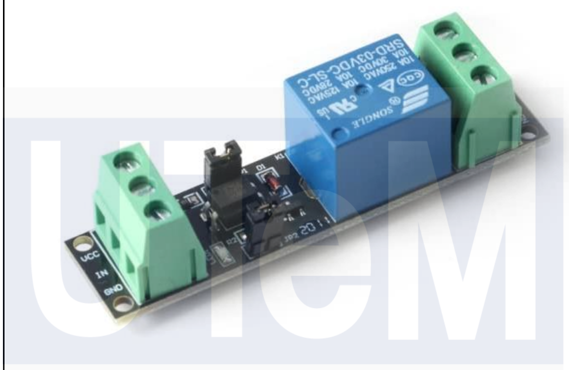	RM6.00
7.	1000mAh Battery 9V With USB Type C charging Rechargeable Port	1		RM20.00

8.	Waterproof switch	1		RM13.50

3.3.2 Block diagram of fish tank waste cleaner.

This block diagram presents an automated fish tank waste cleaner designed to streamline aquarium maintenance. At the core of the system is a microcontroller ESP8266, which controls the entire cleaning process. It communicates with a motor driver that controls two DC motors for movement within the tank water. A relay module serves as an electronic switch, controlled by the microcontroller to activate the water pump as required. An IR sensor is included to assist the cleaner in navigating the tank efficiently and avoiding obstacles. Figure 3.15 shows the block diagram of fish tank waste cleaner.

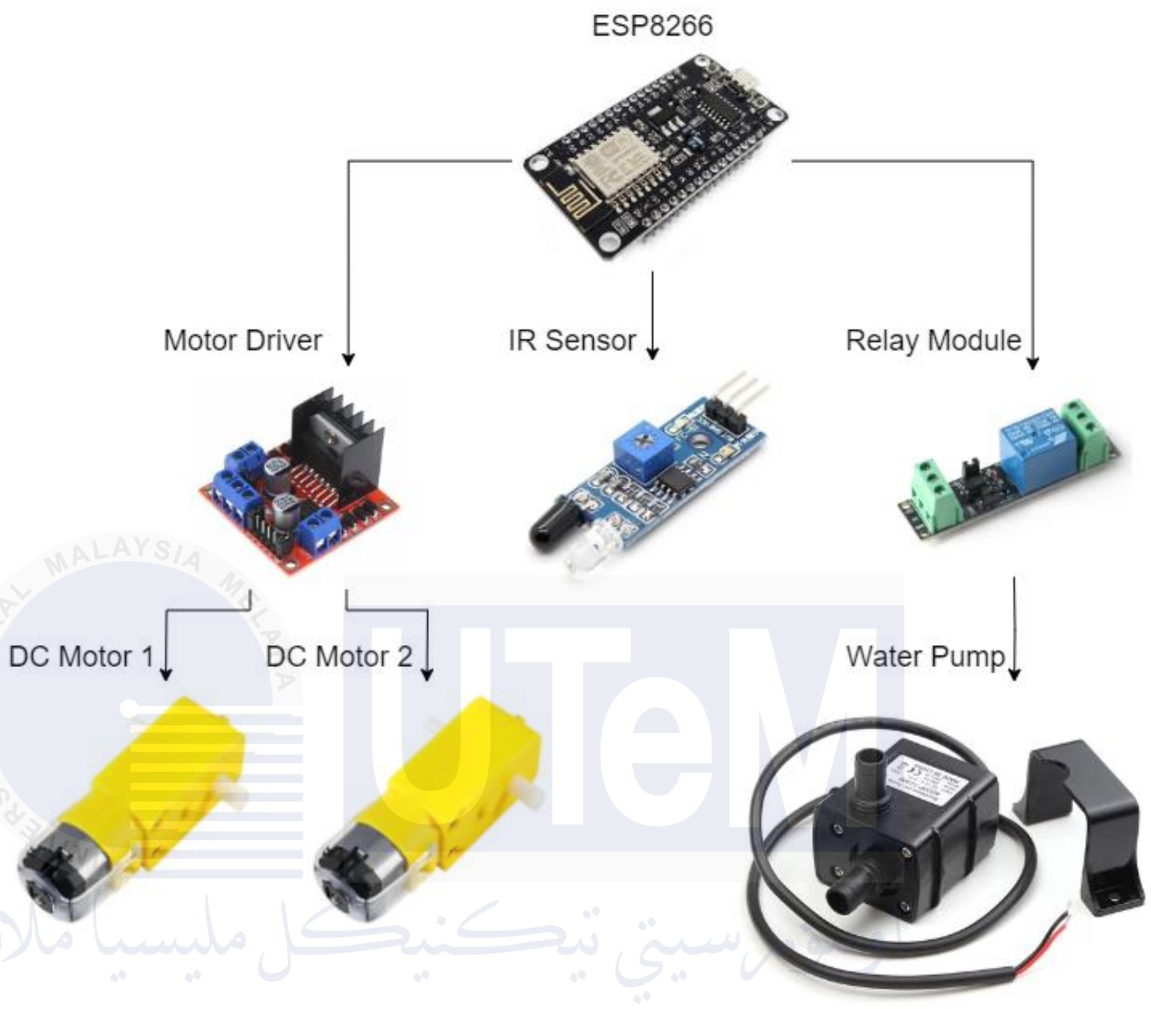

Figure 3.15 Block diagram of fish tank waste cleaner.

3.3.3 Circuit setup for fish tank waste cleaner.

This circuit diagram, created using Proteus software, represents an automated fish tank waste cleaner device. Proteus is a software application utilized for schematic capture, simulation, and PCB (printed circuit board) design. The diagram features a NodeMCU, a microcontroller board based on the ESP8266 chip, which oversees the entire cleaning process. The NodeMCU communicates with a motor driver that manages two DC motors, enabling movement within the tank. A relay module acts as an electronic switch, controlled by the microcontroller to operate the water pump when needed. Additionally, an IR sensor is incorporated to help the cleaner navigate the tank efficiently and avoid obstacles.

To begin creating a schematic in Proteus, start by opening the Proteus Design Suite software and create a new schematic using the file menu, then select new, and select schematic. Select and add required components from the Proteus library by searching through categories or using the search bar. Arrange the components on the schematic workspace, adjusting their orientation and position as necessary. Use the wires tool to connect the components according to the circuit diagram. Optionally, it can simulate the circuit to confirm its functionality before proceeding to PCB design. Finally, save the schematic by navigating to file and selecting save. Figure 3.16 shows the circuit diagram for fish tank waste cleaner.

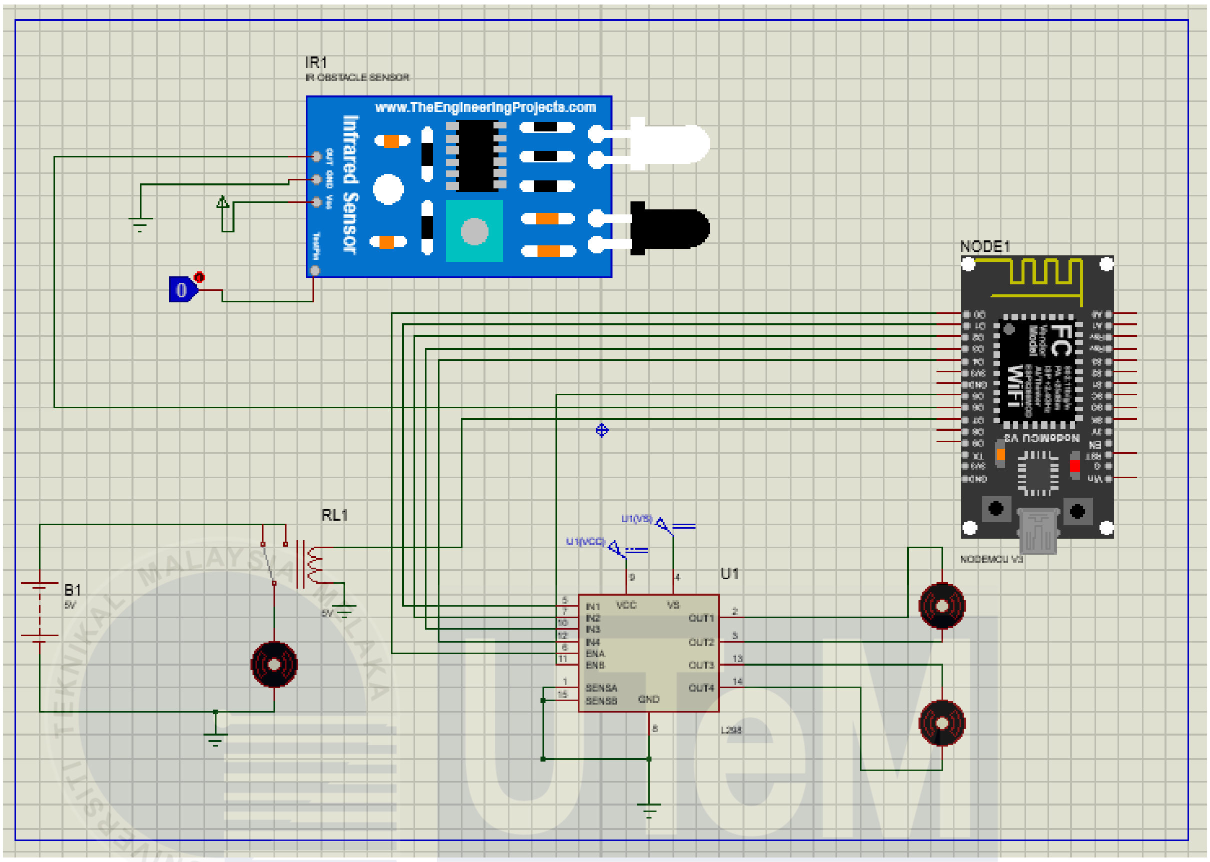

Figure 3.16 Circuit diagram for fish tank waste cleaner.

However, this coding presents a foundational software code for an IoT system based on an ESP8266 microcontroller, serving as the core processor. The system integrates motor control through a two-motor driver, an IR sensor for obstacle detection, and a relay to manage a water pump. During initialization in the setup function, pins for motor control and sensors are configured, and the motors and relay are activated. In the main loop, the system continuously monitors the IR sensor for obstacles. Upon detecting an obstacle, it executes a sequence to avoid it, involving stopping, reversing, and rotating. When no obstacles are detected, the motors proceed forward. This setup supports real-time monitoring and management over Wi-Fi, connecting with the Blynk application to support environmental monitoring and analysis. The entire coding of fish tank waste cleaner shows at **Appendix A**.

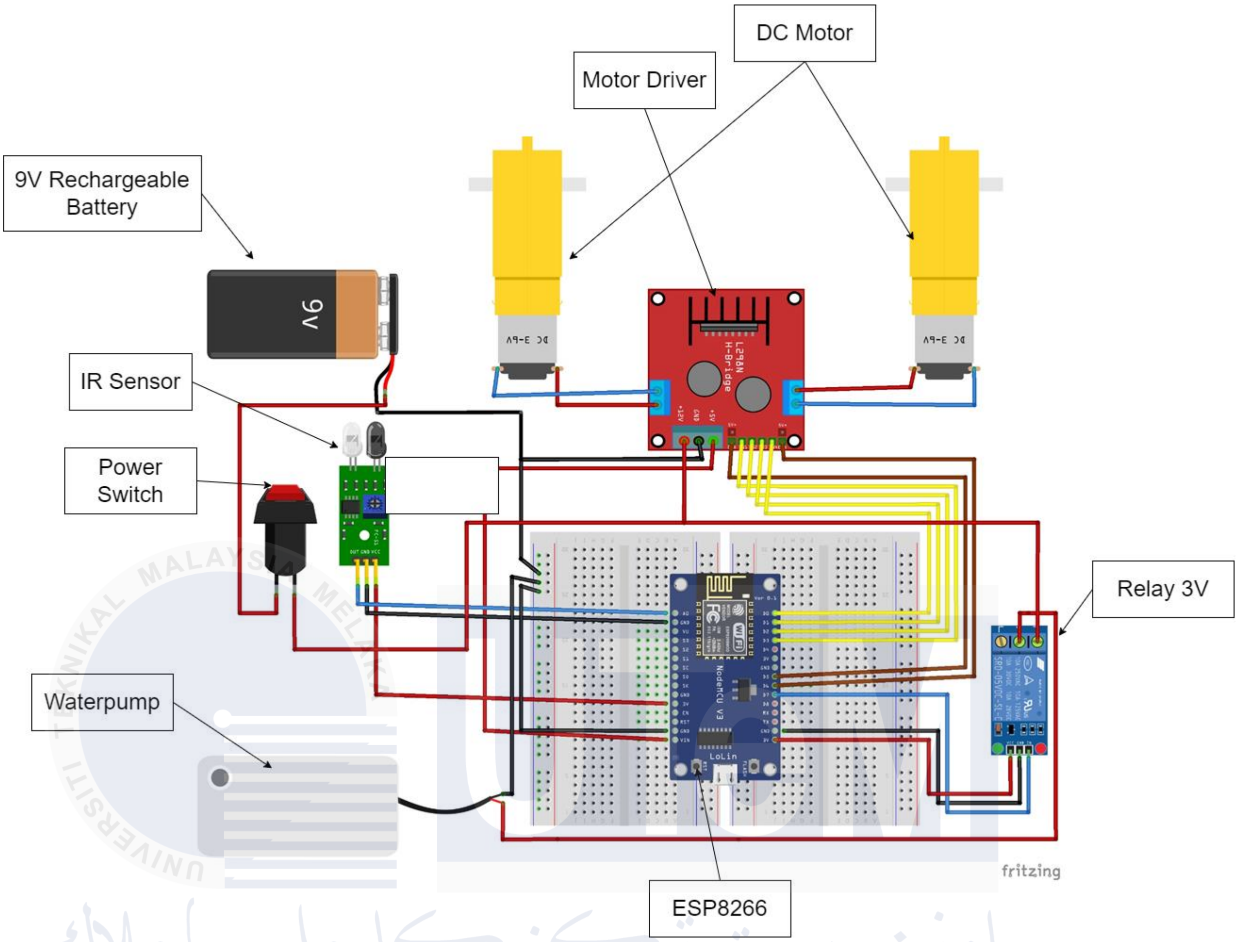

Figure 3.17 Electrical circuit design for fish tank waste cleaner.

Figure 3.17 illustrates electrical circuit design for a fish tank waste cleaner system powered by a 9V rechargeable battery. Created using Fritzing, the diagram visually represents an IoT-enabled system with real-time control capabilities. The setup features an ESP8266 NodeMCU microcontroller, a motor driver (L298N), two DC motors, an IR sensor, a relay module, and a power switch, all interconnected on a circuit board. The 9V rechargeable battery supplies power through the board's power rail to all components. Acting as the central control unit, the ESP8266 processes signals from the IR sensor for obstacle detection and controls the motor driver to operate the waste-cleaning mechanism. The power switch manually activates the battery's power supply, while the relay module ensures safe operation of the water pump.

3.4 Design of fish tank waste cleaner mechanism.

The fish tank waste cleaner's 3D design was carefully developed using SolidWorks software, renowned for its ability to produce detailed and accurate 3D models. The design integrates all key components, including the waste-cleaning mechanism powered by DC motors, the water pump, and dedicated housing for electronics, such as the ESP8266 microcontroller, motor driver, and sensors. SolidWorks enabled precise alignment and component fitting, resulting in a compact and efficient design optimized for standard fish tank dimensions. Furthermore, the design emphasizes ease of assembly, incorporating dedicated provisions for securely mounting the electronics.

3.4.1 Trial design of fish tank waste cleaner.

One of the primary challenges in developing such a device is ensuring it remains submerged and functions properly underwater. SolidWorks is beneficial for designing weight distribution to overcome buoyancy, using fish-safe materials, and suitable weights to help the device sink. Additionally, the electrical components within the main body such as the microcontroller, motor driver, relay module, DC motor, and IR sensor need protection from water damage. SolidWorks can be utilized to design a watertight enclosure with gaskets and O-rings to prevent leaks, and the components themselves may require a conformal coating for added water resistance. Figure 3.18, 3.19, and 3.20 shows the 3D design of the main body, 3D designs of cover water pump part, and 3D design of cover electronic part.

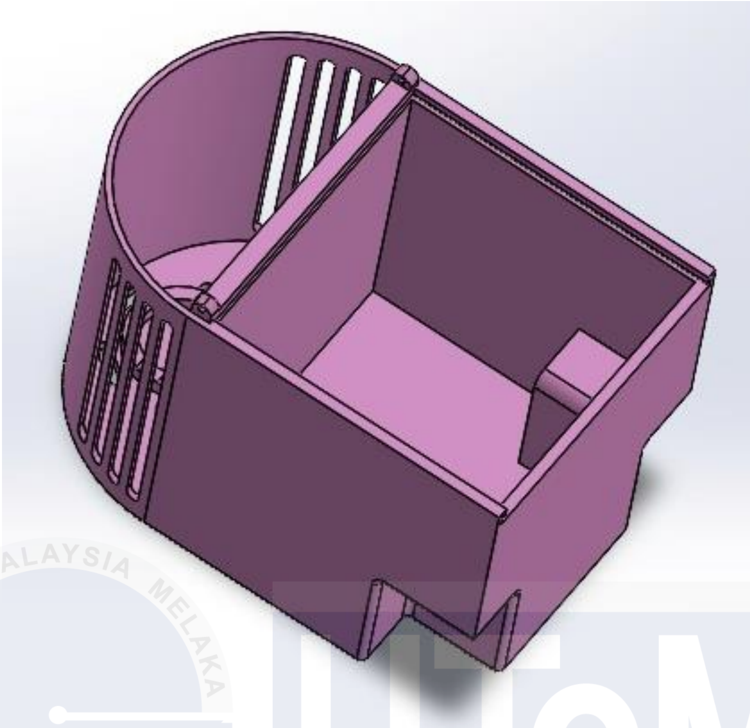

Figure 3.18 3D design of main body.

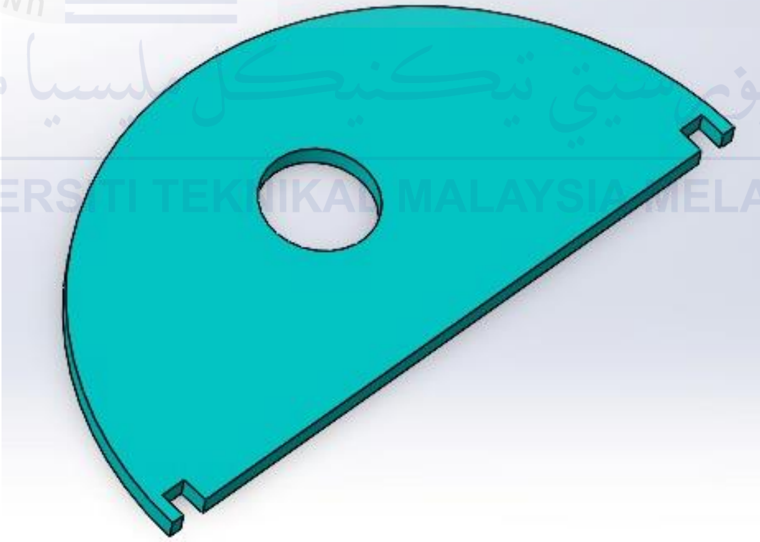

Figure 3.19 3D design of cover water pump part.

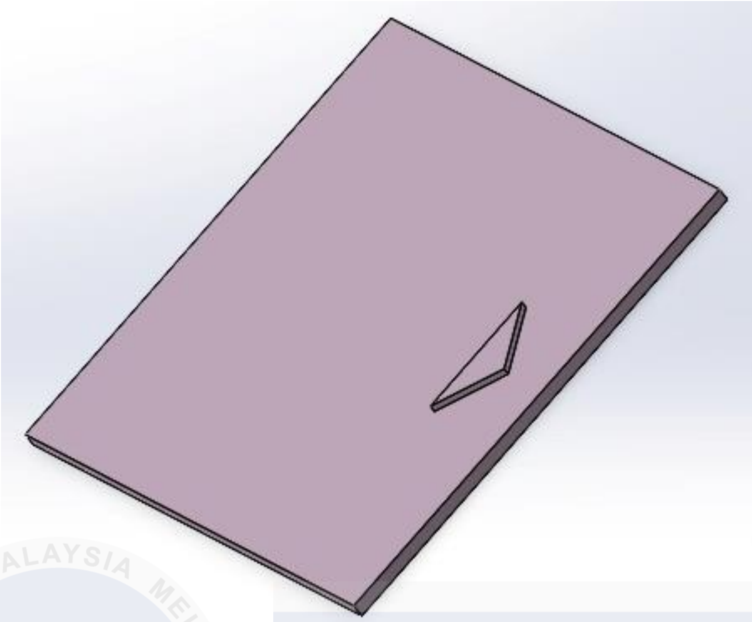

Figure 3.20 3D design of cover electronic part.

3.4.2 Isometric view design of fish tank waste cleaner.

The text labels in the 3D design of the fish tank waste cleaner, created with SolidWorks software, provide essential dimensional information for the device's proper assembly and functionality. These labels include overall dimensions such as length, width, and height, ensuring the cleaner fits within the tank and navigates without obstructions. They detail the precise placement and sizes of internal components like the microcontroller, motor driver, relay module, DC motor, and IR sensor, facilitating optimal operation and ease of assembly. Additionally, the labels specify the weight distribution necessary to overcome buoyancy. The dimensions of the water resistance part, including wall thickness and the sizes of gaskets and O-rings, are also outlined to protect the electrical components from water entry. By accurately defining these dimensions, the text labels ensure the 3D design can be effectively translated into a functional, real-world device, reducing the risk of errors during assembly. Figure 3.21 shows the isometric view of fish tank waste cleaner.

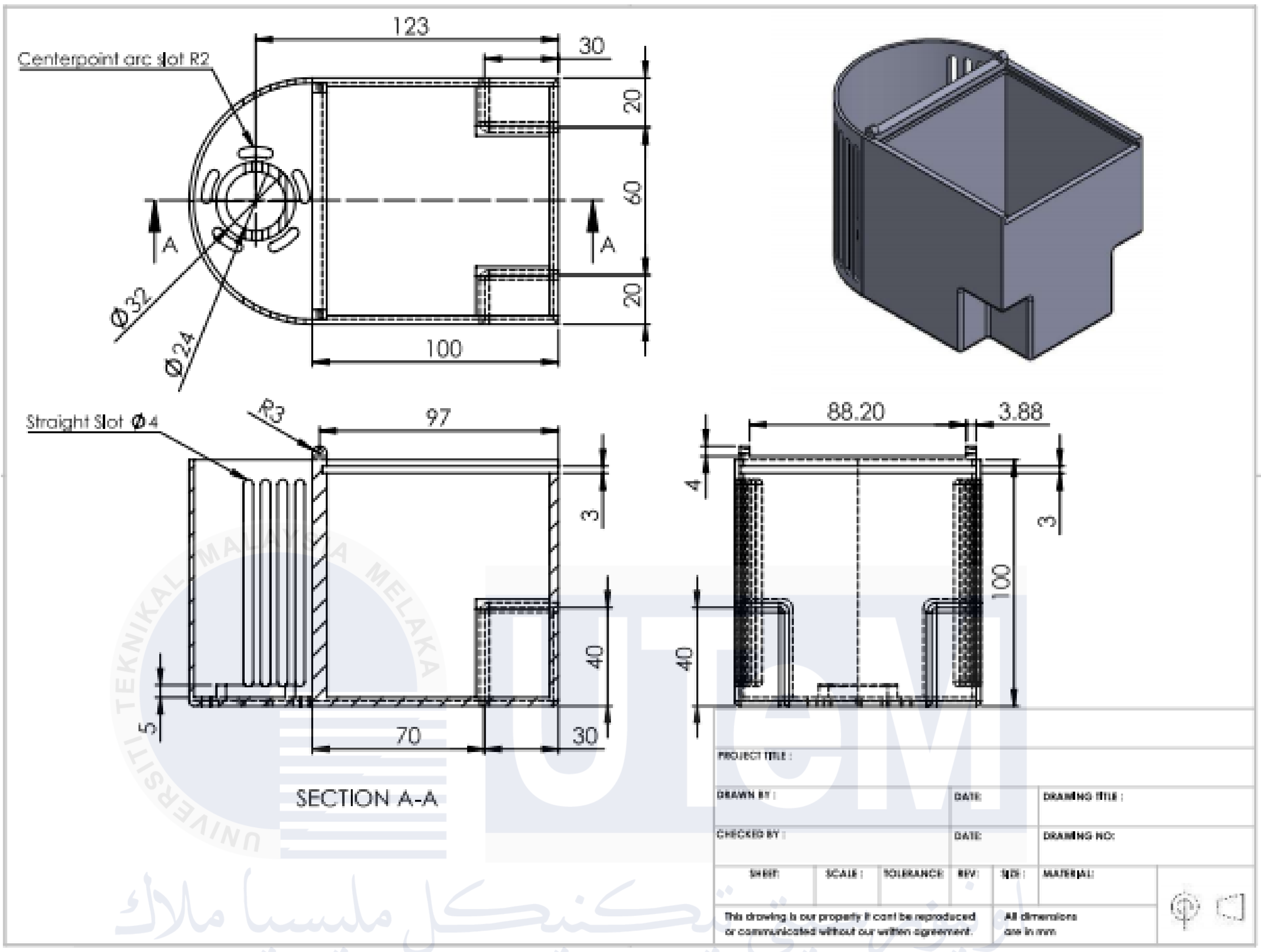

Figure 3.21 Isometric view of fish tank waste cleaner.

3.4.3 Improved design of fish tank waste cleaner.

The second design of the fish tank waste cleaner introduces several improvements and modifications to enhance functionality. The overall measurements have been downscaled to create a more compact and space-efficient design. The front section has been sloped to accommodate a dedicated compartment for the IR sensor, ensuring better alignment for obstacle detection. The IR sensor compartment includes a precise cut hole to securely position the sensor bulb for optimal functionality. Additionally, the water pump has been relocated to a separate compartment, providing better organization and reducing potential interference between components. A designated hole has been added to facilitate clean and secure wiring for the water pump, ensuring easier assembly and maintenance. These enhancements were carefully modeled using SolidWorks, maintaining precision and alignment while optimizing the design for practical use in fish tanks. Figure 3.22, 3.23, 3.24, 3.25, 3.26, 3.27, and 3.28 show overview second design of fish tank waste cleaner, second overview of fish tank waste cleaner, Top view of fish tank waste cleaner, Front view of fish tank waste cleaner, Back view of fish tank waste cleaner, side view of fish tank waste cleaner, and inside view of fish tank waste cleaner.

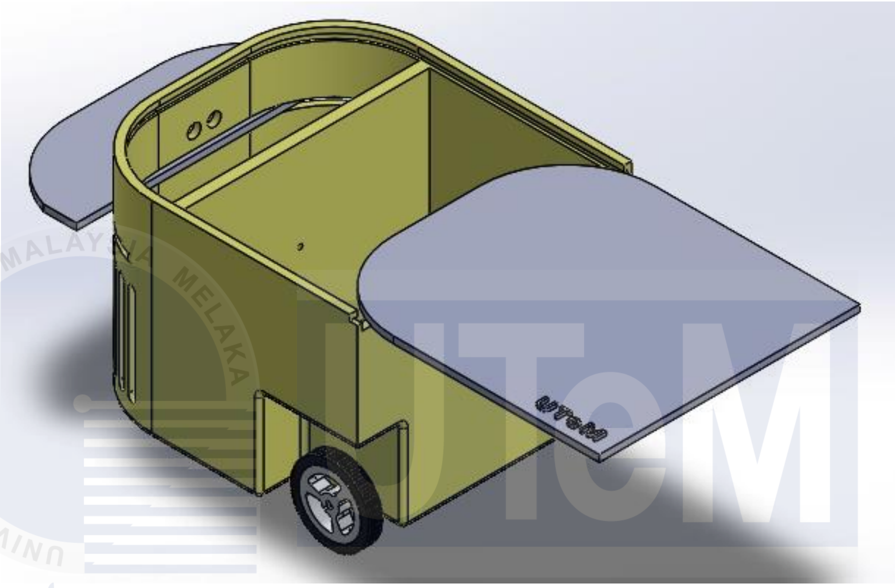

Figure 3.22 Overview second design of fish tank waste cleaner.

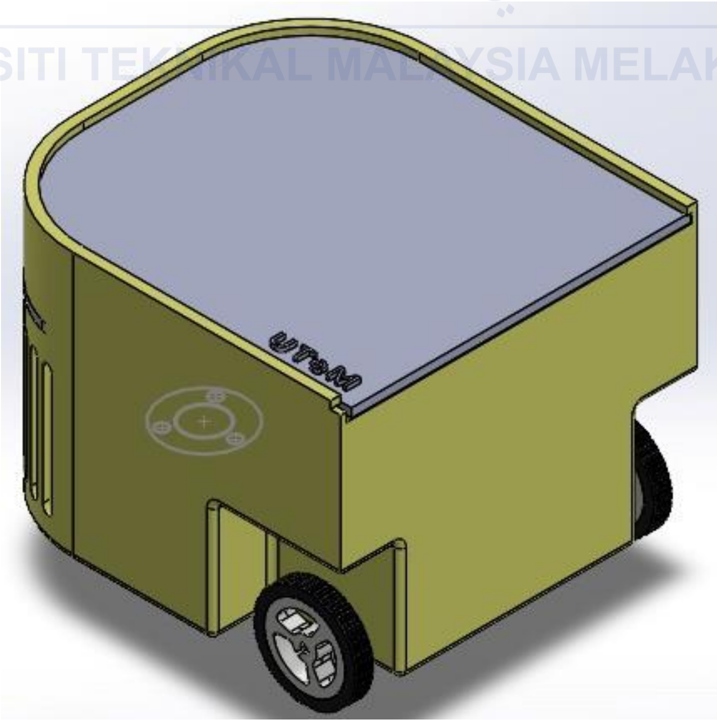

Figure 3.23 Second overview of fish tank waste cleaner.

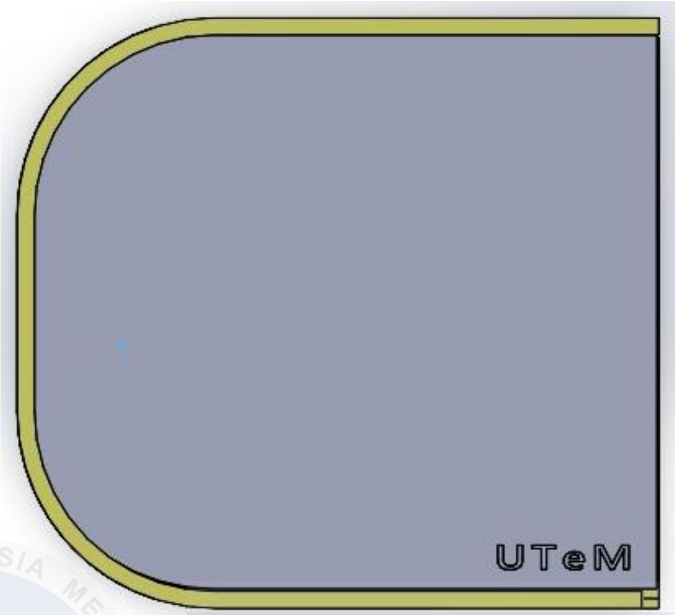

Figure 3.24 Top view of fish tank waste cleaner.

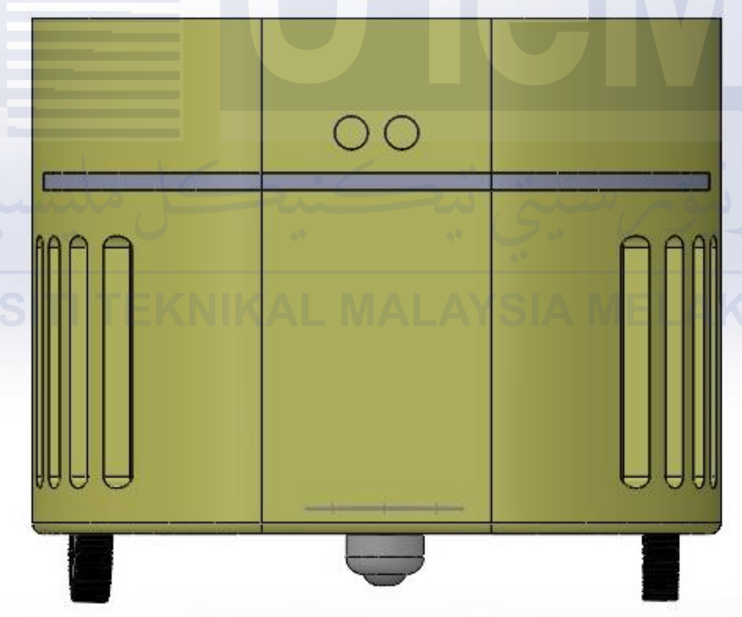

Figure 3.25 Front view of fish tank waste cleaner.

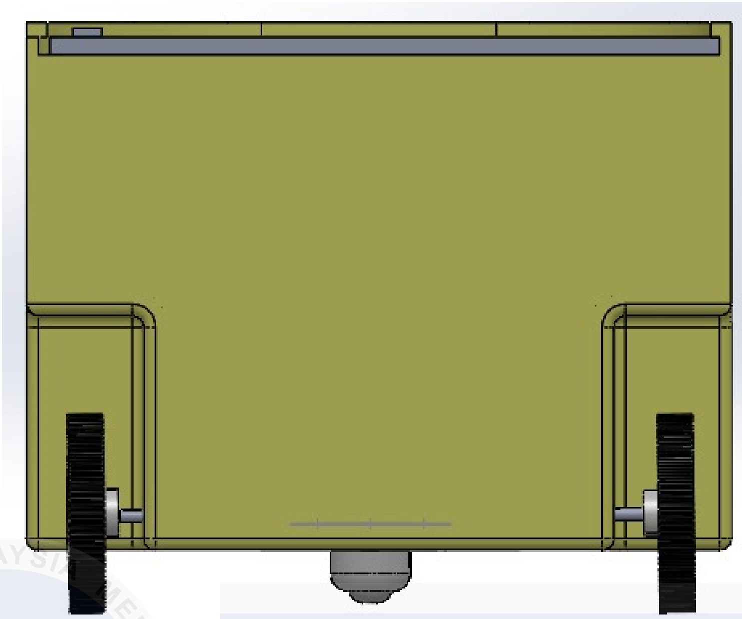

Figure 3.26 Back view of fish tank waste cleaner.

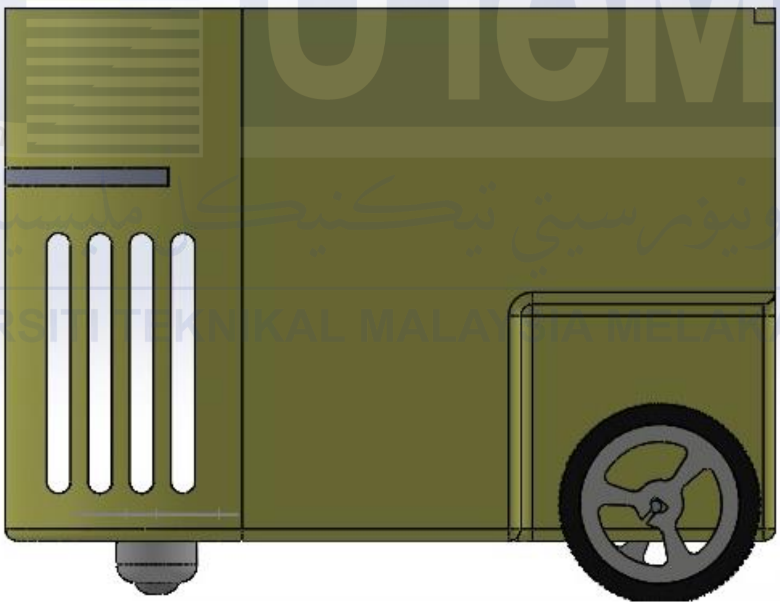

Figure 3.27 Side view of fish tank waste cleaner.

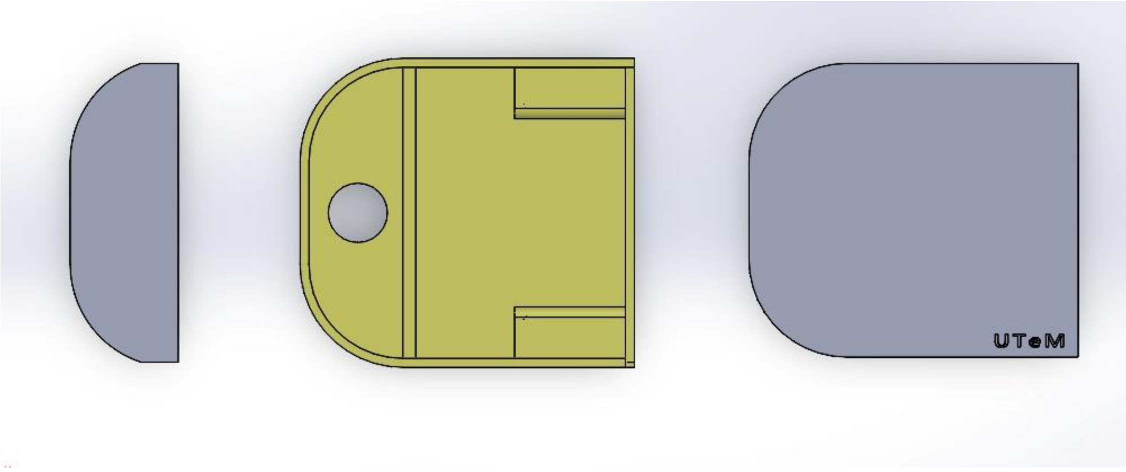

Figure 3.28 Inside view of fish tank waste cleaner.

3.4.4 Isometric view improved design of fish tank waste cleaner.

Figure 3.29 shows the isometric view of the improved design of the fish tank waste cleaner showcases a refined and more efficient layout. This updated design features a compact structure with downscaled measurements for better adaptability to various tank sizes. The front section incorporates a sloped design, creating a dedicated compartment for the IR sensor. This compartment includes a precisely positioned hole for the sensor bulb, ensuring accurate obstacle detection. Additionally, the water pump is housed in a separate compartment, improving organization and minimizing component interference. A dedicated hole is also provided for clean and secure wiring of the water pump, enhancing ease of assembly and maintenance. The isometric view provides a comprehensive perspective of the design, highlighting the improved spatial arrangement and functionality of the system. This updated model, created using SolidWorks, ensures precision, practicality, and an optimized fit for real-world fish tank applications.

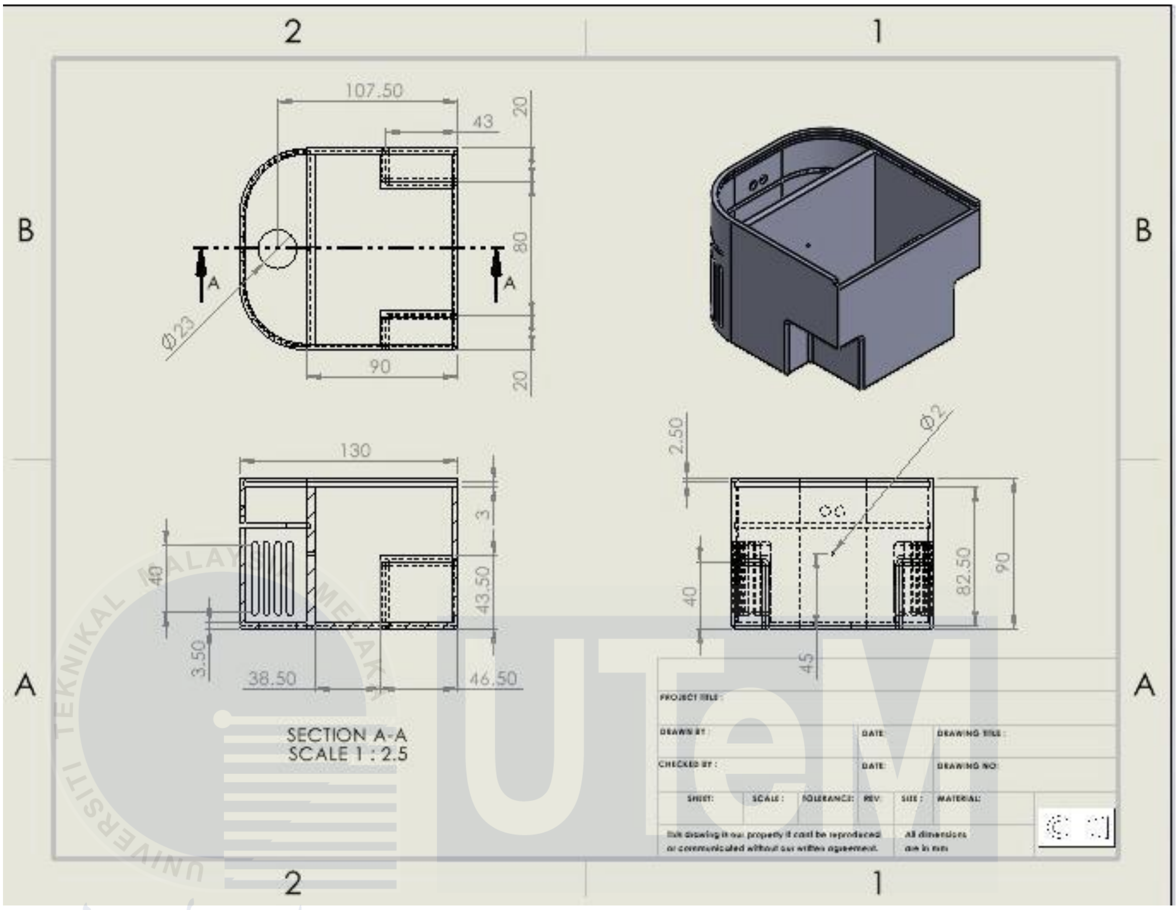

Figure 3.29 Isometric view improved design of fish tank waste cleaner.

3.4.5 Detailed design of fish tank waste cleaner.

The detailed design of the fish tank waste cleaner retains the previous measurements but introduces several enhancements to improve functionality. To ensure the device sinks to the bottom of the tank, 0.5kg weights have been strategically placed on the right, left, and back sides. This addition enhances stability and performance to sink to the bottom of the tank. Furthermore, a switch has been incorporated into the top cap, providing users with a convenient way to manually control the device's power. These modifications aim to optimize both the practical use and ease of operation for the cleaner in a fish tank environment. Figure 3.30, 3.31, 3.32, 3.33, and 3.34 show Overview third design of fish tank waste cleaner, second overview of third design fish tank waste cleaner, top view of third design fish tank waste cleaner, front view of third design fish tank waste cleaner, side view of third design fish tank waste cleaner.

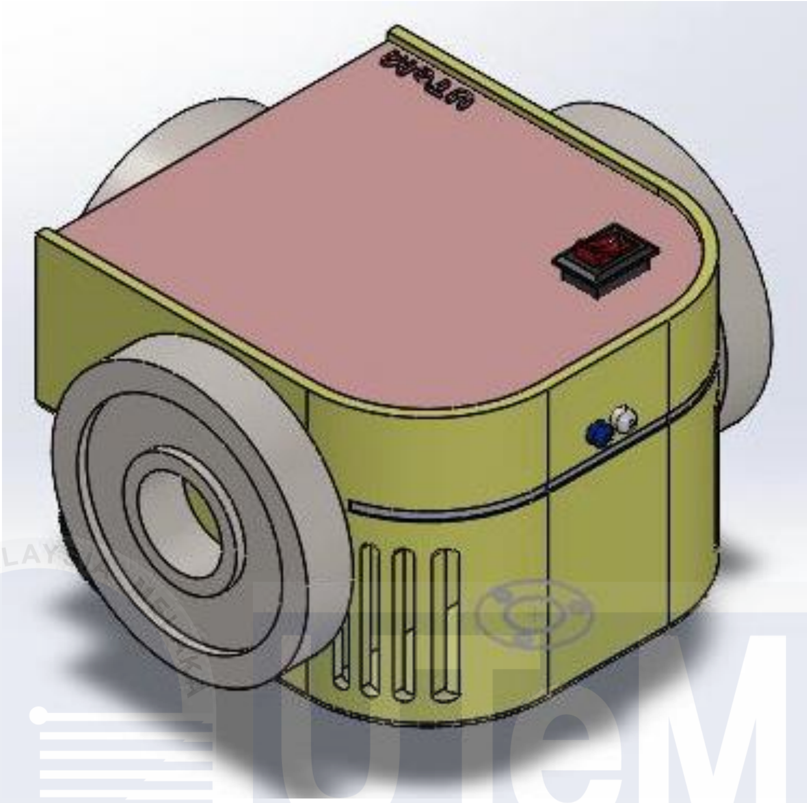

Figure 3.30 Overview third design of fish tank waste cleaner.

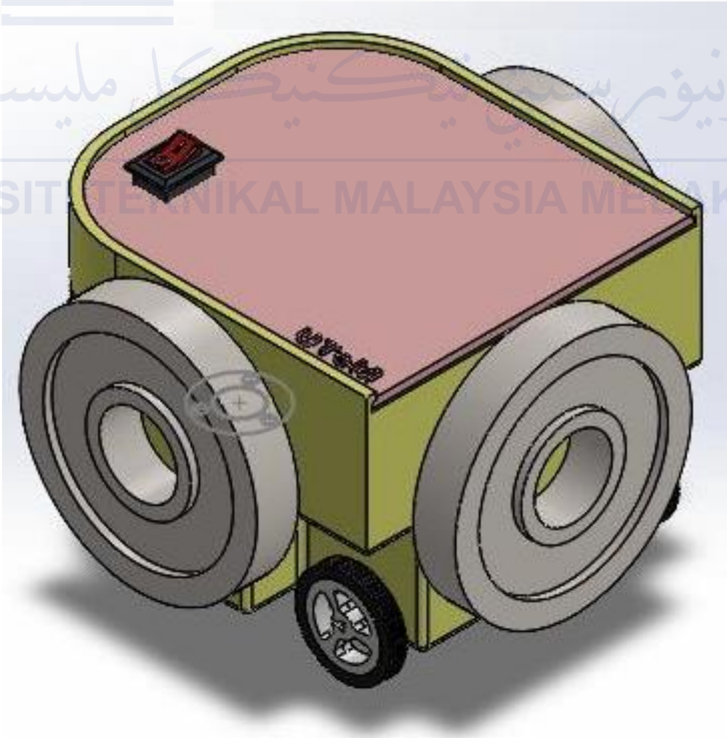

Figure 3.31 Second overview of third design fish tank waste cleaner.

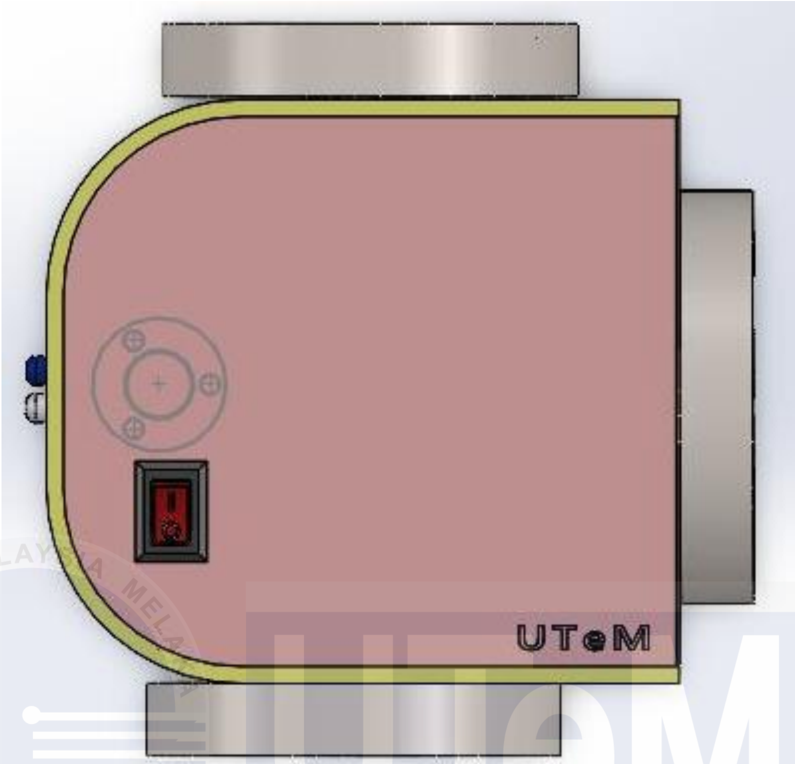

Figure 3.32 Top view of third design fish tank waste cleaner.

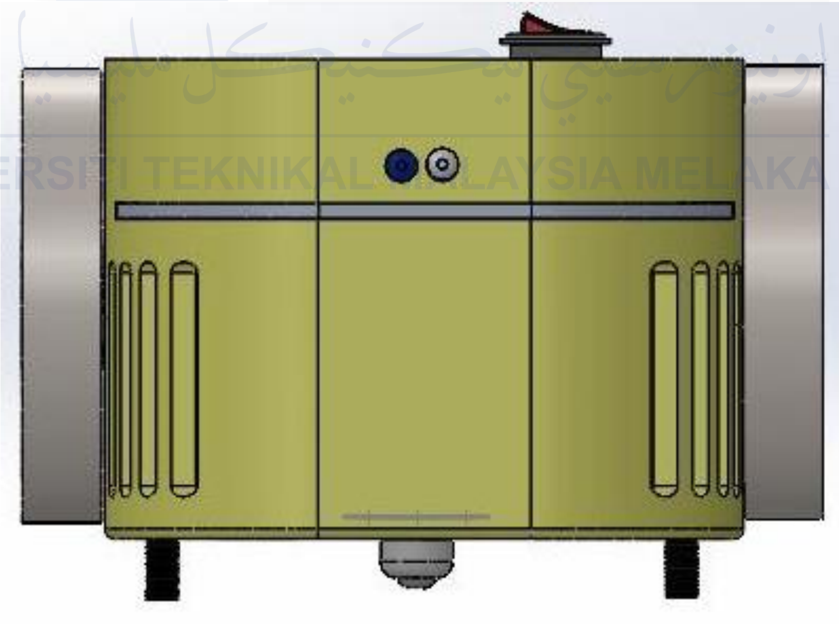
Figure 3.33 Front view of third design fish tank waste cleaner.

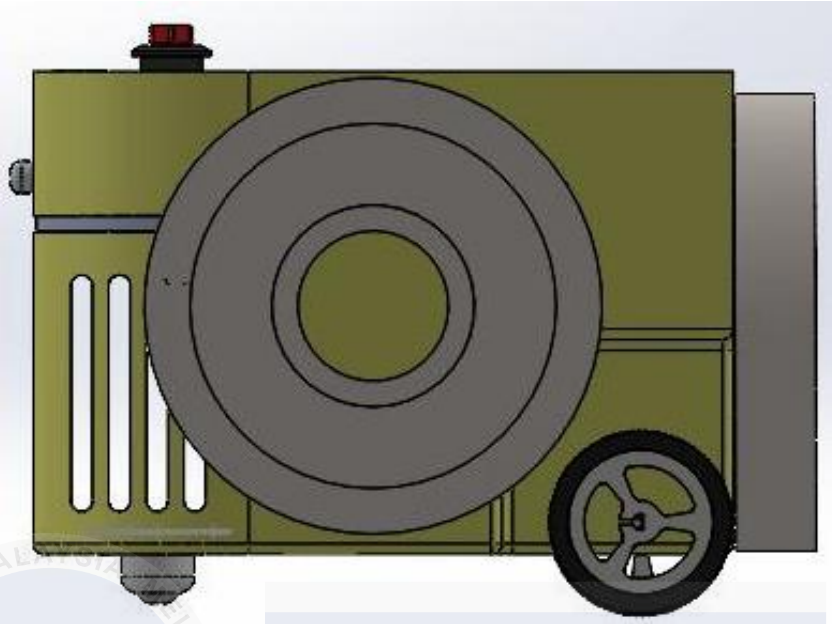

Figure 3.34 Side view of third design fish tank waste cleaner.

3.4.6 Isometric view of detailed design fish tank waste cleaner.

Figure 3.35 shows the isometric view of the detailed design fish tank waste cleaner effectively demonstrates its compact and efficient structure. In this design, the same measurements from previous versions are retained, while 0.5kg weights have been added to the right, left, and back sides of the device to ensure it sinks properly to the bottom of the tank. These weights are integrated into the design for optimal balance and stability. A manual on/off switch is placed on the top cap, allowing users to easily control the device's power. This layout illustrates the precision of the components.

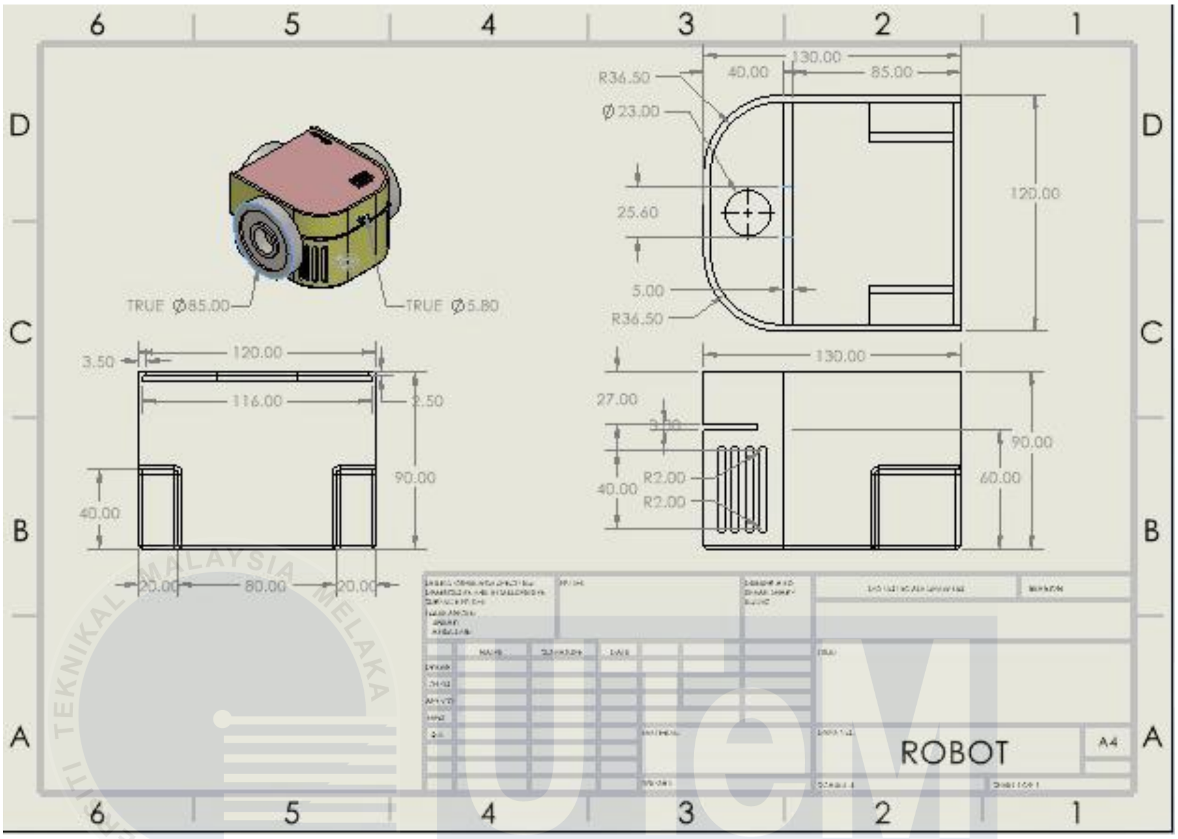

Figure 3.35 Isometric view of third design fish tank waste cleaner.

3.4.7 Final design of fish tank waste cleaner.

The final design of the fish tank waste cleaner was developed to address the limitations of the previous version, which was too heavy to move forward due to the added weight used to counteract buoyancy. Instead of increasing the motor's voltage and torque to make the device sink, the focus shifted to creating a floating design. Buoyancy was achieved using white cork or Styrofoam, allowing the device to remain on the water's surface. A tube was incorporated, extending from the water pump to the bottom of the tank, to efficiently collect debris and waste. For mobility, a propeller was added to the top of the device, enabling it to navigate across the water surface while performing its cleaning tasks. This final design ensures an optimal balance of buoyancy and cleaning functionality, making it an efficient solution for tank maintenance. Figures 3.36, 3.37, and 3.38 illustrate the overview, side view, and back view of the final design of the fish tank waste cleaner.

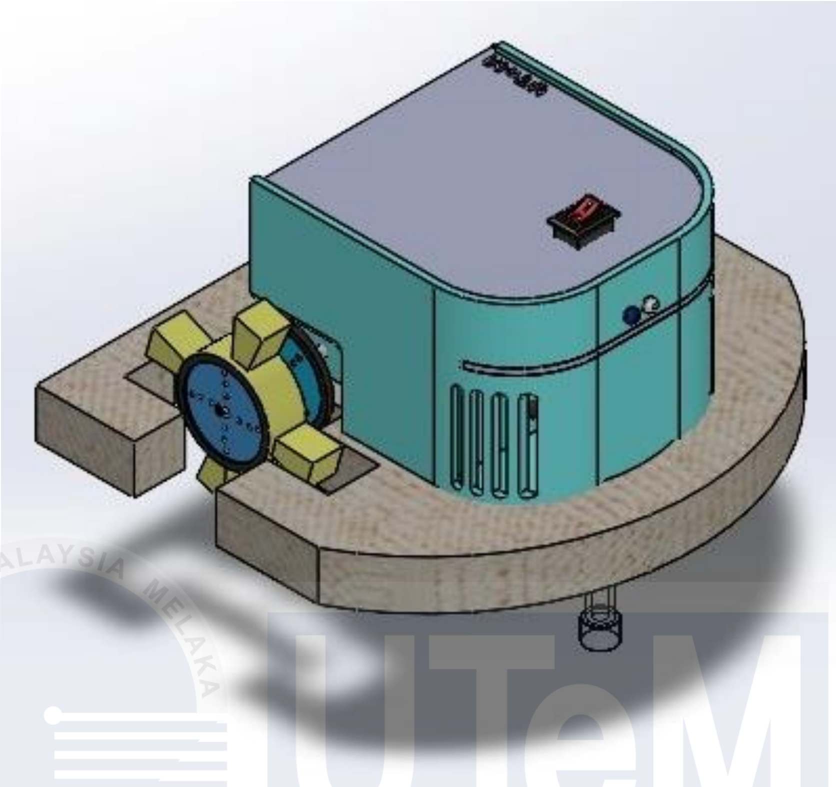

Figure 3.36 Overview the final design of fish tank waste cleaner.

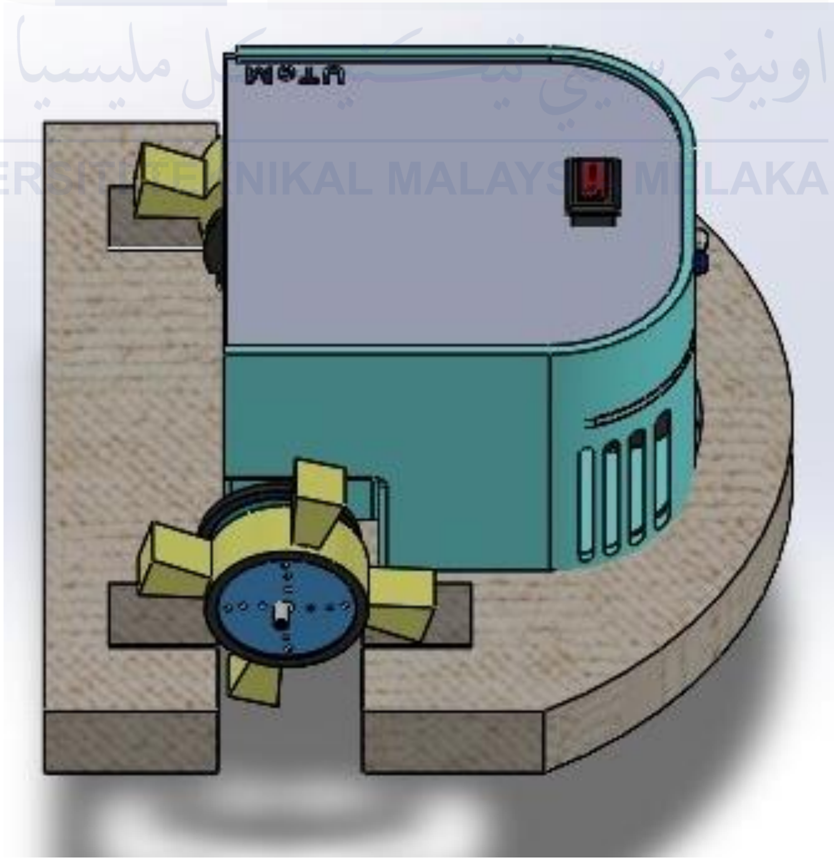

Figure 3.37 Side view the final design of fish tank waste cleaner.

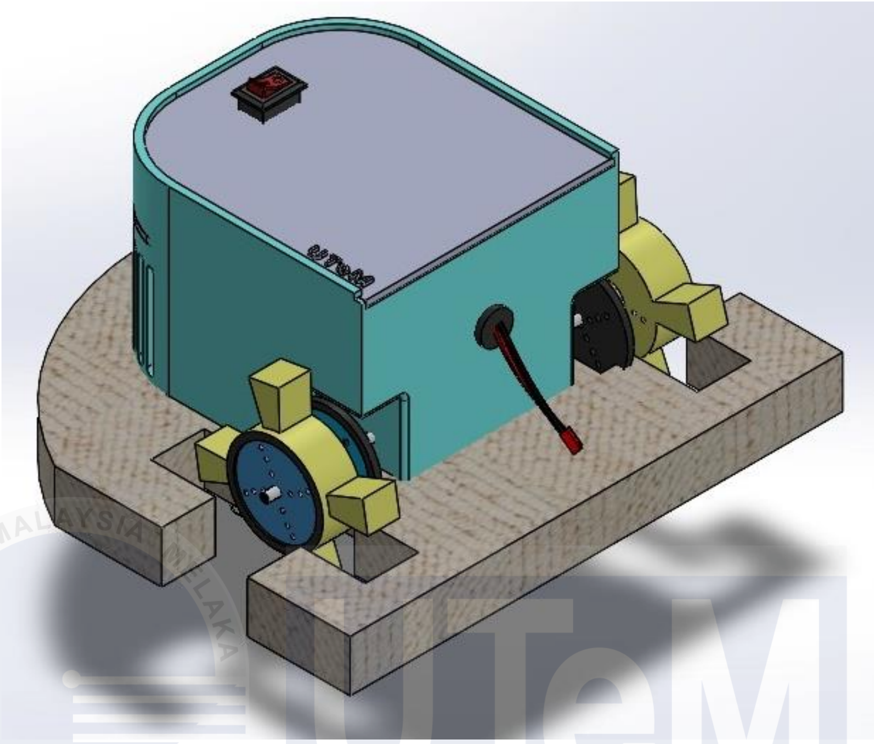

Figure 3.38 Back view the final design of fish tank waste cleaner.

3.4.8 Isometric view of final design fish tank waste cleaner.

The isometric view of the final design of the fish tank waste cleaner offers a three-dimensional perspective that showcases the device's layout. This view provides a clear representation of the device's overall structure, including the floating body made from white cork or Styrofoam, which ensures buoyancy. The tube connected to the water pump, extending towards the bottom of the tank, is visible, indicating its function of sucking up debris and waste. The propeller, mounted at the top of the device, is shown in the isometric view, emphasizing its role in moving the cleaner across the water surface. Figure 3.39 shows the isometric view of final design fish tank waste cleaner.

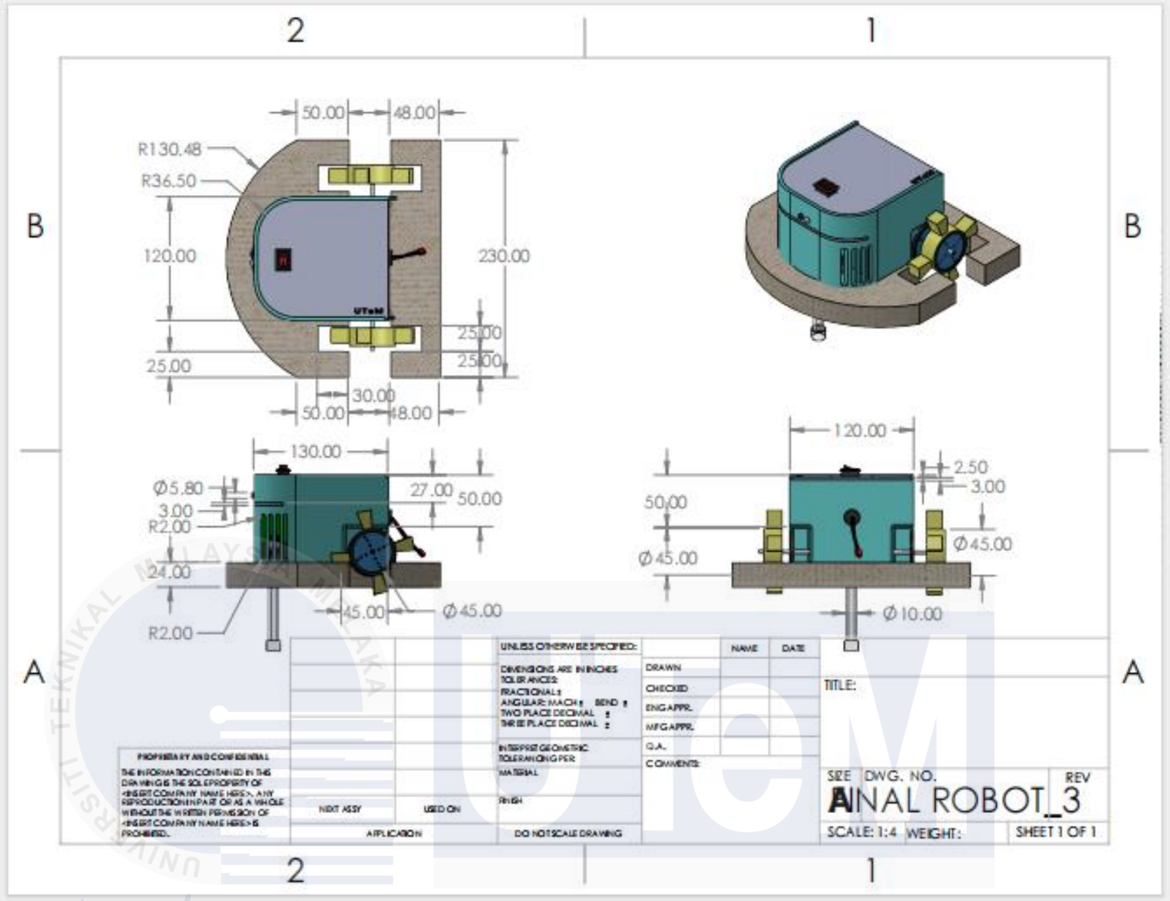

Figure 3.39 Isometric view of final design fish tank waste cleaner.

3.5 Development of IoT system.

The software design for the IoT system fish tank waste cleaner are using the Arduino IDE and the Blynk application. The Arduino IDE is used to write, compile, and upload coding to the ESP8266 microcontroller. This coding encompasses the logic for reading sensor data, controlling the motor and water pump, and managing wireless communication. The Blynk application provides a user-friendly interface for monitoring the device via a smartphone, allowing users to receive real-time data on the system's status.

3.5.1 List of IoT software.

The IoT system consists of two software, each playing a crucial role in the system's operation. All the expenditure on these software is free, as outlined in the corresponding Table 3.4.

Table 3.4 List of IoT software.

No.	Type	Quantity	Model	Price
1.	Arduino IDE	1		FREE
2.	Blynk application	1		FREE

3.5.2 Block diagram of IoT system.

This block diagram depicts a basic software design for an IoT system. The core component is the ESP8266 microcontroller, serving as the brains of the operation. Sensor data collected by the system is then transmitted to a specified platform, which is a Blynk application, enabling real-time environmental monitoring and analysis. This communication typically occurs via Wi-Fi. Figure 3.40 shows the block diagram of the IoT system.

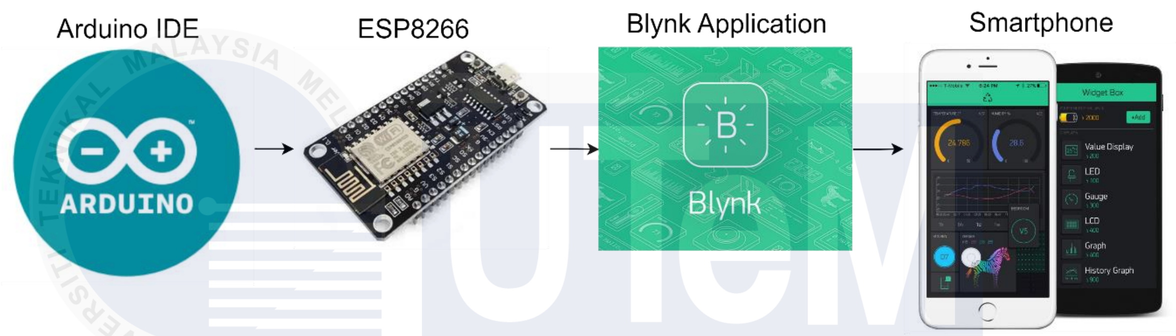

Figure 3.40 Block diagram of IoT system.

3.6 Performance analysis on fish tank waste cleaner.

The performance analysis of the fish tank waste cleaner was conducted within a standard fish tank measuring 60 cm in length, 32 cm in height, and 30 cm in width. These dimensions provided a controlled environment to evaluate the device's functionality, mobility, and cleaning efficiency. The fish tank's size was ideal for testing the maneuverability of the floating design, ensuring the propeller and water pump could operate effectively within confined spaces. Additionally, the depth of 32 cm allowed the tube connected to the water pump to reach the tank's bottom, efficiently removing debris and waste without obstruction. Figures 3.41, and 3.42 show the length of fish tank in cm, width and high of fish tank in cm.

Figure 3.41 Length of fish tank in cm

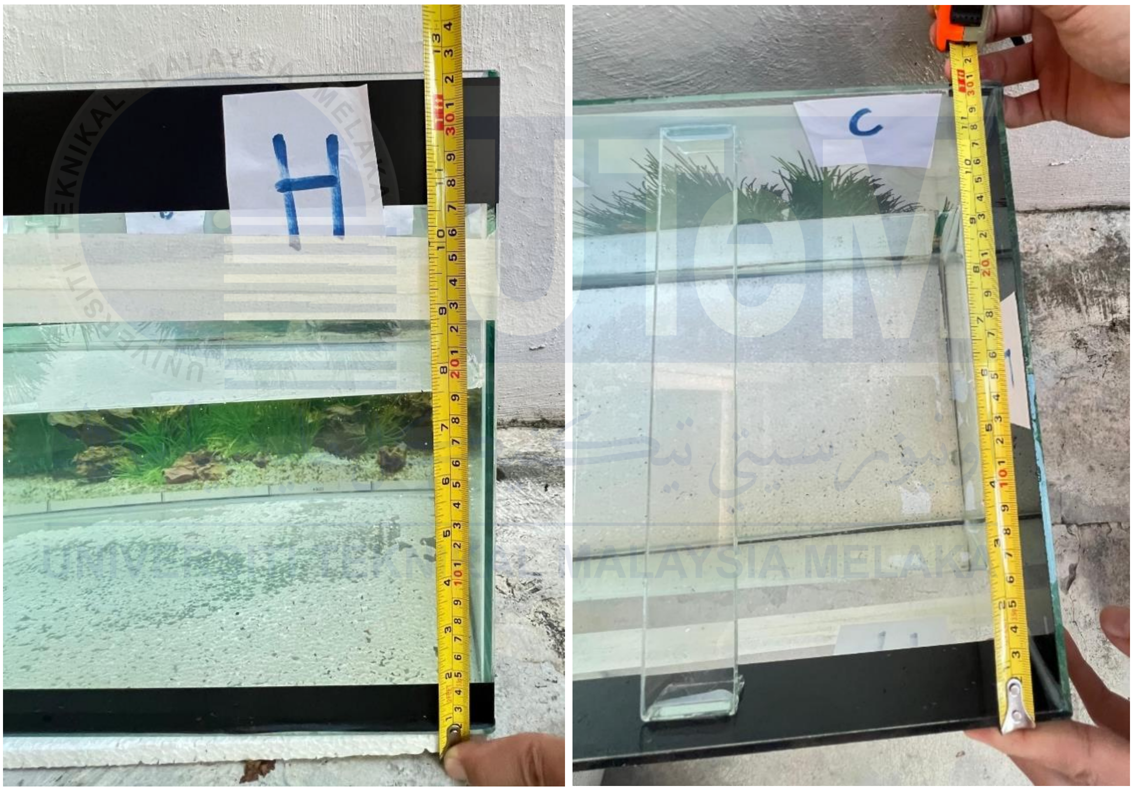

Figure 3.42 Width and high of fish tank in cm

3.6.1 Buoyant force of the fish tank waste cleaner device.

Buoyancy, also known as upthrust, is the force that acts upward, counteracting the downward pull of gravity and preventing a floating object from sinking. When an object is submerged in water, its weight exerts a downward force. Buoyancy opposes this force, with its strength being directly proportional to the volume of fluid displaced by the object essentially, the volume of liquid that the object occupies. Figure 4.43 shows buoyant force equation.

$$B = \rho \times V \times g$$

Figure 3.43 Buoyant force equation

3.6.2 Testing performance of fish tank waste cleaner condition (Case A)

In the detailed design, the fish tank waste cleaner was tested under submerged conditions by adding three iron plates, each weighing 0.5kg, to counter the buoyant force as calculated using the buoyancy force equation. This design successfully allowed the device to remain fully submerged underwater, demonstrating its ability to overcome buoyancy. However, despite achieving submersion, the device could not move forward or perform cleaning tasks due to the excessive weight, which exceeded the motor's capacity to generate enough thrust for mobility.

3.6.3 Testing performance of fish tank waste cleaner condition (Case B)

To address the mobility issue encountered in Case A, the fish tank waste cleaner was redesigned, resulting in the final design. In this iteration, the heavy iron plates were removed, and white cork was added to the base layer to provide sufficient buoyancy, enabling the device to float on the water surface. To ensure efficient cleaning, a tube was attached to the water pump, extending to the bottom of the tank to suck in debris and waste. Additionally, a propeller was integrated at the top of the device to facilitate movement across the tank's surface, allowing it to perform cleaning tasks effectively without the constraints of excessive weight. This redesign optimized both functionality and mobility, making the device more practical for real-world use.

3.7 Gantt chart of the project.

	TASK	PSM1														PSM2													
NO	WEEK	W1	W2	W3	W4	W5	W6	W7	W8	W9	W10	W11	W12	W13	W14	W1	W2	W3	W4	W5	W6	W7	W8	W9	W10	W11	W12	W13	W14
1	Briefing for PSM 1 by JK,PSM,FTKEE																												
2	Project title conformation and registration																												
3	Briefing with supervisor																												
4	Study the project background																												
5	Drafting chapter1 : Introduction																												
6	Task progress evaluation 1																												
7	Drafting chapter 2 : Literature Review																												
8	Table summary Literature review																												
9	Drafting Chapter 3: Methodology																												
10	Work on the software/hardware																												
11	First draft submission to supervisor																												
12	Task progress evaluation 2																												
13	Submission Report to the panel																												
14	Presentation of BDP1																												
15	Drafting Chapter 4: Analyse Data and result																												
16	Data Analyse and result																												
17	Record the result																												
18	Drafting Chapter 5: Conclusion and recommendation																												
19	Compiling Chapter 4 and 5																												
20	Submit latest report to supervisor																												
21	Finalize the report																												
22	Presentation of BDP2																												

3.8 Summary

The fish tank waste cleaner has undergone significant design improvements, focusing on enhancing functionality, organization, and usability. The second design features a more compact and space-efficient layout, with a sloped front section for an IR sensor compartment that ensures precise alignment for obstacle detection. The relocation of the water pump to a separate compartment improves organization and minimizes interference between components, while a dedicated hole allows for secure wiring. These improvements were carefully modeled using SolidWorks to ensure precision. In the third design, 0.5kg weights were added on the right, left, and back sides to help the device sink to the bottom, improving stability. A manual on/off switch was also incorporated for easier operation. The solar charging system hardware setup has been completed, with open circuit voltage (Voc) and short circuit current (Isc) measurements taken and detailed in Chapter 4. The functionality of all components, including the ESP8266 microcontroller, IR sensor, motor driver, DC motors, relay module, and water pump, was successfully simulated in Proteus.

CHAPTER 4

RESULTS AND DISCUSSIONS

4.1 Introduction

The results and discussion section are crucial for presenting and interpreting the findings in the study on the development of a solar-powered fish tank waste cleaner. In the results section, it will be clearly and concisely present the collected data, often using tables, figures, and descriptive statistics to highlight key findings, such as the waste cleaner's efficiency and the solar power charging system's effectiveness, including data that have been collected from the PV panel. The discussion section is where it will be interpreting these results, examining the implications, such as the sustainability and efficiency of using solar power for fish tank maintenance, supported by the analysis of the PV panel data. In this section, it may also propose possible explanations for their findings.

4.2 Data and analysis of solar charging system

The measurement results were collected based on the setup detailed in Chapter 4. Over five days, the voltage and current produced by the solar panel were recorded every two hours, starting at 8:00 AM and ending at 6:00 PM. This consistent data collection method provided a thorough overview of the solar panel's performance throughout the day. The gathered data enabled an analysis of the solar power system's efficiency and effectiveness under varying sunlight conditions.

The measurement of the power output of the PV system over five days, showing a peak during the sun's peak hours and then decreased. This pattern occurs because the sunlight hitting the panel is most intense at midday. However, this data can be changed due to factors like the availability of sunlight and shadows from clouds. The data presented at Table 4.1, 4.2, 4.3, 4.4, 4.5, and 4.6.

Table 4.1 Output power on day 1.

Time (24 hours)	**Current, A (Isc)**	**Voltage, V (Voc)**	**Power, W (P = I x V)**
08:00	0.20	16.0	3.20
10:00	0.48	16.5	7.92
12:00	0.50	17.0	8.50
14:00	0.43	16.5	7.09
16:00	0.40	16.5	6.60
18:00	0.16	15.9	2.54

Table 4.2 Output power on day 2.

Time (24 hours)	**Current, A (Isc)**	**Voltage, V (Voc)**	**Power, W (P = I x V)**
08:00	0.22	16.2	3.56
10:00	0.50	16.8	8.40
12:00	0.50	17.5	8.75
14:00	0.46	16.5	7.59
16:00	0.44	16.5	7.26
18:00	0.20	16.0	3.20

Table 4.3 Output power on day 3.

Time (24 hours)	**Current, A (Isc)**	**Voltage, V (Voc)**	**Power, W (P = I x V)**
08:00	0.22	16.0	3.52
10:00	0.48	16.5	7.92
12:00	0.50	17.0	8.50
14:00	0.45	16.5	7.42
16:00	0.40	16.2	6.48
18:00	0.20	16.0	3.20

Table 4.4 Output power on day 4.

Time (24 hours)	Current, A (Isc)	Voltage, V (Voc)	Power, W (P = I x V)
08:00	0.25	16.0	4.00
10:00	0.50	16.3	8.15
12:00	0.53	17.0	9.01
14:00	0.42	16.5	6.93
16:00	0.38	16.0	6.08
18:00	0.20	16.0	3.20

Table 4.5 Output power on day 5.

Time (24 hours)	Current, A (Isc)	Voltage, V (Voc)	Power, W (P = I x V)
08:00	0.30	16.2	4.86
10:00	0.52	16.4	8.52
12:00	0.55	17.0	9.35
14:00	0.44	16.4	7.21
16:00	0.40	15.9	6.36
18:00	0.35	15.8	5.53

Table 4.6 Output power in five days.

Power, W	**8:00**	**10:00**	**12:00**	**14:00**	**16:00**	**18:00**
Day 1	3.20W	7.92W	8.50W	7.09W	6.60W	2.54W
Day 2	3.56W	8.40W	8.75W	7.59W	7.26W	3.20W
Day 3	3.52W	7.92W	8.50W	7.42W	6.48W	3.20W
Day 4	4.00W	8.15W	9.01W	6.93W	6.08W	3.20W
Day 5	4.86W	8.52W	9.35W	7.21W	6.36W	5.53W

4.2.1 Analysis solar charging system.

The analysis is done based on the collected data in which the data is presented in the graph form. The graphs illustrate the current, voltage, and power output of the solar charging system over a 24-hour period. The power attains with multiplication of voltage and current.

4.2.2 Day 1

On the x-axis, time is labelled from 8:00 AM to 6:00 PM. For the current graph (Figure 4.1), the y-axis ranges from 0 to 0.6 amps. The current starts at around 0.2 amps at 8:00 AM, peaks at approximately 0.5 amps at noon, and then decreases to about 0.2 amps by 6:00 PM. For the voltage graph (Figure 4.2), the y-axis ranges from 10 to 18 volts. The voltage pattern mirrors the current pattern, starting at around 16 volts at 8:00 AM, peaking at about 17.5 volts at noon, and then dropping back to around 16 volts by 6:00 PM. Both graphs reflect the fact that the current and voltage produced by a PV panel depend on sunlight intensity. The PV panel produces the highest current and voltage during peak sun hours, when the sun is highest in the sky. Figure 4.1 and 4.2 shows the graph current versus time and, graph voltage versus time.

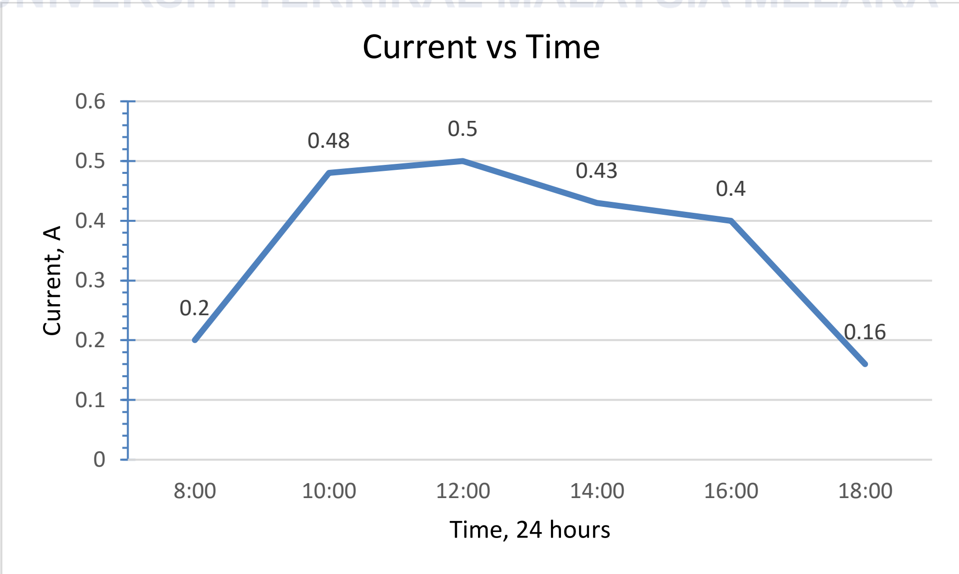

Figure 4.1 Graph current versus time.

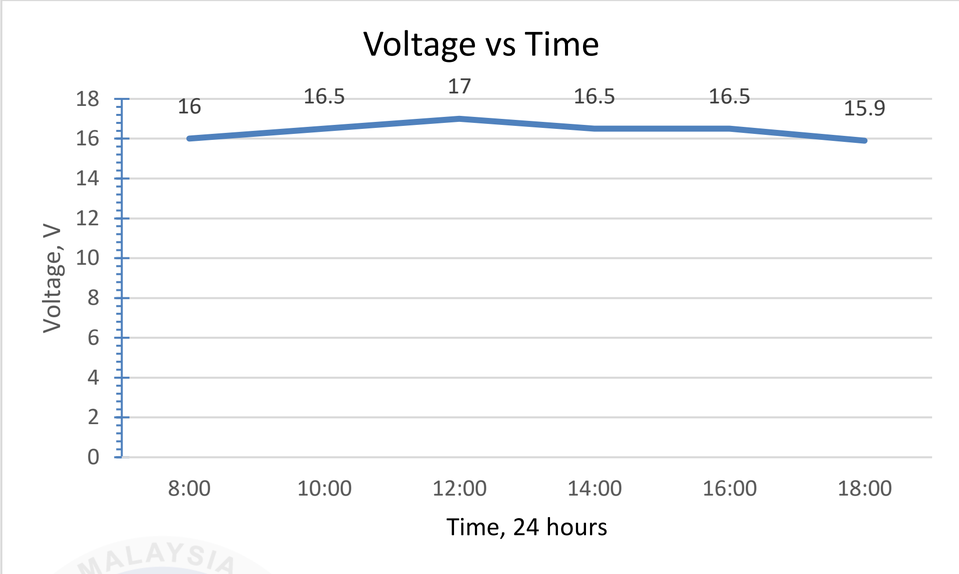

Figure 4.2 Graph voltage versus time.

4.2.3 Day 2

The graphs for day 2 illustrate the current and voltage measured over a 24-hour period. The x-axis represents time in hours, while the y-axis shows the measured values in either amperes (A) for current or volts (V) for voltage. The current graph (Figure 4.3) indicates slight fluctuations throughout the day, with a general increase followed by a decrease. It begins at approximately 0.22 amps at 8:00, peaks at around 0.5 amps at 12:00, and then drops to about 0.2 amps by 18:00. The voltage graph (Figure 4.4) shows a similar trend to the current graph, starting at around 16.2 volts at 8:00 and ending at approximately 16 volts at 18:00. This graph is slightly similar to the graph on the previous day because of the same weather.

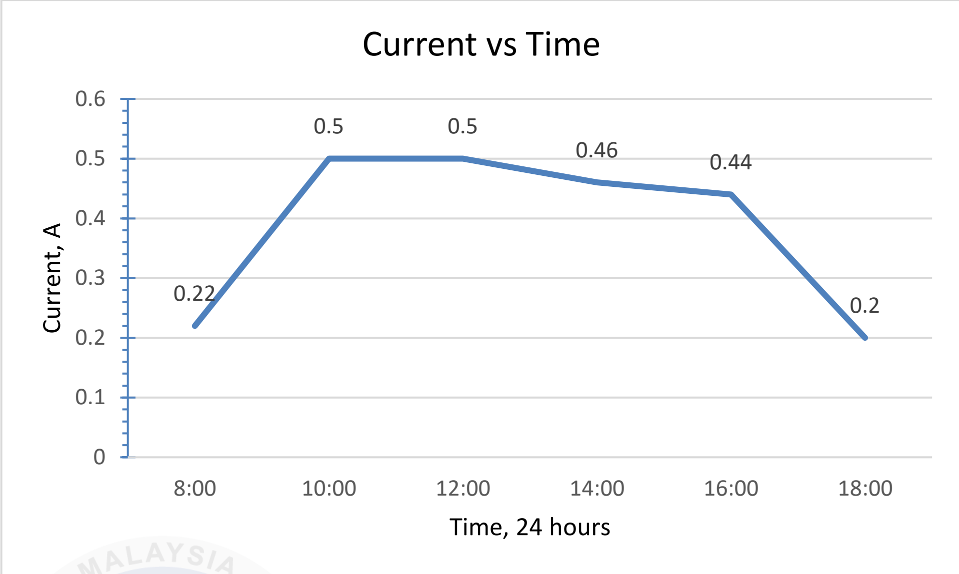

Figure 4.3 Graph current versus time.

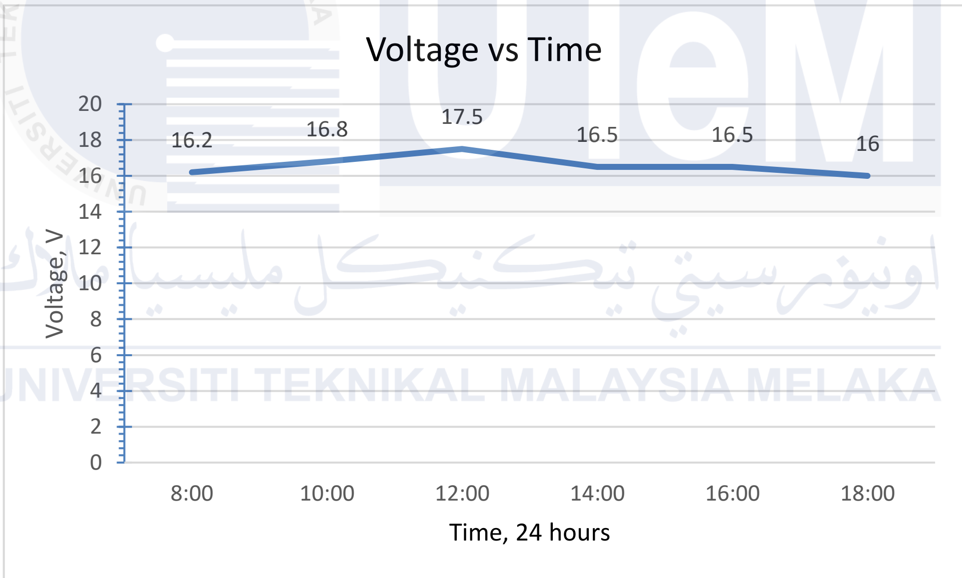

Figure 4.4 Graph voltage versus time.

4.2.4 Day 3

The graphs for day 3 illustrate the current and voltage measured over a 24-hour period. The x-axis represents time in hours, while the y-axis shows the measured values in either amperes (A) for current or volts (V) for voltage. The current graph (Figure 4.5) indicates slight fluctuations throughout the day, with a general increase followed by a decrease. It begins at approximately 0.22 amps at 8:00, peaks at around 0.5 amps at 12:00, and then drops to about 0.2 amps by 18:00. The voltage graph (Figure 4.6) shows a similar trend to the current graph, starting at around 16 volts at 8:00 and ending at approximately 16 volts at

18:00. This graph is slightly similar to the graph on the previous day because of the same weather.

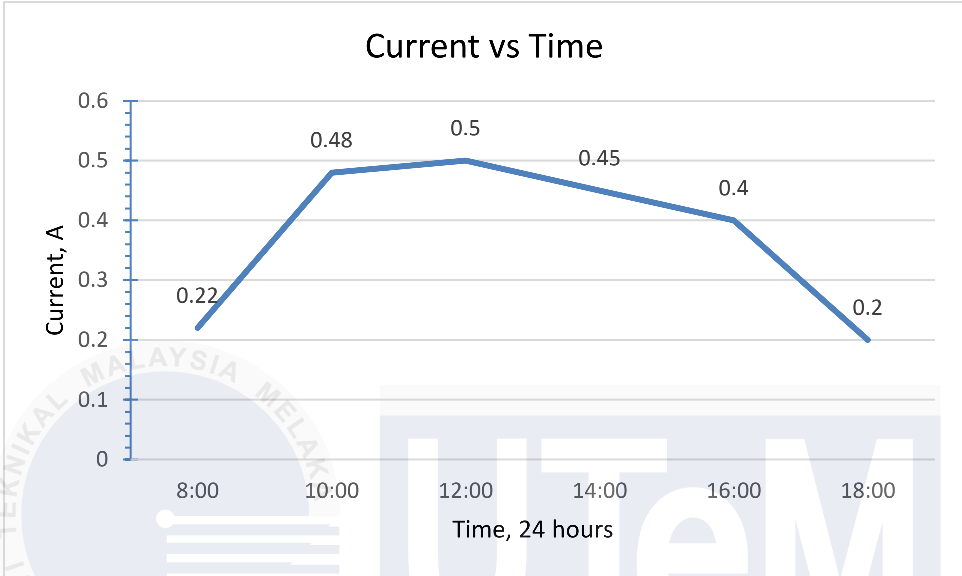

Figure 4.5 Graph current versus time.

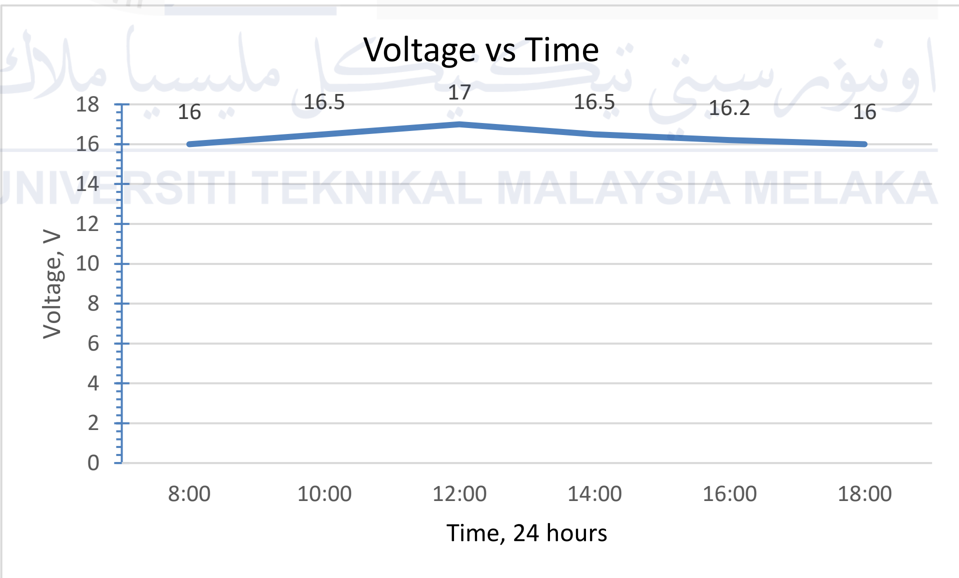

Figure 4.6 Graph voltage versus time.

4.2.5 Day 4

The graphs for day 4 illustrate the current and voltage measured over a 24-hour period. The x-axis represents time in hours, while the y-axis shows the measured values in either amperes (A) for current or volts (V) for voltage. The current graph (Figure 4.7) indicates slight fluctuations throughout the day, with a general increase followed by a decrease. It begins at approximately 0.25 amps at 8:00, peaks at around 0.53 amps at 12:00, and then drops to about 0.2 amps by 18:00. The voltage graph (Figure 4.8) shows a similar trend to the current graph, starting at around 16 volts at 8:00 and ending at approximately 16 volts at 18:00. This graph is slightly similar to the graph on the previous day because of the same weather.

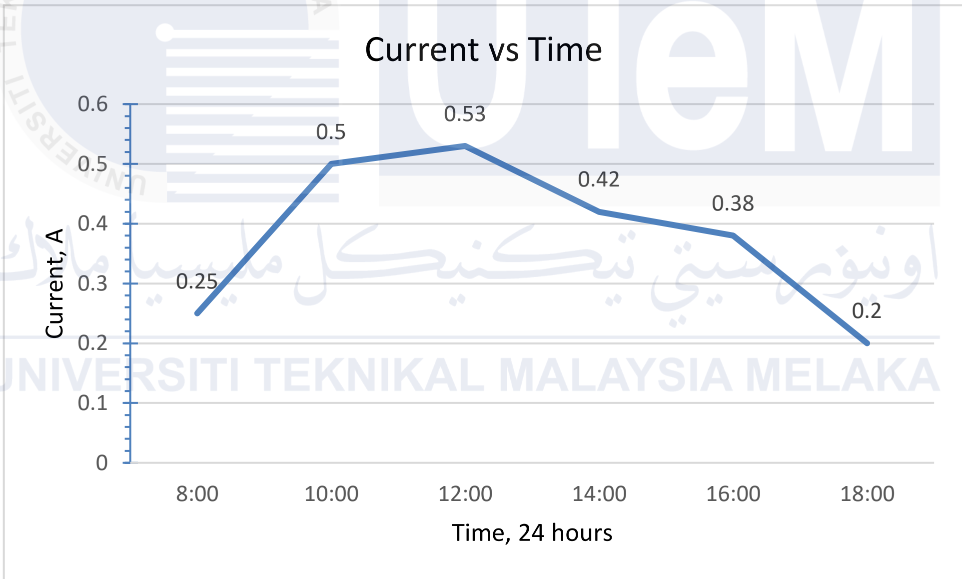

Figure 4.7 Graph current versus time.

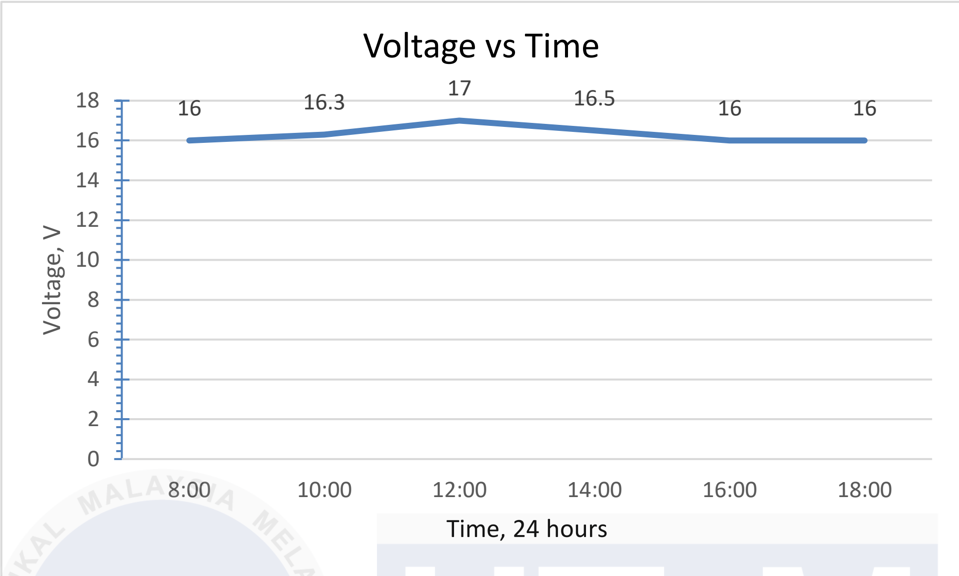

Figure 4.8 Graph voltage versus time.

4.2.6 Day 5

The graphs for day 5 illustrate the current and voltage measured over a 24-hour period. The x-axis represents time in hours, while the y-axis shows the measured values in either amperes (A) for current or volts (V) for voltage. The current graph (Figure 4.9) indicates slight fluctuations throughout the day, with a general increase followed by a decrease. It begins at approximately 0.3 amps at 8:00, peaks at around 0.55 amps at 12:00, and then drops to about 0.35 amps by 18:00. The voltage graph (Figure 4.10) shows a similar trend to the current graph, starting at around 16.2 volts at 8:00 and ending at approximately 15.8 volts at 18:00. This graph is slightly similar to the graph on the previous day because of the same weather.

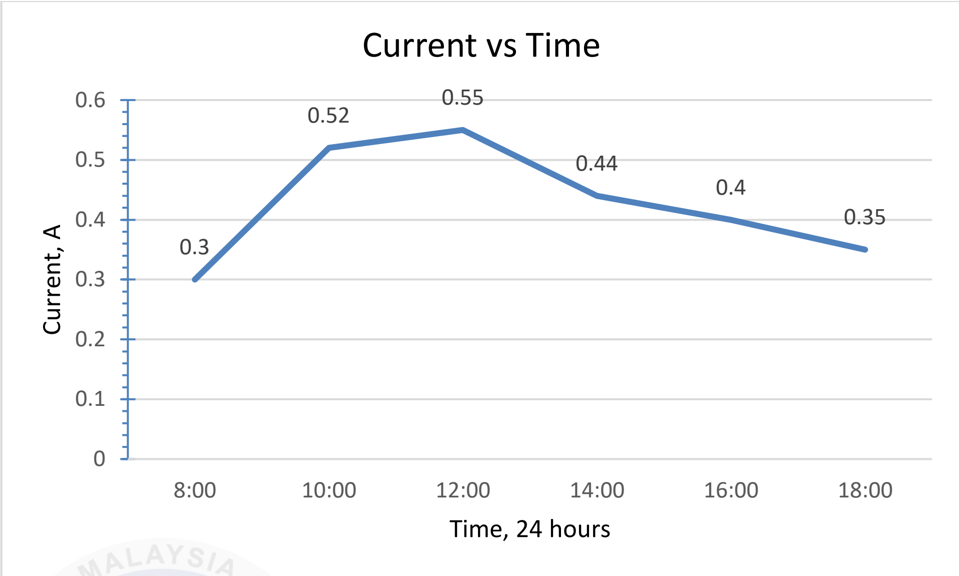

Figure 4.9 Graph current versus time.

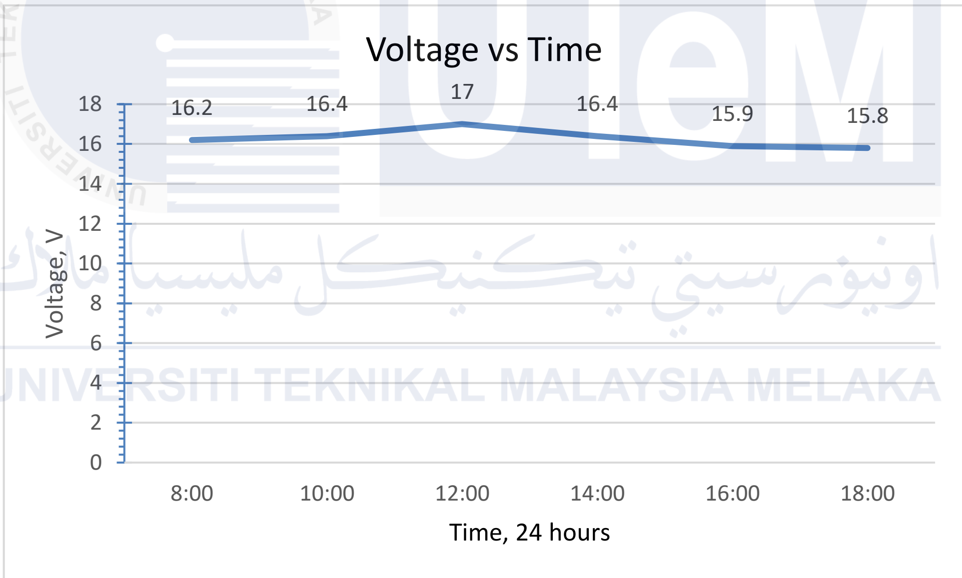

Figure 4.10 Graph voltage versus time.

4.2.7 Combination plot of the data measurement.

The actual short circuit current (Isc) will be different from the current obtained in real-time measurements due to various factors. These include changes in environmental conditions such as temperature and sunlight intensity, which can fluctuate throughout the day and impact solar panel performance. Additionally, real-time measurements may be affected by shading, dust, or other obstructions on the panel surface, which can reduce efficiency. Inaccuracies in measurements can also stem from the quality and calibration of the measuring instruments. Figure 4.11 shows the graph current versus time with short circuit current (Isc).

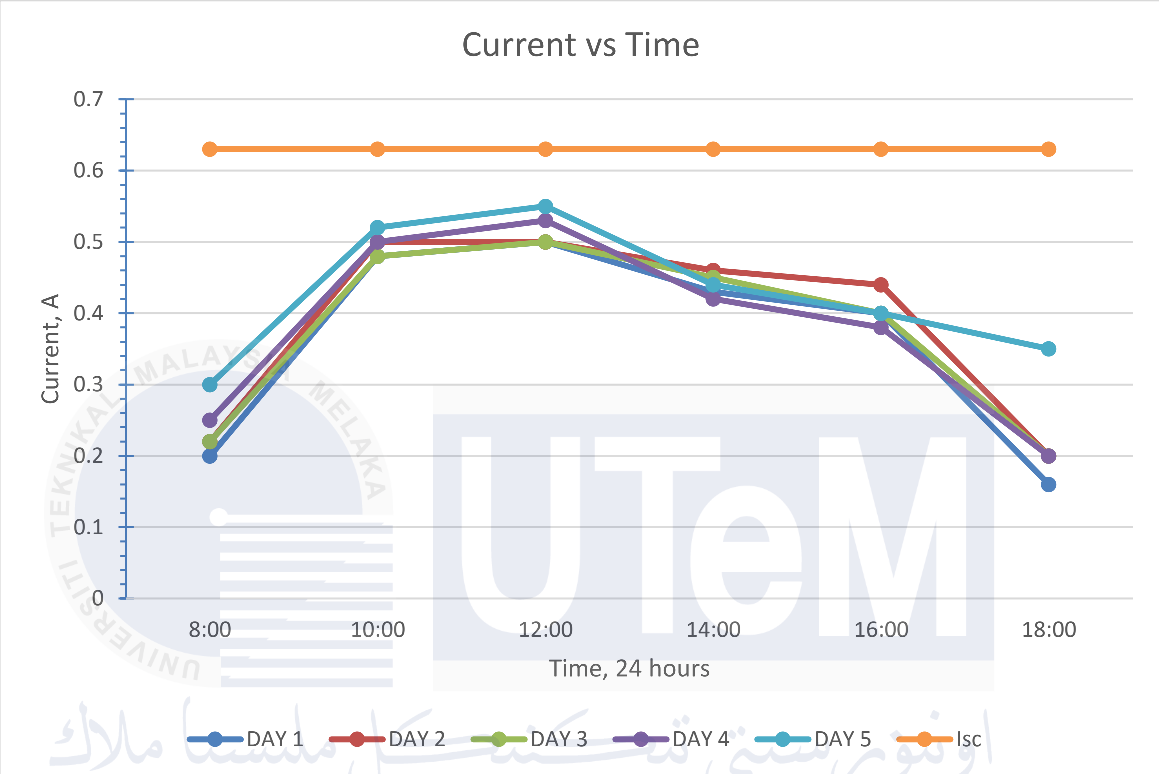

Figure 4.11 Graph current versus time with short circuit current (Isc).

The actual open circuit voltage (Voc) will be different from the voltage obtained in real-time measurements due to several factors. Changes in environmental conditions like temperature, sunlight intensity, and humidity can impact the performance of solar panels over the course of the day. Real-time measurements can also be affected by shading, dirt, or other factors that decrease the panel's efficiency. Moreover, the precision of open circuit voltage (Voc) measurements is heavily influenced by the accuracy and calibration of the measuring instruments used. Figure 4.12 shows the graph Voltage versus time with open circuit voltage (Voc).

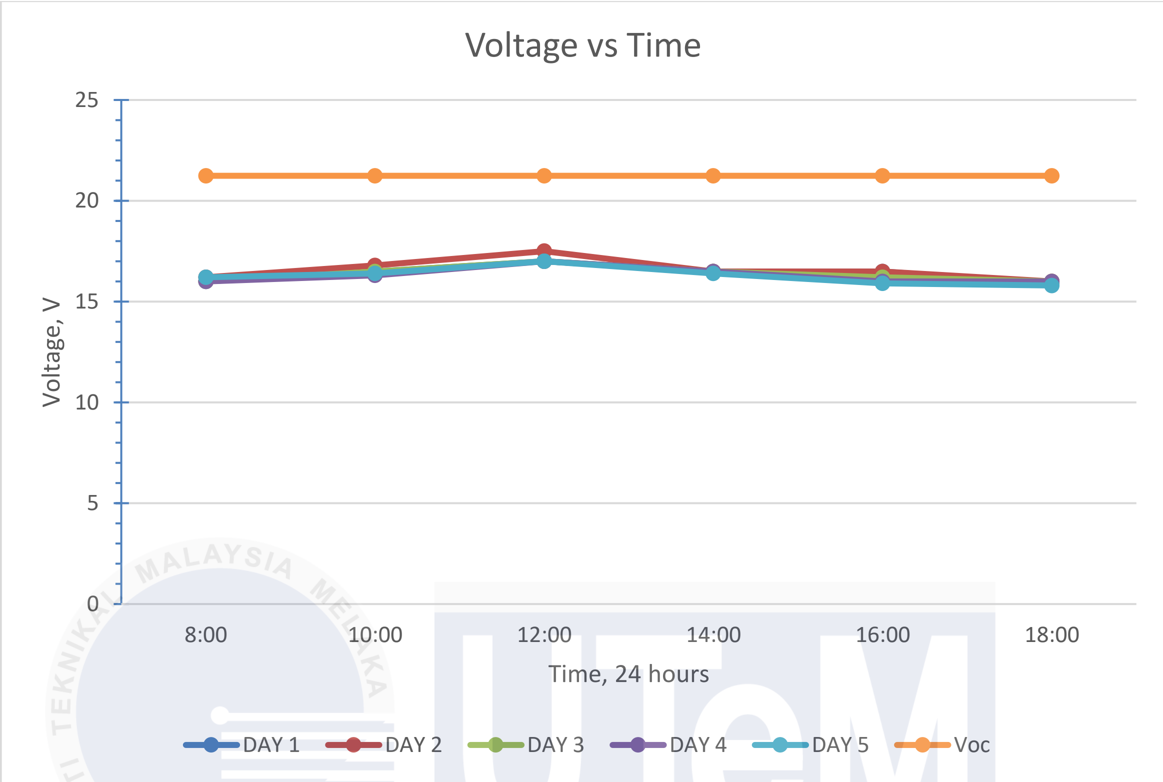

Figure 4.12 Graph Voltage versus time with open circuit voltage (Voc).

Figure 4.13 depicts the power output over time for five days. The x-axis is labeled with time intervals at 8:00, 10:00, 12:00, 14:00, 16:00, and 18:00. The y-axis is labeled in watts, representing power. Each line corresponds to a different day. Day 1 shows the lowest power output, while Day 5 shows the highest. Generally, the power output rises throughout the day, peaking around noon before declining again. Figure 4.13 shows graph power versus time.

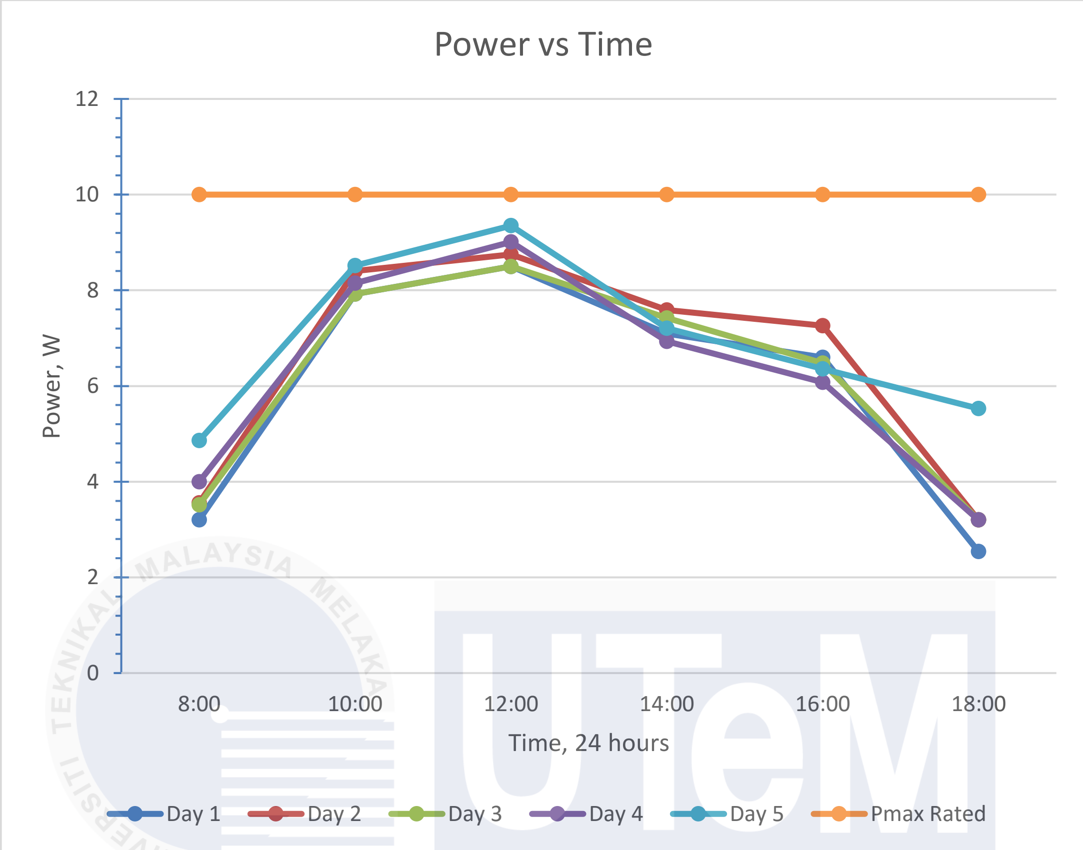

Figure 4.13 Graph power versus time.

4.2.8 Real-time data testing of Solar charging system.

The solar charging system analysis using the PROVA 1011 PV System Analyzer evaluates the performance of a solar panel under varying environmental conditions. It involves measuring critical parameters such as open circuit voltage, short circuit current, maximum power output, efficiency, and fill factor. These metrics provide insights into the panel's ability to convert sunlight into electrical energy and its overall performance relative to its rated specifications. Factors like irradiance and temperature significantly impact the panel's output, with higher irradiance improving performance and elevated temperatures often reducing efficiency. Figure 4.14 shows analysis using the PROVA 1011 PV System.

Figure 4.14 Analysis using the PROVA 1011 PV System.

4.2.9 Real-time data testing on sunny weather.

The solar charging system's performance was evaluated under sunny weather conditions using the PROVA 1011 PV System Analyzer. Key measurements include an open circuit voltage (Voc) of 20.24V and a short circuit current (Isc) of 414mA. The system achieved a maximum power output (Pmax) of 5.434W at a voltage (Vpm) of 14.31V and a current (Ipm) of 379mA. The overall efficiency of the system was recorded at 0.279%, which is considerably lower than expected, possibly due to environmental factors or energy losses. The fill factor (FF) was calculated as 0.646, indicating moderate conversion efficiency relative to theoretical power capability. Figure 4.15 shows data measurement using the PROVA 1011 PV System Analyzer.

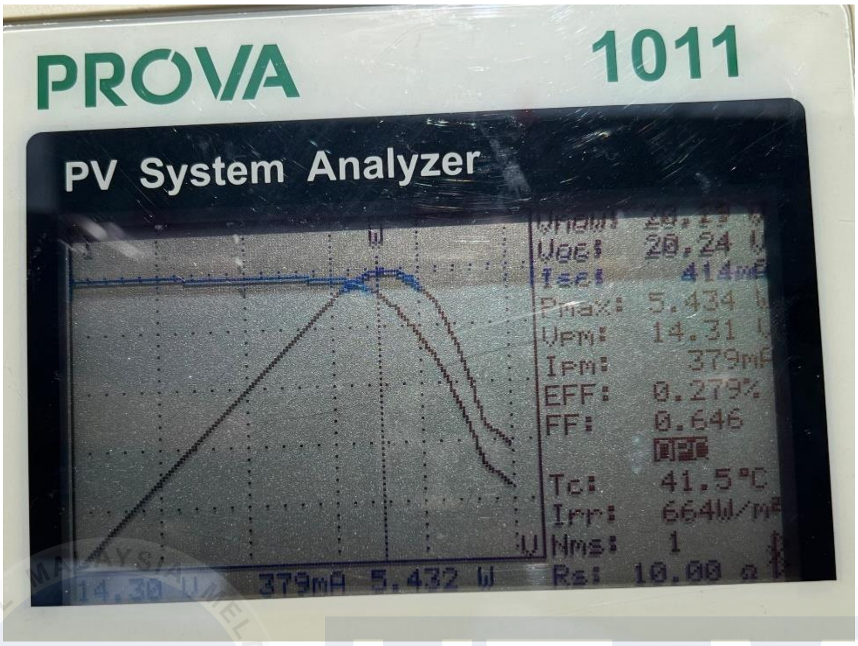

Figure 4.15 Data measurement using the PROVA 1011 PV System Analyzer on sunny weather.

Comparing these results to the solar panel's specifications (Pmax: 10W, Imp: 0.58A, Vmp: 17.5V, Isc: 0.63A, Voc: 21.24V), the measured output is below the rated performance, with the actual maximum power (5.434W) being 54.34% of the rated 10W. This discrepancy could be attributed to several factors, including high panel temperature (Tc: 41.5°C), which negatively impacts voltage, and irradiance (Irr) of 664W/m², which is below the standard test condition (STC) value of 1000W/m². Additionally, the measured operating voltage (Vpm: 14.31V) is lower than the panel's rated maximum power voltage (Vmp: 17.5V), and the operating current (Ipm: 379mA) is below the rated maximum current (Imp: 580mA), indicating suboptimal operating conditions. The solar PV panel specification is presented as in **APPENDIX B**.

4.2.10 Real-time data testing on cloudy weather.

The solar charging system's performance was analyzed under cloudy weather conditions using the PROVA 1011 PV System Analyzer. Key measurements showed an open circuit voltage (Voc) of 19.18V and a short circuit current (Isc) of 154mA. The system achieved a maximum power output (Pmax) of 2.003W at a voltage (Vpm) of 17.32V and a current (Ipm) of 115mA. The overall efficiency was recorded at 0.103%, reflecting the limited power generation capability under low irradiance. The fill factor (FF) was calculated as 0.674, indicating relatively good utilization of theoretical power capacity despite the cloudy conditions. Figure 4.16 shows data measurement using the PROVA 1011 PV System Analyzer on cloudy weather.

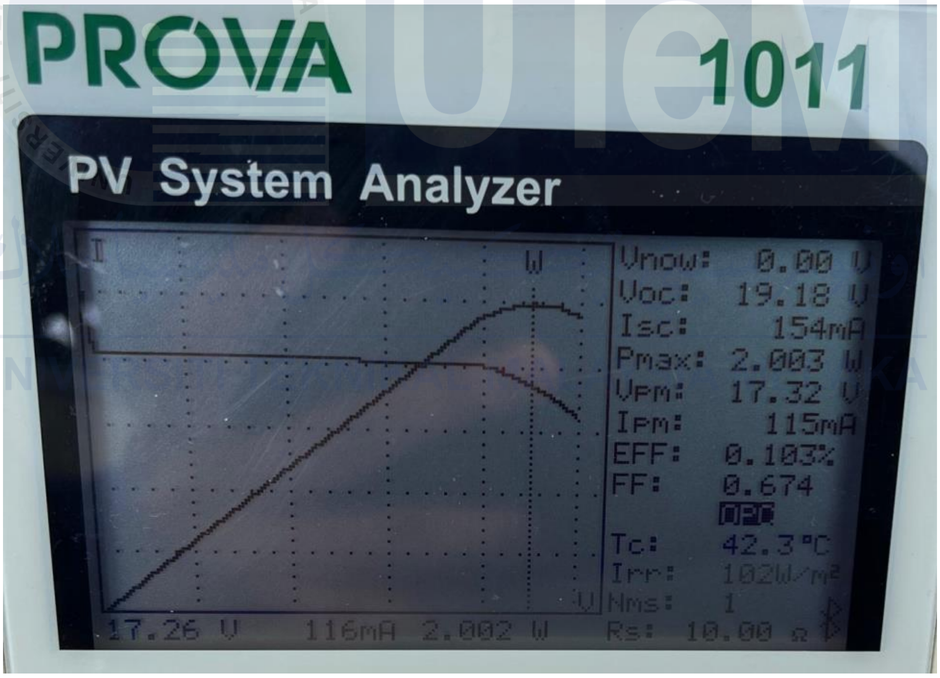

Figure 4.16 Data measurement using the PROVA 1011 PV System Analyzer on cloudy weather.

When compared to the solar panel's specifications (Pmax: 10W, Imp: 0.58A, Vmp: 17.5V, Isc: 0.63A, Voc: 21.24V), the actual output was significantly lower. The maximum power output (2.003W) was only 20.03% of the rated capacity. This reduced performance is primarily due to the low irradiance level of 102W/m², which is well below the standard test condition (STC) value of 1000W/m². Additionally, the panel's operating current (Ipm:

115mA) was far below the rated maximum current (Imp: 580mA), while the operating voltage (Vpm: 17.32V) closely matched the rated maximum power voltage (Vmp: 17.5V). The solar PV panel specification is presented as in **APPENDIX B**.

4.2.11 Real-time data testing of temperature on solar PV panel.

The temperature analysis of the solar PV panel using the fluke pro thermal camera reveals with the average temperature of 42.0°C. The temperature distribution from the top to the bottom of the panel shows a slight variation, with the top of the panel measuring 42.4°C and the bottom measuring 41.2°C. This indicates that the solar panel's surface temperature is relatively uniform, with only a small gradient between the top and bottom sections. The difference of 1.2°C is typical in solar panels as heat tends to accumulate more at the top due to exposure to sunlight. This temperature distribution could influence the panel's efficiency, as higher temperatures generally result in reduced energy conversion efficiency. Figure 4.17 shows data fluke pro thermal camera.

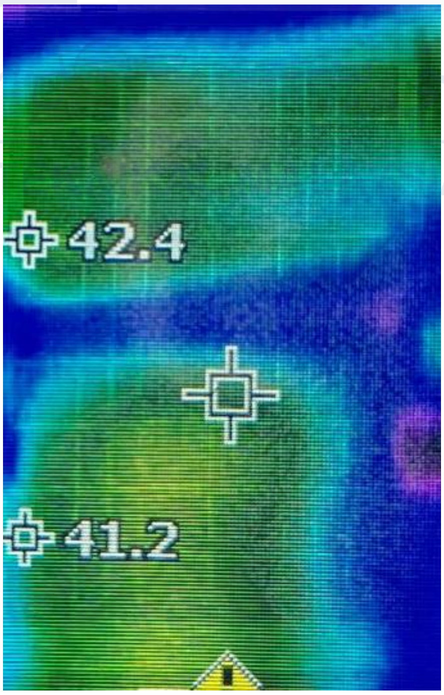

Figure 4.17 Figure 4.17 data fluke pro thermal camera.

4.2.12 Analysis of rechargeable Battery 12V.

Table 4.7 shows the estimated charging progress of a 12V 5Ah sealed lead-acid battery using a 10W polycrystalline solar panel and a PWM charge controller. The charging starts with the battery at 11.63V (0% capacity) and gradually increases until it is fully charged at 12.89V (100% capacity). At 50% capacity, the voltage is about 12.23V, which takes around 3 hours of charging. It takes approximately 6 to 10+ hours to fully charge the battery, depending on sunlight availability. The table highlights how the battery voltage and capacity increase over time during charging. Figure 4.18 shows graph voltage versus time.

Table 4.7 Performance Rechargeable Battery 12V when charging

Time to charge (Hours)	Voltage (V)	Battery capacity (%)
10+	11.63	0%
9	11.70	10%
7.5	11.81	20%
6	11.96	30%
4.5	12.11	40%
3	12.23	50%
2	12.41	60%
1.5	12.51	70%
1	12.65	80%
0.5	12.78	90%
0	12.89	100%

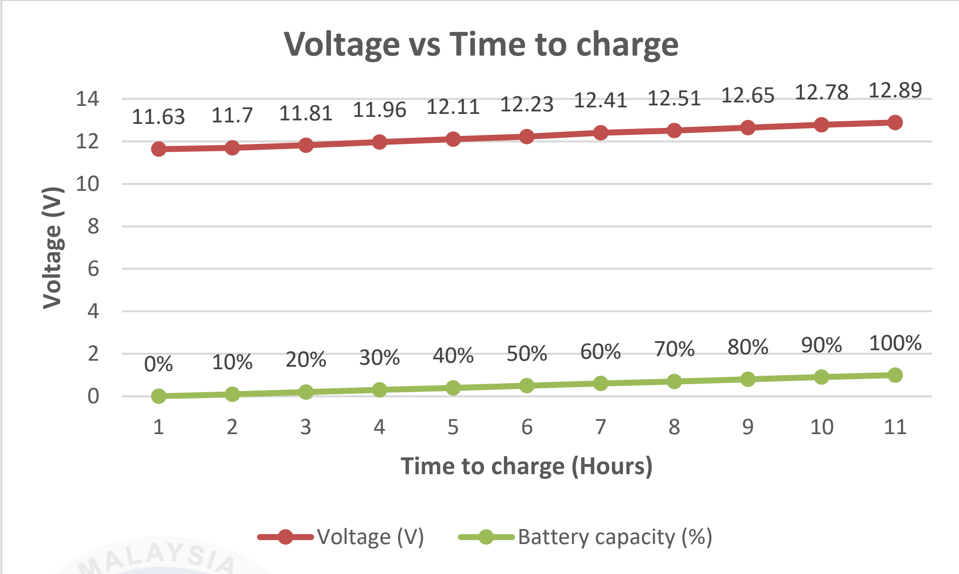

Figure 4.18 Graph voltage versus time.

4.3 Data and analysis of the fish tank waste cleaner's circuitry.

The analysis of the fish tank waste cleaner device includes various tests and simulations to evaluate its functionality and performance. Simulation results confirm that all integrated components, such as the ESP8266 microcontroller, IR sensor, motor driver, DC motors, and water pump, work effectively within the system. The performance of the 9V rechargeable battery was analyzed both during charging and under load, showing stable voltage levels. The IR sensor and water pump were also tested for functionality, ensuring they operated as expected. Manual mode tests were conducted in forward, reverse, and turn right/left conditions, confirming the device's mobility and control. Auto mode tests were performed for both object detection and non-detection scenarios, validating the system's ability to respond accordingly. Additionally, the buoyant force of the device was considered to ensure proper sinking and stability in the water. Finally, real-time experiments demonstrated the overall effectiveness of the fish tank waste cleaner, confirming its operational reliability in cleaning tasks.

4.3.1 Simulation result of the fish tank waste cleaner.

The project comprises several crucial components, each with specific functions. The ESP8266 microcontroller, which has been tested and verified to work correctly, acts as the central control unit. The IR sensor, also functioning properly, is utilized for obstacle detection. The relay module, which is operational, controls the system's electrical circuits, allowing the switching of the water pump. The DC water pump, which has been tested and confirmed to be working, suctions waste from the tank. The motor driver, also functioning as expected, controls the DC motors that provide mobility to the cleaner. Finally, the DC motors themselves are operational and move the cleaner around the tank. Each component has been tested to ensure proper functionality. Table 4.8 outlines the functionality of these components.

Table 4.8 Simulation functionality test

No.	Component	Functionality
1.	ESP8266	OK
2.	IR sensor	OK
3.	Relay module	OK
4.	DC water pump	OK
5.	Motor driver	OK
6.	DC motor	OK

4.3.2 Analysis Rechargeable Battery 9V.

Table 4.9 shows that the 9V rechargeable battery maintains a steady voltage of 9.2V up to 36 minutes, then suddenly drops to 0.1V. This happens because the battery's internal protection circuit (PCM) activates to prevent over-discharge. The PCM detects when the battery's charge is almost completely used up and cuts off the power to protect the battery from damage. When the battery briefly reconnects the battery to a charger, the PCM resets, and the voltage appears normal again (9.2V). However, the battery quickly drops back to 0.1V under load because it is nearly empty. This protection mechanism helps keep the battery safe and extends its lifespan. Figure 4.19 shows graph voltage versus time.

Table 4.9 Performance Rechargeable Battery 9V on load

Time (minutes)	**Voltage (V)**
0	9.2
5	9.2
10	9.2
15	9.2
20	9.2
25	9.2
30	9.2
36	0.1

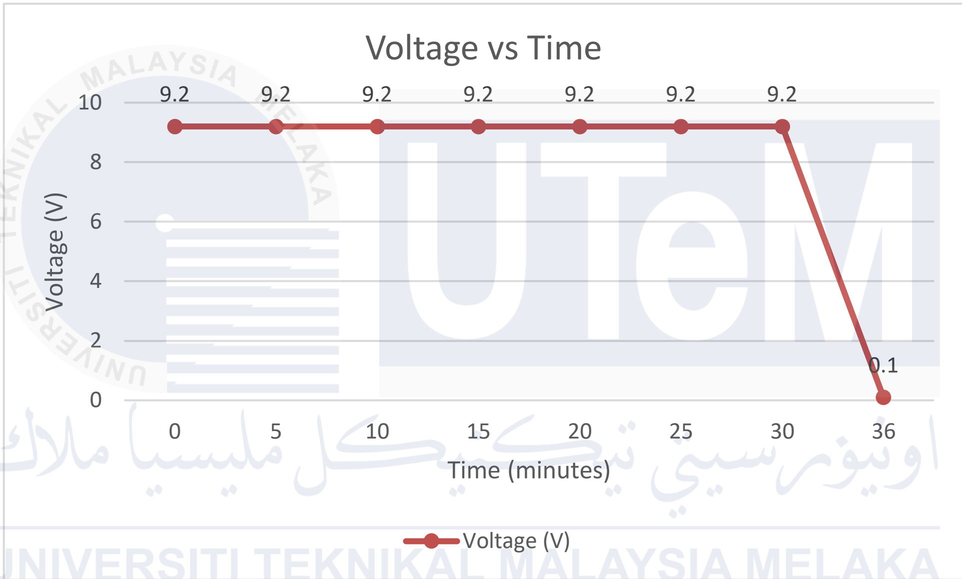

Figure 4.19 Graph voltage versus time.

4.3.3 Rechargeable Battery 9V when charging.

The table 4.10 illustrates the approximate charging percentages of the GTL Energy rechargeable 9V lithium-ion battery, assuming a charging time of 4.5 hours (average of 4–5 hours) with a constant charging current of 200mA. Based on the battery's 1000mAh capacity, it takes approximately 5 hours (1000 ÷ 200 = 5 hours) for a full charge, with charging percentages calculated linearly over time. During the charging process, the red light remains illuminated, indicating the battery is still charging, while the green light activates once the battery reaches full charge (100%). The table assumes the battery is charged using a USB Type-C port delivering a consistent 200mA current, which is the maximum supported by the battery's charging specifications. If a lower-current USB port is used, the charging time may increase. Figure 4.20 shows graph charging percentage versus time.

Table 4.10 Performance Rechargeable Battery 9V when charging

Time (Hours)	Time (Minutes)	Charging Percentage (%)	Charging Indicator
0.0	0	0%	Red Light
0.5	30	11%	Red Light
1.0	60	22%	Red Light
1.5	90	33%	Red Light
2.0	120	44%	Red Light
2.5	150	56%	Red Light
3.0	180	67%	Red Light
3.5	210	78%	Red Light
4.0	240	89%	Red Light
4.5	270	100%	Green Light

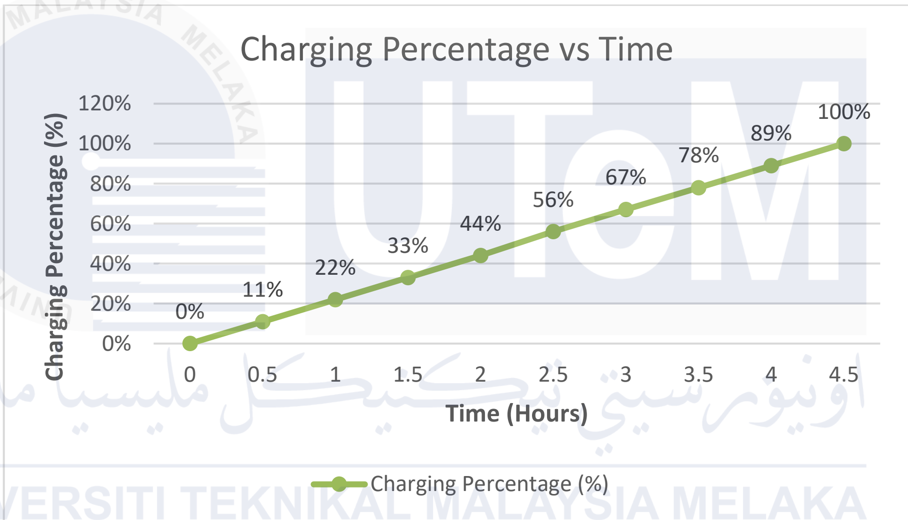

Figure 4.20 Graph charging percentage versus time.

4.3.4 IR Sensor functionality test.

Table 4.11 shows the results of a functionality test performed on an IR sensor. The test aimed to verify the sensor's ability to detect obstacles. 10 individual tests were conducted. Across 10 tests, the IR sensor successfully detected the obstacle, as indicated by the "OK" result for each test. This demonstrates that the IR sensor is functioning correctly and reliably detects obstacles within its range.

Table 4.11 Functionality test of IR Sensor

Number of tests	Detected
1	OK
2	OK
3	OK
4	OK
5	OK
6	OK
7	OK
8	OK
9	OK
10	OK

4.3.5 Water pump functionality test.

Table 4.12 summarizes the functionality tests conducted on the water pump under different power switch conditions. Across 10 tests, the water pump operates correctly when the power switch is turned ON, keeping the water pump ON. Similarly, when the power switch is turned OFF, the water pump turns OFF as expected. In all cases, the functionality of the system is marked as OK, indicating that the water pump operates reliably and as designed under both ON and OFF conditions of the power switch. This consistency confirms the system's proper functionality and responsiveness to the power switch state.

Table 4.12 Functionality test of water pump

Number of tests	Power Switch	Water Pump	Power Switch	Water Pump	Functionality
1	ON	ON	OFF	OFF	OK
2	ON	ON	OFF	OFF	OK
3	ON	ON	OFF	OFF	OK
4	ON	ON	OFF	OFF	OK
5	ON	ON	OFF	OFF	OK
6	ON	ON	OFF	OFF	OK
7	ON	ON	OFF	OFF	OK
8	ON	ON	OFF	OFF	OK
9	ON	ON	OFF	OFF	OK
10	ON	ON	OFF	OFF	OK

4.3.6 Manual mode analysis on forward condition.

Table 4.13 presents the results of 10 tests conducted in manual mode under the forward condition. In each test, the virtual forward button is activated (ON), causing both Motor 1 and Motor 2 to move forward while the water pump remains operational (ON). The functionality is consistently marked as OK across all tests, confirming that the system operates correctly and reliably in manual mode when the forward condition is engaged. This demonstrates the system's ability to execute forward movement with proper coordination of motors and water pump functionality.

Table 4.13 Results of 10 tests conducted in manual mode under the forward condition

Number of tests	Virtual Forward Button	Motor 1	Motor 2	Water Pump	Functionality
1	ON	Forward	Forward	ON	OK
2	ON	Forward	Forward	ON	OK
3	ON	Forward	Forward	ON	OK
4	ON	Forward	Forward	ON	OK
5	ON	Forward	Forward	ON	OK
6	ON	Forward	Forward	ON	OK
7	ON	Forward	Forward	ON	OK
8	ON	Forward	Forward	ON	OK
9	ON	Forward	Forward	ON	OK
10	ON	Forward	Forward	ON	OK

4.3.7 Manual mode analysis on reverse condition.

Table 4.14 summarizes the outcomes of 10 tests conducted in manual mode under the reverse condition. In each test, the virtual reverse button is activated (ON), causing both Motor 1 and Motor 2 to move in reverse while the water pump remains operational (ON). The functionality is consistently recorded as OK across all tests, indicating that the system performs effectively and reliably in manual mode when the reverse condition is activated. This confirms the system's capability to execute reverse movement with proper coordination between the motors and the water pump.

Table 4.14 Results of 10 tests conducted in manual mode under the reverse condition

Number of tests	Virtual Reverse Button	Motor 1	Motor 2	Water Pump	Functionality
1	ON	Reverse	Reverse	ON	OK
2	ON	Reverse	Reverse	ON	OK
3	ON	Reverse	Reverse	ON	OK
4	ON	Reverse	Reverse	ON	OK
5	ON	Reverse	Reverse	ON	OK
6	ON	Reverse	Reverse	ON	OK
7	ON	Reverse	Reverse	ON	OK
8	ON	Reverse	Reverse	ON	OK
9	ON	Reverse	Reverse	ON	OK
10	ON	Reverse	Reverse	ON	OK

4.3.8 Manual mode analysis on turn right condition.

Table 4.15 presents the results of 10 tests conducted in manual mode under the turn-right condition. When the virtual right button is activated (ON), Motor 1 moves in reverse while Motor 2 moves forward, enabling the system to turn right. Simultaneously, the water pump remains operational (ON). In all tests, the functionality is marked as OK, confirming that the system operates effectively and reliably in executing a right-turn with proper coordination between the motors and the water pump.

Table 4.15 Results of 10 tests conducted in manual mode under the turn right condition

Number of tests	Virtual Right Button	Motor 1	Motor 2	Water Pump	Functionality
1	ON	Reverse	Forward	ON	OK
2	ON	Reverse	Forward	ON	OK
3	ON	Reverse	Forward	ON	OK
4	ON	Reverse	Forward	ON	OK
5	ON	Reverse	Forward	ON	OK
6	ON	Reverse	Forward	ON	OK
7	ON	Reverse	Forward	ON	OK
8	ON	Reverse	Forward	ON	OK
9	ON	Reverse	Forward	ON	OK
10	ON	Reverse	Forward	ON	OK

4.3.9 Manual mode analysis on turn left condition.

Table 4.16 presents the results of 10 tests conducted in manual mode under the turn-left condition. When the virtual left button is activated (ON), Motor 1 moves in forward while Motor 2 moves reverse, enabling the system to turn left. Simultaneously, the water pump remains operational (ON). In all tests, the functionality is marked as OK, confirming that the system operates effectively and reliably in executing a right-turn with proper coordination between the motors and the water pump.

Table 4.16 Results of 10 tests conducted in manual mode under the turn left condition

Number of tests	Virtual Left Button	Motor 1	Motor 2	Water Pump	Functionality
1	ON	Forward	Reverse	ON	OK
2	ON	Forward	Reverse	ON	OK
3	ON	Forward	Reverse	ON	OK
4	ON	Forward	Reverse	ON	OK
5	ON	Forward	Reverse	ON	OK
6	ON	Forward	Reverse	ON	OK
7	ON	Forward	Reverse	ON	OK
8	ON	Forward	Reverse	ON	OK
9	ON	Forward	Reverse	ON	OK
10	ON	Forward	Reverse	ON	OK

4.3.10 Auto mode analysis on not detect object condition

The table 4.17 summarizes the performance of a system operating in auto mode when no object is detected. In all 10 tests conducted, both Motor 1 and Motor 2 consistently moved forward, the water pump remained turned ON, and the system functionality was verified as OK. This indicates that the system performed as expected, maintaining normal operation without any issues in the absence of object detection.

Table 4.17 Results of 10 tests conducted in auto mode under not detect object condition

Number of tests	Detect object	Motor 1	Motor 2	Water Pump	Functionality
1	NO	Forward	Forward	ON	OK
2	NO	Forward	Forward	ON	OK
3	NO	Forward	Forward	ON	OK
4	NO	Forward	Forward	ON	OK
5	NO	Forward	Forward	ON	OK
6	NO	Forward	Forward	ON	OK
7	NO	Forward	Forward	ON	OK
8	NO	Forward	Forward	ON	OK
9	NO	Forward	Forward	ON	OK
10	NO	Forward	Forward	ON	OK

4.3.11 Auto mode analysis on detected object condition

Table 4.18 illustrates the system's operational response upon detecting an object. In Step 1, both Motor 1 and Motor 2 stop, while the water pump remains ON, with functionality performing as expected. Step 2 sees both motors reversing for 0.5 seconds, the water pump staying ON, and functionality remaining intact. Following this, in Step 3, Motor 1 reverses while Motor 2 moves forward for 0.4 seconds, executing a slight right turn, with the water pump continuing to operate as intended. Lastly, in Step 4, when no object is detected, both motors move forward, the water pump stays ON, and the system operates normally. This sequence highlights the system's effective response to object detection, ensuring uninterrupted functionality under varying conditions.

Table 4.18 Results of 10 tests conducted in auto mode under detect object condition

Detect object	Number of steps	Motor 1	Motor 2	Water Pump	Functionality
YES	1	Stop	Stop	ON	OK
YES	2	Reverse (0.5 second)	Reverse (0.5 second)	ON	OK
YES	3	Reverse (0.4 second)	Forward (0.4 second)	ON	OK
NO	4	Forward	Forward	ON	OK

4.4 Real-time result mechanism of fish tank waste cleaner.

The real-time result mechanism of the fish tank waste cleaner involves various stages of testing and design refinement. The real-time trial testing design focuses on evaluating the device's initial functionality and performance in the water, ensuring it can perform the cleaning task effectively. As the design progresses, the real-time improved testing design is implemented to address any issues identified in the trial phase, such as optimizing the movement or improving waste collection efficiency. The real-time detailed testing design further refines the mechanism, ensuring the device maintains proper buoyancy and stability while efficiently collecting debris. Finally, the real-time final testing design is carried out to verify that the system works seamlessly, with adjustments made based on earlier feedback, ensuring that the fish tank waste cleaner operates optimally under all conditions.

4.4.1 Real-time trial testing design.

The real-time trial testing design of the fish tank waste cleaner involved evaluating its functionality and performance in a controlled environment. The design was conducted using a prototype created with 3D printing technology, utilizing 347.41 grams of filament, ensuring a precise and lightweight structure suitable for underwater operations. Detailed assessments included the top and side views of the design to analyze its external structure, alignment, and overall dimensions. Additionally, the inside view of the trial design was examined to ensure proper integration and arrangement of internal components, such as the ESP8266 microcontroller, motor driver, DC motors, IR sensor, water pump, and rechargeable battery. Figures 4.21, 4.22, and 4.23 show the real-time trial testing design using 3D printed, top and side view of trial design fish tank waste cleaner, and inside view of trial design fish tank waste cleaner.

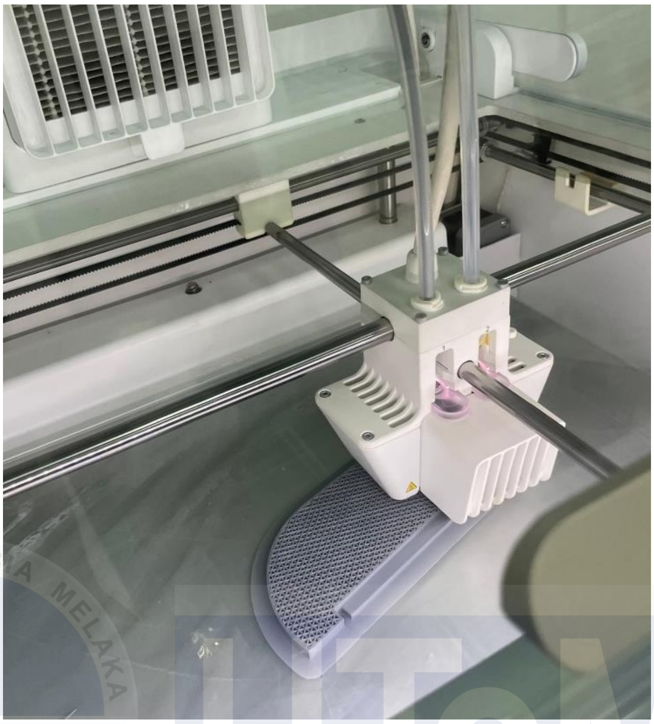

Figure 4.21 Real-time trial testing design using 3D printed

Figure 4.22 Top and side view of trial design fish tank waste cleaner

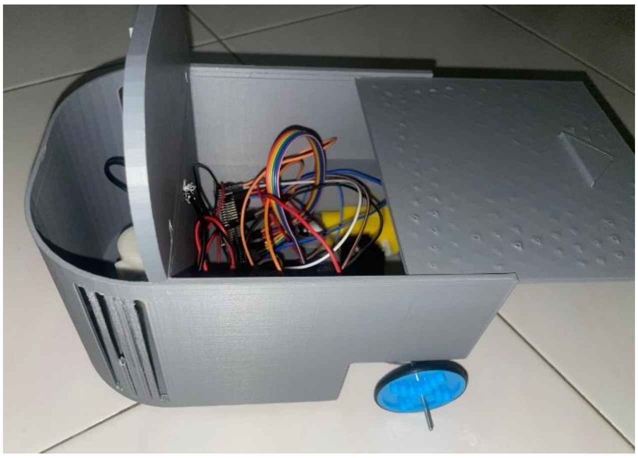

Figure 4.23 Inside view of trial design fish tank waste cleaner

4.4.2 Real-time improved testing design.

The real-time improved testing design of the fish tank waste cleaner involved downscaling the device's size to enhance efficiency within the tank. This updated design maintained the functionality of the original prototype while optimizing its dimensions for better performance in smaller spaces. The top view of the improved design highlighted the compact layout and strategic placement of critical components, including the water pump, motor assembly, and sensors. The side view revealed the streamlined profile of the device, ensuring reduced drag and smoother movement through water. The inside view showcased the restructured internal compartment, with neatly organized electrical components such as the ESP8266 microcontroller, rechargeable battery, and motor driver. Figures 4.24, 4.25, and 4.26 show the top view of improved design fish tank waste cleaner, side view of improved design fish tank waste cleaner, and inside view of improved design fish tank waste cleaner.

Figure 4.24 Top view of improved design fish tank waste cleaner

Figure 4.25 Side view of improved design fish tank waste cleaner

Figure 4.26 Inside view of improved design fish tank waste cleaner

4.4.3 Real-time detailed testing design.

The real-time detailed testing design of the fish tank waste cleaner incorporated additional weight using iron plates to counteract the buoyancy force and ensure the device sank to the bottom of the tank for optimal cleaning performance. The side view of the detailed design displayed the strategic placement of the iron plates along the device's body, ensuring balanced weight distribution for stable operation underwater. The front view highlighted the compact and robust design, with an unobstructed pathway for the cleaning mechanism and water pump to function effectively. Figures 4.27 and 4.28 show the side view of detailed design fish tank waste cleaner, front view of detailed design fish tank waste cleaner.

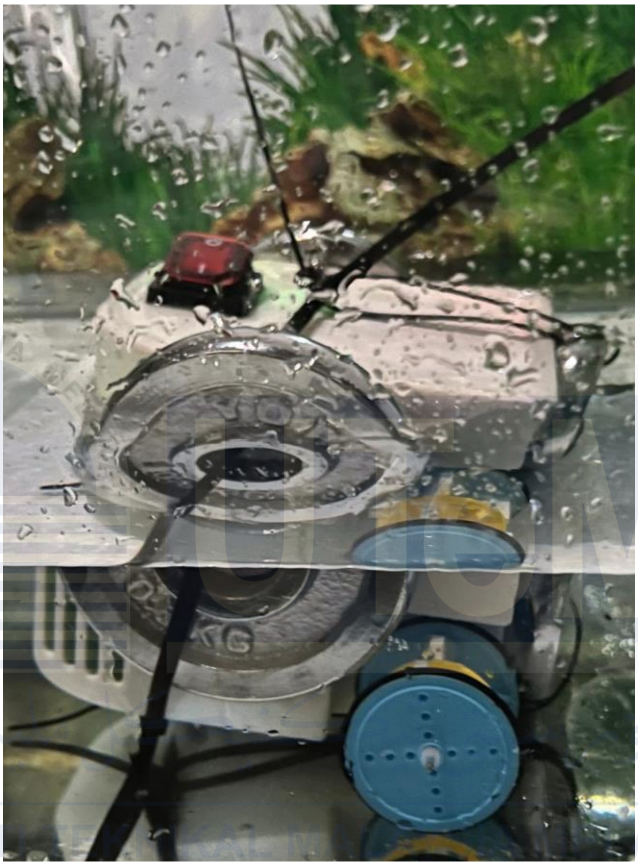

Figure 4.27 Side view of detailed design fish tank waste cleaner

Figure 4.28 Front view of detailed design fish tank waste cleaner

4.4.4 Real-time final testing design.

The real-time final testing design of the fish tank waste cleaner demonstrates the full functionality of the device in action. The overview of the real-time final testing design provides a comprehensive look at how all components are integrated and aligned, ensuring optimal performance. The top view highlights the floating body, constructed from materials like white cork or Styrofoam. The device's propeller, visible from the top, ensures movement across the water surface, while the motor and pump work in unison to keep the system running smoothly. In the real-time performance test on water, the device is shown in action, floating on the tank's surface and efficiently cleaning by sucking up waste, verifying its effectiveness and confirming that the design improvements, such as the use of buoyant materials and the addition of a propeller, contribute to the overall functionality of the cleaner. Figures 4.29, 4.30, and 4.31 show the overview of real-time final testing design, top view of real-time final testing design, and real-time final testing design perform on water.

Figure 4.29 Overview of real-time final testing design.

Figure 4.30 Top view of real-time final testing design.

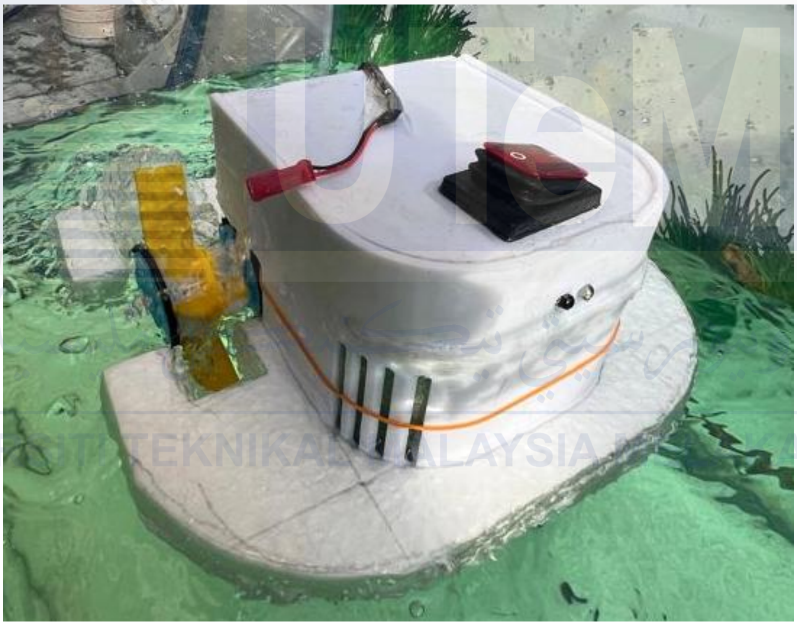
Figure 4.31 Real-time final testing design perform on water.

4.5 Result of IoT system

The IoT system for the fish tank waste cleaner device is powered by the Blynk platform, providing a user-friendly interface for real-time monitoring and control. Through the Blynk application on a smartphone, this project can effortlessly manage the device's operations, including switching between manual and auto modes, controlling motor movement, and activating the water pump.

4.5.1 Blynk interface of a fish tank waste cleaner device.

The Blynk interface for the fish tank waste cleaner device utilizes five virtual buttons to control the device's operation, offering both manual and automatic modes. The virtual pins in the Blynk app are mapped as follows: V0 is used to toggle between auto and manual mode, with auto mode enabling the system to function autonomously based on sensor input, while manual mode allows for direct control via the other buttons. In manual mode, V1 controls moving the device forward, V2 reverses its direction, V3 turns it right, and V4 turns it left. These buttons send signals to the ESP8266 microcontroller, which then activates the corresponding motor control functions (e.g., moveForward(), moveReverse(), turnRight(), turnLeft()). Additionally, the system can activate the water pump based on the mode and manual control inputs, ensuring optimal operation during waste cleaning. When auto mode is activated, the device uses an IR sensor to detect objects in its path, and if an obstacle is detected, the device automatically reverses, turns, and moves forward again to continue cleaning. Figures 4.32, 4.33, and 4.34 show blynk interface on manual mode, blynk interface on auto mode, blynk interface of blynk cloud on laptop.

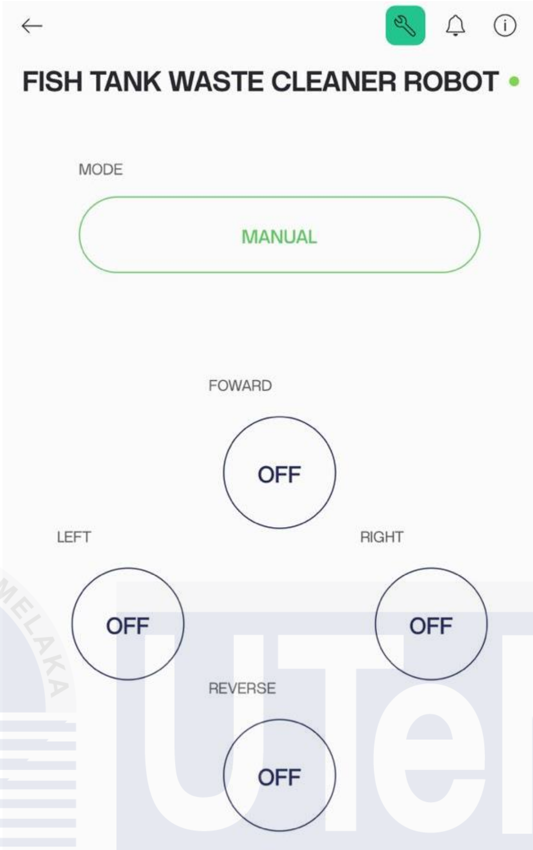

Figure 4.32 Blynk interface on manual mode.

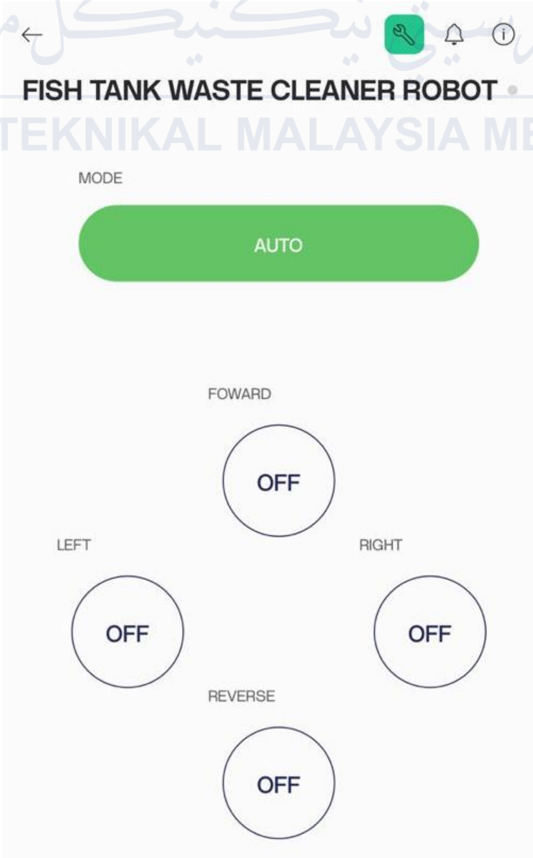

Figure 4.33 Blynk interface on auto mode.

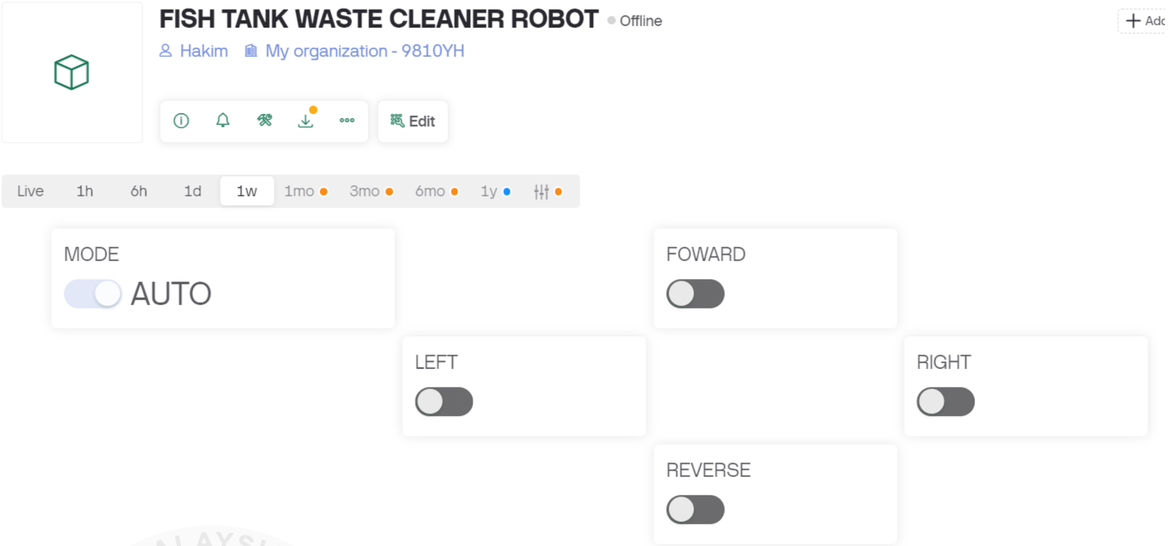

Figure 4.34 Blynk interface of blynk cloud on laptop.

4.6 Result performance analysis on fish tank waster cleaner.

The performance analysis of the fish tank waste cleaner demonstrates its efficiency and adaptability across various conditions. Result buoyant force of fish tank waste cleaner revealed that the detailed design (Case A) successfully countered buoyancy by adding iron plates, allowing the device to fully submerge; however, it became too heavy to move. In the real-time result on detailed design of fish tank waste cleaner device (Case A), the added weight ensured stability but hindered mobility, highlighting the need for redesign. The real-time result on final design of fish tank waste cleaner device (Case B) introduced a floating mechanism using white cork and a propeller for movement, resolving the weight issue while effectively collecting debris through a water pump tube. Finally, the real-time result on auto mode to cover all areas in the fish tank showed the device's ability to navigate all eight designated points, completing the task in 1 minute and 42 seconds. While certain points took longer due to corners, the device’s IR sensor and motor performed reliably, demonstrating its capability for comprehensive cleaning.

4.6.1 Result buoyant force of fish tank waste cleaner.

The buoyant force acting on the fish tank waste cleaner device is calculated based on the fluid type (water) with a density of 1000 kg/m^3 and a displaced volume of 1,404,000 mm^3, resulting in a buoyant force of 13.769 N. This indicates that the displaced water has a mass of 1.404 kg. To ensure the device sinks to the bottom of the tank, three 0.5 kg iron plates were added, increasing the device's total mass. This added weight counters the upward buoyant force, allowing the device to overcome the upthrust and maintain stability at the bottom of the tank for effective operation. Figure 4.22 shows buoyant force testing of the fish tank waste cleaner device for 15 minutes.

Figure 4.22 Buoyant force testing of the fish tank waste cleaner device for 15 minutes.

4.6.2 Real time result on detailed design of fish tank waste cleaner device (case A).

In the real-time experiment, the fish tank waste cleaner device was initially tested with the water level set at half the height of the device, enabling it to remain submerged and operational at the bottom of the tank. This controlled adjustment ensured stability and effective waste cleaning performance. The added weight of an iron plate attached to the device's body provided sufficient balance and sinkability, allowing it to stay securely at the bottom. The device was controlled in real time using the Blynk application on a smartphone, enabling smooth and responsive movement across the tank bottom. This setup successfully demonstrated the device's capability to clean fish tank waste efficiently under practical conditions.

However, when the aquarium was filled to its maximum water level, resulting in the device being fully submerged, several challenges arose. The ESP8266 microcontroller, which relies on Wi-Fi connectivity, automatically disconnected due to water's interference with signal transmission, rendering remote control functionality ineffective. Additionally, the weight of the device, compounded by the added iron plate, exceeded the motor's capacity to generate enough thrust for movement. While other components, such as the water pump and cleaning mechanism, continued to function as intended, the inability to maintain Wi-Fi connectivity and movement limited the overall performance under fully submerged conditions. These findings highlight the need for further design adjustments, such as improved connectivity solutions and higher-torque motors, to optimize the device for fully submerged operation.

Figures 4.35, 4.36, and 4.37 show real time overview of fish tank waste cleaner device, top view of real time result of fish tank waste cleaner device, and real time controlling using the Blynk application.

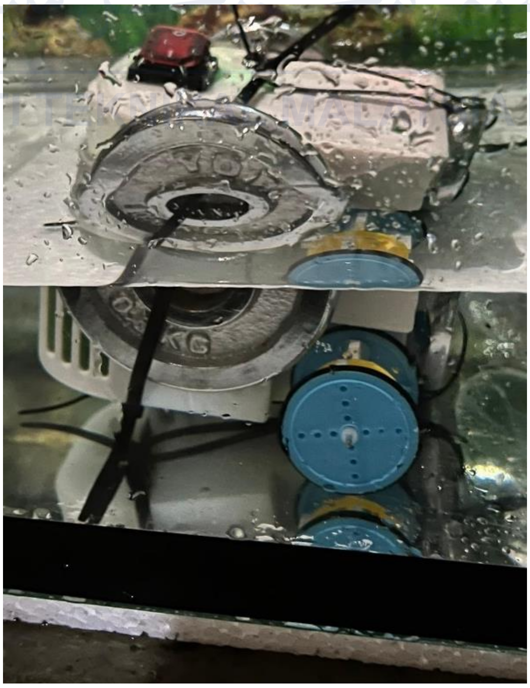

Figure 4.35 Real time overview of fish tank waste cleaner device.

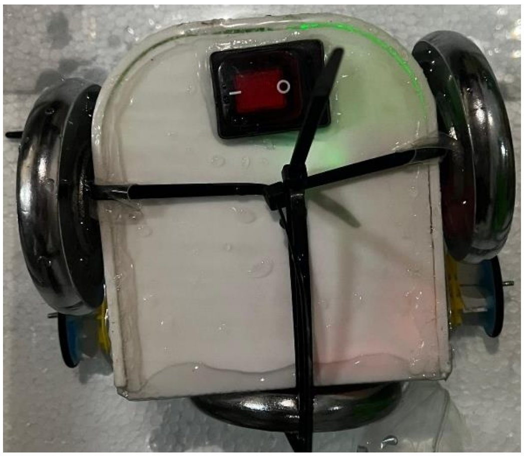

Figure 4.36 Top view of real time result of fish tank waste cleaner device.

Figure 4.37 Real time controlling using the Blynk application

4.6.3 Real time result on final design of fish tank waste cleaner device (case B).

The real-time testing of the final design for the fish tank waste cleaner device (Case B) demonstrated significant improvements over the previous iterations. To address the issue of the device being unable to move due to excessive weight, the redesign incorporated a floating mechanism using a white cork base layer, which provided buoyancy. This modification eliminated the need for the heavy iron plates, allowing the motor to function efficiently without being burdened by excess weight. Additionally, a propeller was installed at the rear of the device to enable smooth movement on the water's surface.

A tube was also integrated into the design, extending from the water pump to the bottom of the tank, to effectively suck debris and waste from the tank floor. The real-time results showed that the floating method successfully resolved the movement issues, with the device operating smoothly in both manual and auto modes, controlled via the Blynk application on a smartphone. The ESP8266 microcontroller maintained a stable Wi-Fi connection throughout the operation, ensuring seamless remote control and monitoring. The waste collection system, powered by the water pump and the attached tube, effectively gathered debris from the tank, demonstrating the device's efficiency and reliability in practical conditions. These results highlight the effectiveness of the final design in overcoming previous limitations and achieving optimal performance. Figure 4.38 Real time overview on final design of fish tank waste cleaner device. Figure 4.39 Real time overview on running forward condition. Figures 4.38, 4.39, 4.40, 4.41, and 4.42 show the real time overview on final design of fish tank waste cleaner device, real time overview on running forward condition, real time controlling of final design using the Blynk application, real time result of collecting waste using waterpump, and real time result of flowing water using waterpump.

Figure 4.38 Real time overview on final design of fish tank waste cleaner device.

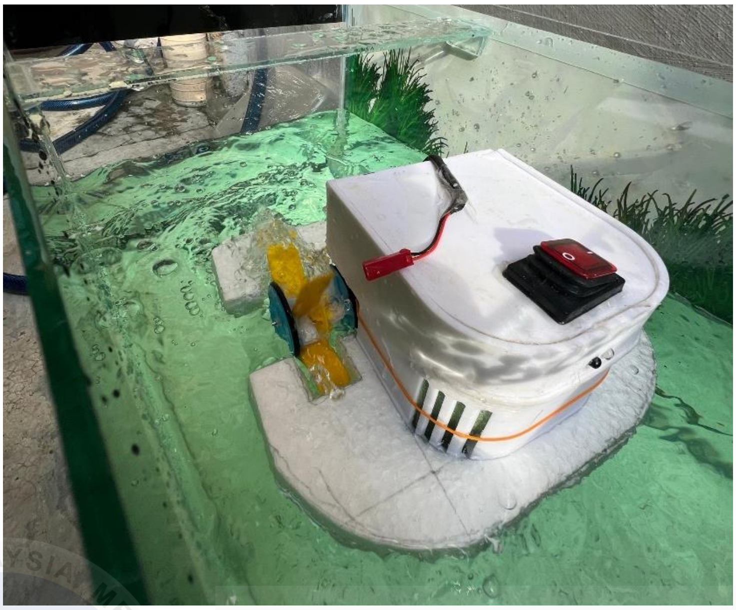

Figure 4.39 Real time overview on running forward condition.

Figure 4.40 Real time controlling of final design using the Blynk application.

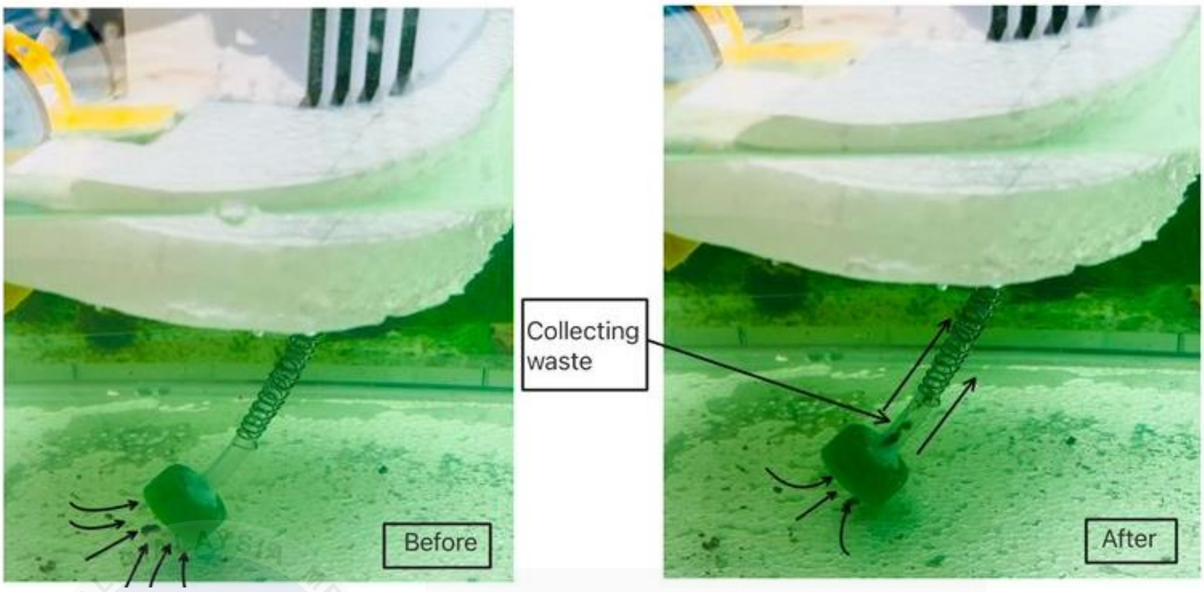

Figure 4.41 Real time result of colleting waste using waterpump.

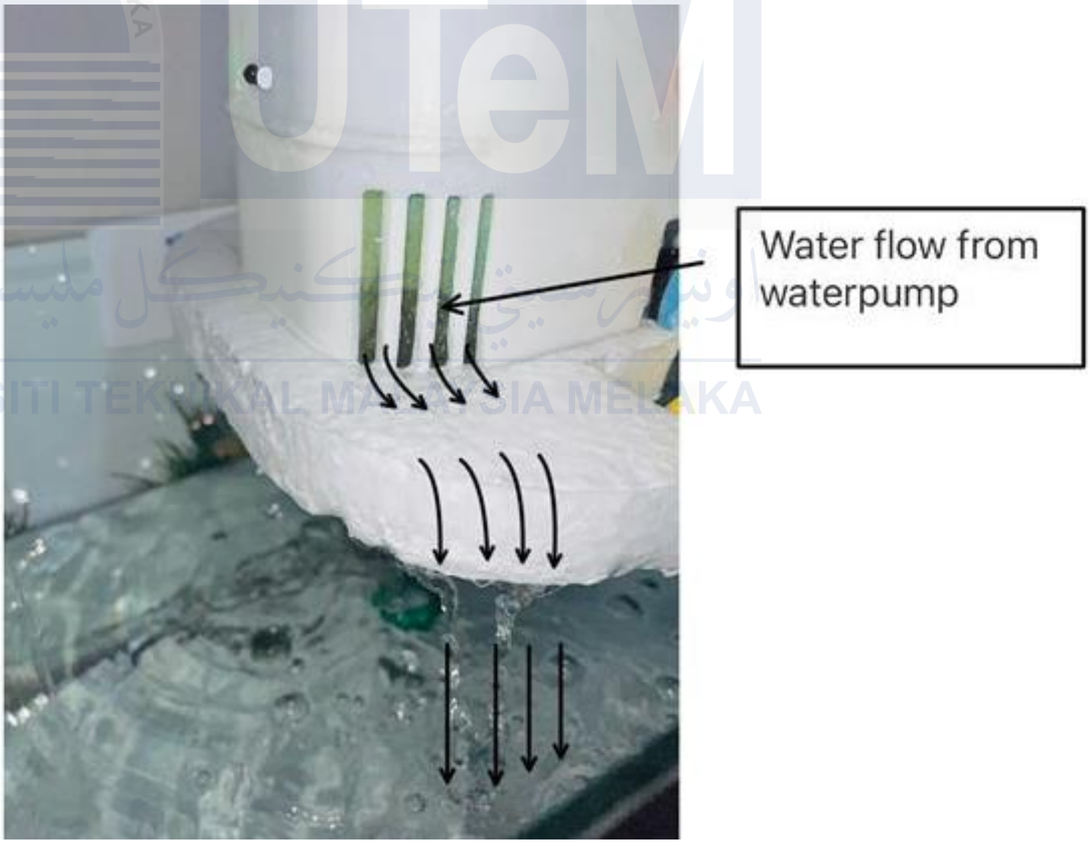

Figure 4.42 Real time result of flowing water using waterpump.

4.6.4 Real time result on auto mode to cover all area in fish tank.

To evaluate the performance of the fish tank waste cleaner, eight specific points (A, B, C, D, E, F, G, H) were marked to ensure the device covered the entire fish tank. Using a stopwatch on a smartphone, the time taken to reach each point was recorded as follows: point 1 (13.09 seconds), point 2 (11.18 seconds), point 3 (6.11 seconds), point 4 (17.73 seconds), point 5 (6.41 seconds), point 6 (34.23 seconds), point 7 (11.63 seconds), and point 8 (1.61 seconds). The total time to cover all areas was 1 minute and 42.03 seconds. Certain points, such as point 6, required more time due to the corners of the aquarium, which made it slightly challenging for the IR sensor to detect obstacles and for the motor to make precise turns. However, this was not a significant issue, as the IR sensor successfully detected obstacles, and the motor adjusted its path, albeit with slightly longer lap times at specific points. To address this, using a larger aquarium would allow for smoother navigation and reduce the time taken to cover corner areas, further optimizing the device's performance. Table 4.19 shows the real time result on auto mode to cover all area in fish tank.

Table 4.19 Real time result on auto mode to cover all area in fish tank.

Point	Lap Time (seconds)
1 (Lap 1)	13.09
2 (Lap 2)	11.18
3 (Lap 3)	6.11
4 (Lap 4)	17.73
5 (Lap 5)	6.41
6 (Lap 6)	34.23
7 (Lap 7)	11.63
8 (Lap 8)	1.61
Total Time	**102.03 (1 min 42.03 sec)**

Figure 4.43 8 point at fish tank.

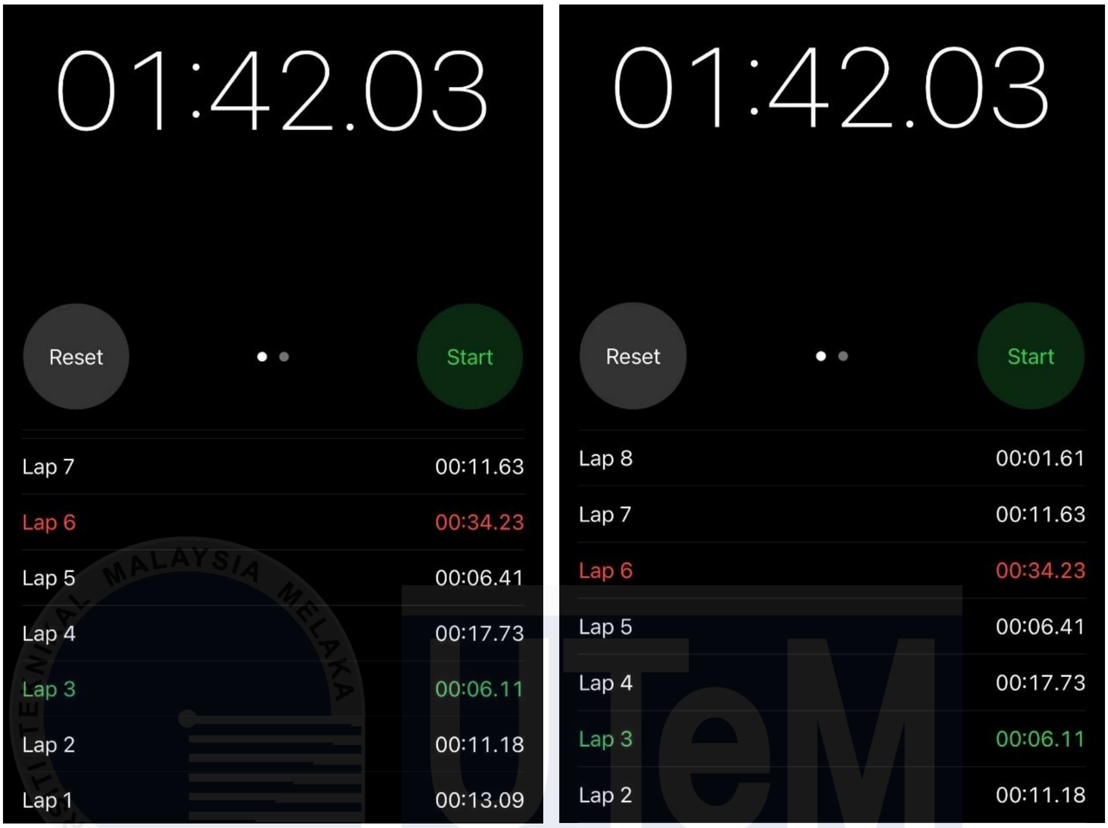

Figure 4.44 Time taken using stopwatch in smartphone.

4.7 Summary

In summary, the comprehensive analysis of the solar charging system, rechargeable batteries, and various components of the fish tank waste cleaner device highlights the system's efficiency and functionality. The solar panel, rated at 10 watts, demonstrated consistent current and voltage outputs, with performance peaking around noon. The highest power output was observed on Day 5, likely due to improved weather conditions. Performance tests on the 12V and 9V batteries, IR sensor, and water pump confirmed their reliability, with the IR sensor performing accurately over 10 trials. The buoyant force of the fish tank waste cleaner device was also tested, confirming its stability under varying water levels.

Relating this to the fish tank waste cleaner’s real-time results, the device's performance was tested in both detailed (Case A) and final (Case B) designs. The detailed design (Case A) showed the device's ability to operate effectively when submerged, though movement was hindered due to the added weight. In contrast, the final design (Case B) resolved this issue by using buoyant materials like white cork, allowing the device to float and perform more efficiently. Real-time tests under auto mode demonstrated the cleaner’s ability to cover the entire fish tank, with smooth movement and effective debris collection in all areas, showing the device's suitability for the cleaning task. The successful integration of the Blynk app further enhanced the device's control, allowing seamless operation in both manual and auto modes.

This analysis validates the fish tank waste cleaner's overall efficiency and functionality, demonstrating a stable power supply and reliable performance under various conditions. The system, which operates in both solar and manual/auto modes, provides an effective solution for cleaning fish tanks while ensuring consistent performance across different situations.

CHAPTER 5

CONCLUSION AND RECOMMENDATIONS

5.1 Conclusion

This chapter provides a detailed explanation of the primary objectives aimed at developing a fish tank waste cleaner powered by a solar charging system. The core goals included implementing a solar power charging system, designing an underwater fish tank waste cleaner, and analyzing the performance of this solar-powered underwater cleaner through real-time experiments. The solar charging system was successfully implemented, as demonstrated by the results presented in Chapter 4, thus achieving the first objective. Additionally, the simulation of the fish tank waste cleaner using Proteus software effectively confirmed the functionality of all integrated components, such as the ESP8266 microcontroller, IR sensor, motor driver, DC motors, relay module, and DC water pump. These components were successfully simulated, demonstrating their correct operation within the system.

However, further research is necessary to fully enable the system to operate while submerged in the tank. One key issue is the limitation of Wi-Fi signals (2.4 GHz), which are electromagnetic waves that do not travel well through water due to its high dielectric properties. To address this, the system will need improved methods for reliable communication in underwater environments, such as using external antennas for better signal strength. Additionally, further research is needed to overcome the buoyancy effect. To counterbalance the device’s weight after adding necessary components to keep it submerged, stronger motors or alternative design modifications might be required.

Furthermore, the sensor detection system, currently using an IR sensor, can be impacted by water refraction and temperature fluctuations, and thus replacing it with a more reliable sensor, such as a waterproof ultrasonic sensor, should be considered. Lastly, research is needed to redesign the electrical compartment to allow easy troubleshooting and maintenance. Currently, the system uses glue for sealing, which allows for only a single instance of troubleshooting before fully sealing the compartment. The new design should enable the compartment to be opened and closed for easier maintenance without compromising its waterproof integrity, ensuring the device operates efficiently and reliably in real-world, submerged conditions.

5.2 Future Works

As part of future improvements for the fish tank waste cleaner system, addressing the challenges related to Wi-Fi connectivity in aquatic environments is essential. The current system, relying on Wi-Fi signals at 2.4 GHz, encounters difficulties in maintaining a reliable connection due to the refractive and attenuative properties of water. Freshwater and saltwater have high dielectric constants and conductivity, respectively, which hinder signal propagation, leading to poor performance in submerged conditions. To mitigate this, one potential improvement would be the integration of an external antenna with the ESP8266 module. By using models like the ESP8266-07 or ESP8266-12F, which support external antennas via U.FL or IPEX connectors, a stronger Wi-Fi signal can be achieved. This antenna can be positioned outside the waterproof compartment, using a sealed cable gland, to bypass the water's interference. This approach would significantly enhance the reliability and range of the system's Wi-Fi performance, ensuring consistent communication for remote control via the Blynk app, even in the challenging aquatic environment.

Another important area of future development lies in the power and movement of the fish tank waste cleaner device. To overcome the effects of buoyancy, which currently restricts the cleaner's ability to stay grounded at the tank's bottom, a more powerful DC motor could be employed. By increasing the motor voltage, the device would have the necessary force to counteract the buoyancy and remain stable while operating efficiently. This upgrade would enhance the device's overall performance, especially in larger or deeper tanks where the forces at play can be more significant.

Additionally, replacing the existing IR sensor with a waterproof ultrasonic sensor would improve the device's obstacle detection capability. Ultrasonic sensors are not only more accurate for detecting objects at various distances, but they also function better in water environments compared to IR sensors, which can be affected by water refraction and temperature fluctuations. The ultrasonic sensor would provide more precise data for navigating the tank, helping the device avoid obstructions and perform cleaning tasks more effectively.

Incorporating a more user-friendly and maintainable design, the electrical compartment of the device can be made accessible for troubleshooting. This compartment would be equipped with a screw-based design, featuring threaded holes to ensure a secure fit, and could be easily opened or closed for maintenance purposes. To maintain full waterproofing and protect the electrical components from water exposure, a gasket or O-ring would be used around the compartment's opening. This would prevent water from seeping into the electrical components, ensuring durability and reliability even under submerged conditions.

These future enhancements, including improved Wi-Fi connectivity, stronger motors, more accurate sensors, and a user-friendly, waterproof electrical compartment, would elevate the functionality and efficiency of the fish tank waste cleaner. The device would become more reliable, durable, and adaptable to various tank sizes and water conditions, ultimately improving its overall performance and ease of maintenance.

REFERENCES

[1] S. Mousavi and G. Farahani, “Introducing a new method of automatic cleaning of the PV array surface using a suction robot,” *Mechatronics*, vol. 85, Aug. 2022, doi: 10.1016/j.mechatronics.2022.102845.

[2] R. K. Behara and A. K. Saha, “Analysis of Wind Characteristics for Grid-Tied Wind Turbine Generator Using Incremental Generative Adversarial Network Model,” *IEEE Access*, vol. 12, pp. 38315–38334, 2024, doi: 10.1109/ACCESS.2024.3372862.

[3] F. Y. C. Albert, C. H. S. Mason, C. K. J. Kiing, K. S. Ee, and K. W. Chan, “Remotely operated solar-powered mobile metal detector robot,” in *Procedia Computer Science*, Elsevier B.V., 2014, pp. 232–239. doi: 10.1016/j.procs.2014.11.057.

[4] A. B. Tatar, A. K. Tanyildizi, and B. Tasar, “A Conceptual Design of Solar-Powered Water Surface Garbage Cleaning Robot,” in *2023 4th International Conference on Artificial Intelligence, Robotics and Control, AIRC 2023*, Institute of Electrical and Electronics Engineers Inc., 2023, pp. 78–82. doi: 10.1109/AIRC57904.2023.10303130.

[5] K. Kalyani Radha and M. Ashok Chakravarthy, “Fabrication of solar robotic vacuum cleaner,” *Mater Today Proc*, Aug. 2023, doi: 10.1016/j.matpr.2023.06.401.

[6] Y. Ma, K. Xie, Y. Zhao, H. Yang, and D. Zhang, “Bi-objective Layout Optimization for Multiple Wind Farms Considering Sequential Fluctuation of Wind Power Using Uniform Design,” *CSEE Journal of Power and Energy Systems*, vol. 8, no. 6, pp. 1623–1635, Nov. 2022, doi: 10.17775/CSEEJPES.2020.03350.

[7] X. Feng, S. Lin, W. Liu, W. Liang, and M. Liu, “Distributionally Robust Optimal Dispatch of Offshore Wind Farm Cluster Connected by VSC-MTDC Considering Wind Speed Correlation,” *CSEE Journal of Power and Energy Systems*, vol. 9, no. 3, pp. 1021–1035, May 2023, doi: 10.17775/CSEEJPES.2021.06970.

[8] Y. Yu, Y. Wu, and Q. Sheng, “Optimal Scheduling Strategy of Cascade Hydropower Plants under the Joint Market of Day-Ahead Energy and Frequency Regulation,” *IEEE Access*, vol. 9, pp. 87749–87762, 2021, doi: 10.1109/ACCESS.2021.3071491.

[9] J. Tong, W. Liu, J. Mao, and M. Ying, “Role and Development of Thermal Power Units in New Power Systems,” *IEEE Journal of Radio Frequency Identification*, vol. 6, pp. 837–841, 2022, doi: 10.1109/JRFID.2022.3205465.

[10] E. Doroudchi, H. Khajeh, and H. Laaksonen, “Increasing Self-Sufficiency of Energy Community by Common Thermal Energy Storage,” *IEEE Access*, vol. 10, pp. 85106–85113, 2022, doi: 10.1109/ACCESS.2022.3195242.

[11] M. Voss, J. F. Heinekamp, S. Krutzsch, F. Sick, S. Albayrak, and K. Strunz, “Generalized Additive Modeling of Building Inertia Thermal Energy Storage for Integration into Smart Grid Control,” *IEEE Access*, vol. 9, pp. 71699–71711, 2021, doi: 10.1109/ACCESS.2021.3078802.

[12] Z. Wang *et al.*, “Study on the Optimal Configuration of a Wind-Solar-Battery-Fuel Cell System Based on a Regional Power Supply,” *IEEE Access*, vol. 9, pp. 47056–47068, 2021, doi: 10.1109/ACCESS.2021.3064888.

[13] H. Shi, C. Gan, K. Ni, Y. Chen, and Y. Hu, “Uniform Thermal Energy Distribution Scheme for Wireless Heat Transfer System Based on Inherent Topology and Thermal Coupling,” *IEEE Trans Power Electron*, 2022, doi: 10.1109/TPEL.2022.3188499.

[14] B. K and R. N, “Design of remote monitored solar powered grasscutter robot with obstacle avoidance using IoT,” *Global Transitions Proceedings*, vol. 3, no. 1, pp. 109–113, Jun. 2022, doi: 10.1016/j.gltp.2022.04.023.

[15] J. Farrokhi Derakhshandeh *et al.*, “A comprehensive review of automatic cleaning systems of solar panels,” *Sustainable Energy Technologies and Assessments*, vol. 47, Oct. 2021, doi: 10.1016/j.seta.2021.101518.

[16] V. A. Raj, P. N. Rao, R. Prasanna Alagokulesh, and M. Jeeva, "Trash Sweep Medi-waste separator," *Mater Today Proc*, vol. 64, pp. 655–660, Jan. 2022, doi: 10.1016/j.matpr.2022.05.155.

[17] R. Gopalakrishnan, U. Ramani, K. U. Maheswari, and M. Thilagaraj, "Design and Development of Controller Based Automatic Ground Cleaning Robot," in *Proceedings - 6th International Conference on Computing Methodologies and Communication, ICCMC 2022*, Institute of Electrical and Electronics Engineers Inc., 2022, pp. 491–494. doi: 10.1109/ICCMC53470.2022.9753828.

[18] K. Wei, Z. Zhang, and Z. Zhou, "Design of a new composite underwater hull cleaning robot," *J Sea Res*, vol. 198, Apr. 2024, doi: 10.1016/j.seares.2024.102488.

[19] H. Su, S. Liu, L. Zhang, Y. Chen, and C. Yang, "Biofouling recognition and boundary tracking control for underwater cleaning robots," *Ocean Engineering*, vol. 295, Mar. 2024, doi: 10.1016/j.oceaneng.2024.116707.

[20] L. Chen, R. Cui, W. Yan, H. Xu, H. Zhao, and H. Li, "Design and climbing control of an underwater robot for ship hull cleaning," *Ocean Engineering*, vol. 274, Apr. 2023, doi: 10.1016/j.oceaneng.2023.114024.

[21] T. B. Asafa, T. M. Afonja, E. A. Olaniyan, and H. O. Alade, "Development of a vacuum cleaner robot," *Alexandria Engineering Journal*, vol. 57, no. 4, pp. 2911–2920, Dec. 2018, doi: 10.1016/j.aej.2018.07.005.

[22] J. Khan, U. Bhapkar, J. Bhat, A. Chougule, and S. Sangale, "Design and development of smart solar powered street sweeping machine," in *Materials Today: Proceedings*, Elsevier Ltd, 2021, pp. 8663–8667. doi: 10.1016/j.matpr.2021.03.662.

[23] "Miniature_Water_Surface_Garbage_Cleaning_Robot".

[24] SCAD College of Engineering and Technology and Institute of Electrical and Electronics Engineers, *Proceedings of the 4th International Conference on Trends in Electronics and Informatics (ICOEI 2020) : 15-17, June 2020*.

[25] M. Manikandan, R. Suriya, K. K. Prawin, and C. Rajasekaran, "Design of Sensor Assisted Lake Water Cleaning Robot Using Internet of Things," in *Proceedings - 2023 3rd International Conference on Pervasive Computing and Social Networking, ICPCSN 2023*, Institute of Electrical and Electronics Engineers Inc., 2023, pp. 1077–1084. doi: 10.1109/ICPCSN58827.2023.00183.

[26] Y. Wang, Y. Zhao, Y. Wu, S. Zhang, and J. Wang, "A Multi-sensor Intelligent Surface Garbage Cleaning Robot," in *2021 IEEE International Conference on Mechatronics and Automation, ICMA 2021*, Institute of Electrical and Electronics Engineers Inc., Aug. 2021, pp. 797–801. doi: 10.1109/ICMA52036.2021.9512614.

[27] R. K. Megalingam, K. S. Shanmukh, A. Ashvin, and P. N. Reddy, "Design and Simulation of Autonomous Water Tank Cleaning robot in Gazebo," in *3rd International Conference on Power, Energy, Control and Transmission Systems, ICPECTS 2022 - Proceedings*, Institute of Electrical and Electronics Engineers Inc., 2022. doi: 10.1109/ICPECTS56089.2022.10047423.

[28] Z. Chen *et al.*, "Experimental Demonstration of over 14 AL Underwater Wireless Optical Communication," *IEEE Photonics Technology Letters*, vol. 33, no. 4, pp. 173–176, Feb. 2021, doi: 10.1109/LPT.2020.3048786.

[29] L. J. Bradley and N. G. Wright, "Optimising SD Saving Events to Maximise Battery Lifetime for Arduino™/Atmega328P Data Loggers," *IEEE Access*, vol. 8, pp. 214832–214841, 2020, doi: 10.1109/ACCESS.2020.3041373.

[30] J. Riedemann *et al.*, “Design and building of an automatic alternator synchronizer based on open-hardware arduino platform,” *IEEE Access*, vol. 7, pp. 105116–105122, 2019, doi: 10.1109/ACCESS.2019.2932294.

[31] R. Kamath, M. Balachandra, and S. Prabhu, “Raspberry Pi as Visual Sensor Nodes in Precision Agriculture: A Study,” *IEEE Access*, vol. 7, pp. 45110–45122, 2019, doi: 10.1109/ACCESS.2019.2908846.

[32] S. Karthikeyan, R. Aakash Raj, M. V. Cruz, L. Chen, J. L. Ajay Vishal, and V. S. Rohith, “A Systematic Analysis on Raspberry Pi Prototyping: Uses, Challenges, Benefits, and Drawbacks,” *IEEE Internet Things J*, vol. 10, no. 16, pp. 14397–14417, Aug. 2023, doi: 10.1109/JIOT.2023.3262942.

[33] V. Barral Vales, O. C. Fernandez, T. Dominguez-Bolano, C. J. Escudero, and J. A. Garcia-Naya, “Fine Time Measurement for the Internet of Things: A Practical Approach Using ESP32,” *IEEE Internet Things J*, vol. 9, no. 19, pp. 18305–18318, Oct. 2022, doi: 10.1109/JIOT.2022.3158701.

[34] A. Baingane and G. Slaughter, “A Glucose Monitoring System with Remote Data Access,” *IEEE Trans Nanobioscience*, vol. 19, no. 4, pp. 622–626, Oct. 2020, doi: 10.1109/TNB.2020.3002453.

[35] R. Muniz, J. Diaz, F. Nuno, M. J. Prieto, and A. M. Pernia, “A smart power meter to recharge electric vehicles in communal parking areas,” *IEEE Internet Things J*, vol. 6, no. 2, pp. 3448–3454, Apr. 2019, doi: 10.1109/JIOT.2018.2885171.

[36] H. R. Lim *et al.*, “Evaluation of Real-Time Monitoring on the Growth of Spirulina Microalgae: Internet of Things and Microalgae Technologies,” *IEEE Internet Things J*, vol. 11, no. 2, pp. 3274–3281, Jan. 2024, doi: 10.1109/JIOT.2023.3296525.

[37] Waluyo, A. Widura, F. Hadiatna, and D. Anugerah, “Fuzzy-Based Smart Farming and Consumed Energy Comparison Using the Internet of Things,” *IEEE Access*, vol. 11, pp. 69241–69251, 2023, doi: 10.1109/ACCESS.2023.3291616.

[38] R. Vishaal, P. Raghavan, R. Rajesh, S. Michael, and M. R. Elara, “Design of Dual Purpose Cleaning Robot,” in *Procedia Computer Science*, Elsevier B.V., 2018, pp. 518–525. doi: 10.1016/j.procs.2018.07.065.

[39] A. Natarajan, V. Krishnasamy, and M. Singh, “A Machine Learning Approach to Passive Human Motion Detection Using WiFi Measurements From Commodity IoT Devices,” *IEEE Trans Instrum Meas*, vol. 72, 2023, doi: 10.1109/TIM.2023.3272374.

[40] B. Y. Ooi, W. L. Beh, X. Y. Kh’ng, S. Y. Liew, and S. Shirmohammadi, “Using Compressive Sampling to Fill Interbatch Data Gap From Low-Cost IoT Vibration Sensor,” *IEEE Internet Things J*, vol. 9, no. 12, pp. 9820–9830, Jun. 2022, doi: 10.1109/JIOT.2022.3151051.

[41] M. M, V. T S, B. V, S. Rao, and G. P S, “Smart vacuum cleaner,” *Global Transitions Proceedings*, vol. 2, no. 2, pp. 553–558, Nov. 2021, doi: 10.1016/j.gltp.2021.08.051.

[42] A. Abubakkar, R. Achuthan, S. Gowri Shankar, S. K. Yeasigan, and K. Manoj Kumar, “Design and fabrication of mobile app-controlled floor sweeper,” in *Materials Today: Proceedings*, Elsevier Ltd, 2021, pp. 365–369. doi: 10.1016/j.matpr.2021.09.557.

[43] N. Western, X. Kong, and M. S. Erden, “Design of a train cleaning robot for the train carriage interior,” in *Procedia CIRP*, Elsevier B.V., 2021, pp. 804–809. doi: 10.1016/j.procir.2021.05.040.

[44] T. Guo, Z. D. Deng, X. Liu, D. Song, and H. Yang, “Development of a new hull adsorptive underwater climbing robot using the Bernoulli negative pressure effect,” *Ocean Engineering*, vol. 243, Jan. 2022, doi: 10.1016/j.oceaneng.2021.110306.

[45] H. Chen, G. Tang, Y. Huang, J. Wang, and H. Huang, “Adaptive model-parameter-free nonsingular fixed-time sliding mode control for underwater cleaning vehicle,” *Ocean Engineering*, vol. 262, Oct. 2022, doi: 10.1016/j.oceaneng.2022.112239.

[46] B. Wang, Z. Ni, Y. Shen, S. Zhang, Q. Shen, and X. wei Niu, “Design and analysis of a wheel-leg compound variable curvature ship hull cleaning robot,” *Ocean Engineering*, vol. 266, Dec. 2022, doi: 10.1016/j.oceaneng.2022.112755.

[47] W. Zhao, F. Han, X. Qiu, X. Peng, Y. Zhao, and J. Zhang, “Research on the identification and distribution of biofouling using underwater cleaning robot based on deep learning,” *Ocean Engineering*, vol. 273, Apr. 2023, doi: 10.1016/j.oceaneng.2023.113909.

[48] Q. Tang *et al.*, “Study on the performance of vortex suction cup for an underwater inspection robot,” *Ocean Engineering*, vol. 300, May 2024, doi: 10.1016/j.oceaneng.2024.117462.

[49] T. Kita and T. Tanaka, “Prototyping of Automatic Navigation of Underwater Robot for Underwater Visual Inspection,” in *2023 IEEE International Symposium on Underwater Technology, UT 2023*, Institute of Electrical and Electronics Engineers Inc., 2023. doi: 10.1109/UT49729.2023.10103377.

[50] D. Gogoi, A. Bharatee, and P. K. Ray, “Implementation of battery storage system in a solar PV-based EV charging station,” *Electric Power Systems Research*, vol. 229, Apr. 2024, doi: 10.1016/j.epsr.2024.110113.

[51] J. Nishanthy, S. Charles Raja, and J. Jeslin Drusila Nesamalar, “Feasibility analysis of solar PV system in presence of EV charging with transactive energy management for a community-based residential system,” *Energy Convers Manag*, vol. 288, Jul. 2023, doi: 10.1016/j.enconman.2023.117125.

[52] R. Fachrizal *et al.*, “Urban-scale energy matching optimization with smart EV charging and V2G in a net-zero energy city powered by wind and solar energy,” *eTransportation*, vol. 20, May 2024, doi: 10.1016/j.etran.2024.100314.

[53] M. E. Zayed, M. M. Aboelmaaref, and M. Chazy, “Design of solar air conditioning system integrated with photovoltaic panels and thermoelectric coolers: Experimental analysis and machine learning modeling by random vector functional link coupled with white whale optimization,” *Thermal Science and Engineering Progress*, vol. 44, Sep. 2023, doi: 10.1016/j.tsep.2023.102051.

[54] S. Prasath Kumar, A. Ravindiran, S. Meganathan, N. Oral Roberts, and N. Anbarasi, “Swarm robot materials handling paradigm for solar energy conservation,” in *Materials Today: Proceedings*, Elsevier Ltd, 2020, pp. 3924–3928. doi: 10.1016/j.matpr.2021.02.402.

[55] M. ElSayed, A. Foda, and M. Mohamed, “Autonomous drone charging station planning through solar energy harnessing for zero-emission operations,” *Sustain Cities Soc*, vol. 86, Nov. 2022, doi: 10.1016/j.scs.2022.104122.

[56] H. M. Khalid *et al.*, “Dust accumulation and aggregation on PV panels: An integrated survey on impacts, mathematical models, cleaning mechanisms, and possible sustainable solution,” *Solar Energy*, vol. 251. Elsevier Ltd, pp. 261–285, Feb. 01, 2023. doi: 10.1016/j.solener.2023.01.010.

[57] M. Vega-Heredia *et al.*, “Design and modelling of a modular window cleaning robot,” *Autom Constr*, vol. 103, pp. 268–278, Jul. 2019, doi: 10.1016/j.autcon.2019.01.025.

APPENDICES

Appendix A

Coding for a fish tank waste cleaner.

```
// Blynk and ESP8266 Libraries
#define BLYNK_PRINT Serial
#include <ESP8266WiFi.h>
#include <BlynkSimpleEsp8266.h>

// Blynk Auth Token and WiFi Credentials
#define BLYNK_AUTH_TOKEN "Rzqzi37pS42nCvs8C7j14AbIesCIN0Sb" // Enter your
Blynk Auth Token
char auth[] = BLYNK_AUTH_TOKEN;
char ssid[] = "12345678";  // Enter your WiFi name
char pass[] = "12345678";          // Enter your WiFi password

// Motor control pins
const int motor1Pin1 = 0;  // IN1 on L298N
const int motor1Pin2 = 4;  // IN2 on L298N
const int motor2Pin1 = 5;  // IN3 on L298N
const int motor2Pin2 = 16; // IN4 on L298N
const int ENA = 14;       // ENA pin for Motor 1 speed control
const int ENB = 12;       // ENB pin for Motor 2 speed control

// Additional component pins
const int irSensorPin = A0;  // IR sensor input pin
const int waterPumpPin = 13; // GPIO pin for water pump control

// Variables for control and thresholds
const int distanceThreshold = 50; // Threshold for object detection
bool autoMode = false;           // Auto or Manual Mode
bool systemActive = false;       // System ON/OFF status

// Function Prototypes
void moveForward();
void moveReverse();
void turnLeft();
void turnRight();
void stopMotors();
void controlWaterPump(bool state);

// Blynk Virtual Pins:
// V0: Mode Auto/Manual Button
// V1: Forward Button (Manual Mode)
```

```
// V2: Reverse Button (Manual Mode)
// V3: Right Button (Manual Mode)
// V4: Left Button (Manual Mode)

// Toggle Mode (Auto/Manual)
BLYNK_WRITE(V0) {
  autoMode = param.asInt(); // Update autoMode state
  systemActive = autoMode;  // System active in Auto Mode only
  if (autoMode) {
    Serial.println("Auto Mode Activated");
    controlWaterPump(true); // Turn ON water pump in Auto Mode
  } else {
    Serial.println("Manual Mode Activated");
    controlWaterPump(false); // Turn OFF water pump initially in Manual Mode
    stopMotors();           // Stop motors when switching to Manual Mode
  }
}

// Manual Control Buttons with Momentary Behavior
BLYNK_WRITE(V1) { // Forward Button
  if (!autoMode) {
    if (param.asInt()) { // Button pressed
      systemActive = true;
      controlWaterPump(true);
      moveForward();
    } else { // Button released
      stopMotors();
    }
  }
}

BLYNK_WRITE(V2) { // Reverse Button
  if (!autoMode) {
    if (param.asInt()) { // Button pressed
      systemActive = true;
      controlWaterPump(true);
      moveReverse();
    } else { // Button released
      stopMotors();
    }
  }
}

BLYNK_WRITE(V3) { // Right Button
  if (!autoMode) {
    if (param.asInt()) { // Button pressed
      systemActive = true;
      controlWaterPump(true);
      turnRight();
    } else { // Button released
```

```
      stopMotors();
    }
  }
}

BLYNK_WRITE(V4) { // Left Button
  if (!autoMode) {
    if (param.asInt()) { // Button pressed
      systemActive = true;
      controlWaterPump(true);
      turnLeft();
    } else { // Button released
      stopMotors();
    }
  }
}

void setup() {
  Serial.begin(9600);
  Blynk.begin(auth, ssid, pass, "blynk.cloud", 80);

  // Motor Pins Setup
  pinMode(motor1Pin1, OUTPUT);
  pinMode(motor1Pin2, OUTPUT);
  pinMode(ENA, OUTPUT);
  pinMode(motor2Pin1, OUTPUT);
  pinMode(motor2Pin2, OUTPUT);
  pinMode(ENB, OUTPUT);

  // Water Pump Setup
  pinMode(waterPumpPin, OUTPUT);
  controlWaterPump(false); // Ensure water pump is OFF at startup

  analogWrite(ENA, 200); // Set motor speed (80%)
  analogWrite(ENB, 200);

  Serial.println("System Ready");
}

void loop() {
  Blynk.run();

  if (autoMode) {
    // **Mode 1: Auto Mode**
    int distanceValue = analogRead(irSensorPin); // Read IR sensor value
    int distance = map(distanceValue, 0, 1023, 0, 100);

    Serial.print("Distance: ");
    Serial.print(distance);
    Serial.println(" cm");
```

```
    if (distance < distanceThreshold) {
      // If object detected, reverse, turn slightly right, and move forward again
      Serial.println("Object Detected! Reversing...");
      stopMotors();
      moveReverse();
      delay(500); // Reverse for 0.5 second
      stopMotors();
      delay(300);  // Small pause
      Serial.println("Slight Turn Right...");
      turnRight();
      delay(400); // Slight turn right for 0.4 second
      stopMotors();
      delay(300);  // Small pause
      Serial.println("Moving Forward...");
      moveForward();
    } else {
      // If no object detected, keep moving forward
      moveForward();
    }
    controlWaterPump(true); // Ensure water pump stays ON in Auto Mode
  } else if (!autoMode && !systemActive) {
    // **System OFF in Manual Mode**
    stopMotors();
    controlWaterPump(false); // Turn OFF water pump
  }
}

// Motor Control Functions
void moveForward() {
  Serial.println("Moving Forward");
  digitalWrite(motor1Pin1, HIGH);
  digitalWrite(motor1Pin2, LOW);
  digitalWrite(motor2Pin1, HIGH);
  digitalWrite(motor2Pin2, LOW);
}

void moveReverse() {
  Serial.println("Moving Reverse");
  digitalWrite(motor1Pin1, LOW);
  digitalWrite(motor1Pin2, HIGH);
  digitalWrite(motor2Pin1, LOW);
  digitalWrite(motor2Pin2, HIGH);
}

void turnLeft() {
  Serial.println("Turning Left");
  digitalWrite(motor1Pin1, HIGH);
  digitalWrite(motor1Pin2, LOW);
  digitalWrite(motor2Pin1, LOW);
```

```
  digitalWrite(motor2Pin2, HIGH);
}

void turnRight() {
  Serial.println("Turning Right");
  digitalWrite(motor1Pin1, LOW);
  digitalWrite(motor1Pin2, HIGH);
  digitalWrite(motor2Pin1, HIGH);
  digitalWrite(motor2Pin2, LOW);
}

void stopMotors() {
  Serial.println("Motors Stopped");
  digitalWrite(motor1Pin1, LOW);
  digitalWrite(motor1Pin2, LOW);
  digitalWrite(motor2Pin1, LOW);
  digitalWrite(motor2Pin2, LOW);
  delay(50);
}

// Water Pump Control Function
void controlWaterPump(bool state) {
  if (state) {
    Serial.println("Water Pump ON");
    digitalWrite(waterPumpPin, HIGH); // Turn ON water pump
  } else {
    Serial.println("Water Pump OFF");
    digitalWrite(waterPumpPin, LOW);  // Turn OFF water pump
  }
}
```

Appendix B

Specification of polycrystalline.

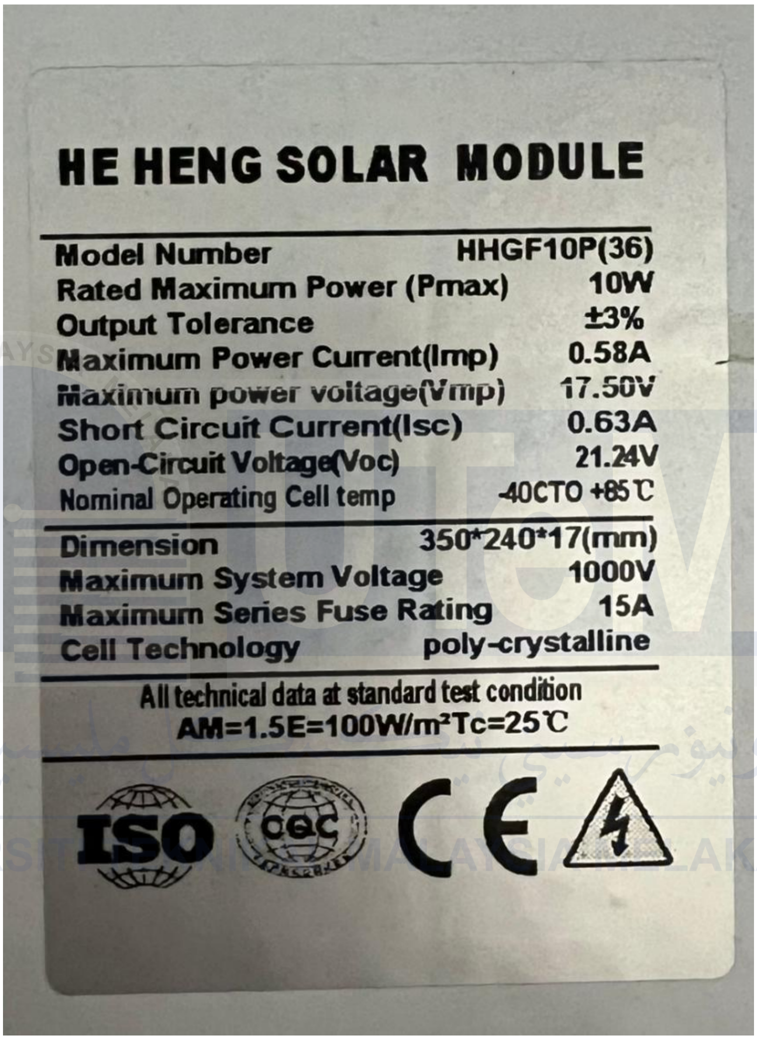

Appendix C

Pinouts of ESP8266.

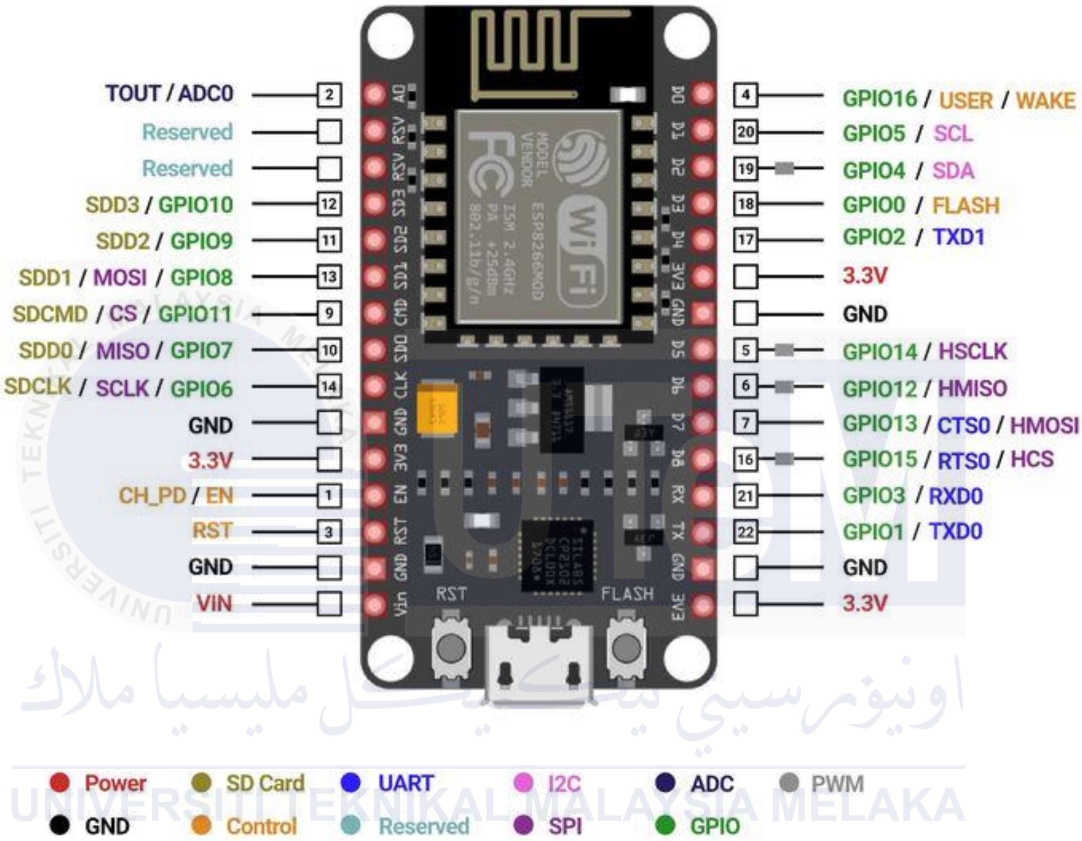

Appendix D

Pinouts of motor driver.

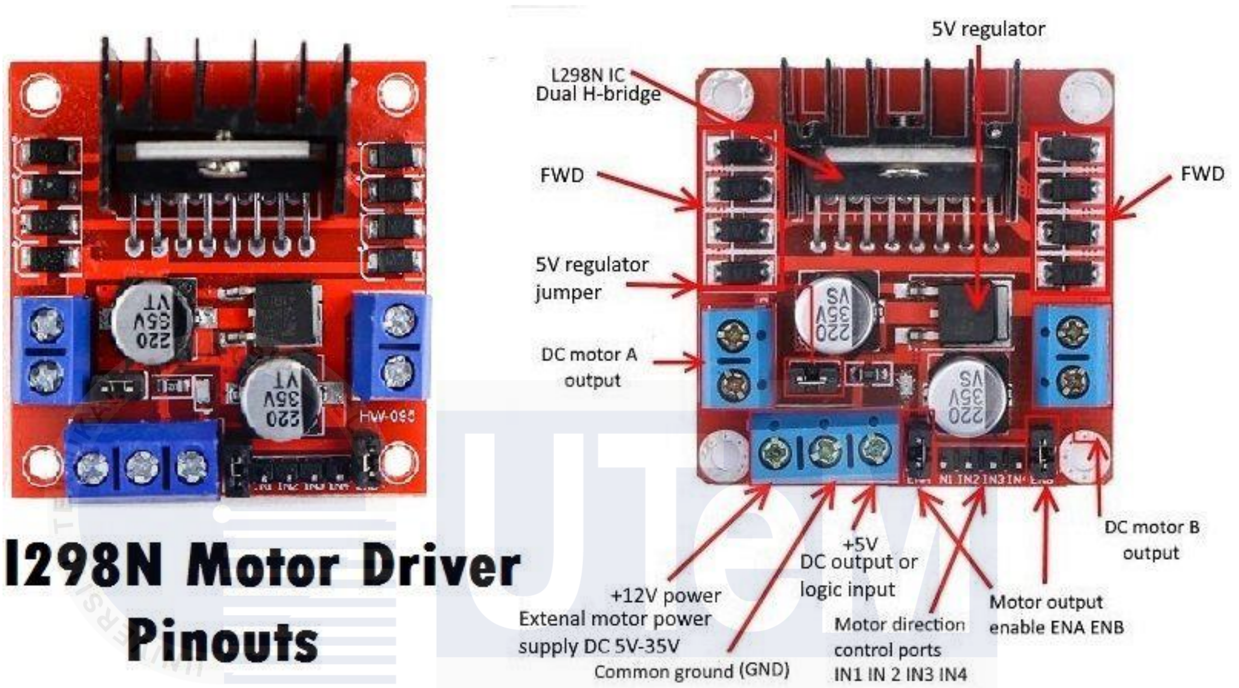

Appendix E

Pinouts of relay module.

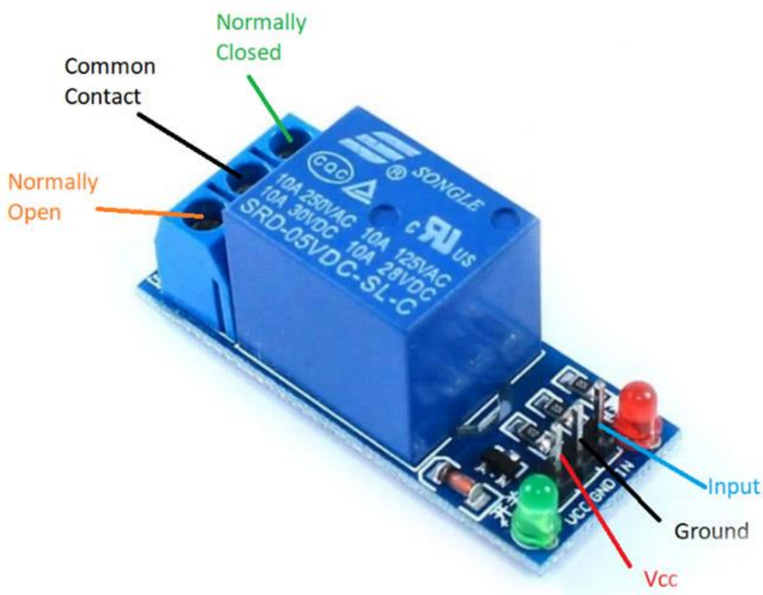

Appendix F

Pinouts of IR sensor.